

Regulation of L-periaxin by the Ubiquitin/Proteasome pathway

A.Sylvia Vasiliou

Ph.D.

University of Edinburgh

Preclinical Veterinary Sciences

2001



DECLARATION

I declare that I composed this thesis and that the work described in it is my own except where indicated.

CONTENTS

DECLARATION	
TABLE OF CONTENTS	i
LIST OF FIGURES	viii
LIST OF TABLES	x
ABBREVIATIONS	xi
ABSTRACT	xv
ACKNOWLEDGEMENTS	xvii
1 INTRODUCTION	1
1.1 INTRODUCTION	1
1.2 MYELINATION IN THE PERIPHERAL NERVOUS SYSTEM	3
1.2.1 Myelinated fibers	3
1.2.1.1 Myelin and its formation	
1.2.1.2 The structure and chemical composition of PNS myelin	9
1.3 ROLE OF THE SCHWANN CELL IN PERIPHERAL MYELINATION	17
1.3.1 Embryological development of the Schwann cell	17
1.3.2 Determination of the Schwann cell phenotype	18
1.3.3 Factors involved in Schwann cell proliferation and differentiation	20
1.3.4 Axon-Schwann cell interactions determine the length of the myelin segment and induce the formation of a basal lamina	21
1.3.5 Schwann cells and their precursors control neuronal survival and development	22
1.3.6 Schwann cells regulate their own survival via an autocrine mechanism	23

1.4	PERIAXIN: A PROTEIN EXPRESSED BY MYELIN-FORMING SCHWANN CELLS	24
1.4.1	Periaxin isoforms and the structure of the periaxin gene	26
1.4.2	Primary structure and developmental regulation of periaxin	26
1.4.3	L-periaxin participates in a dystroglycan transmembrane complex	29
1.4.4	Periaxin null mice display peripheral demyelination and neuropathic pain	33
1.4.5	Mutations in human periaxin are responsible for Dejerine-Sottas neuropathy (DSN) and Charcot-Marie-Tooth Disease 4F(CMT4F)	34
1.5	DETECTION OF SPECIFIC INTERACTIONS BETWEEN PROTEINS: THE YEAST TWO- HYBRID APPROACH	35
1.6	INTRACELLULAR CONTROL OF PROTEIN ABUNDANCE	38
1.6.1	The ubiquitin pathway of protein degradation	38
1.6.2	Discovery of an energy-dependent proteolytic process mediated by ubiquitin	39
1.6.3	Components of the ubiquitination machinery	43
1.6.3.1	E1 ubiquitin activating enzyme	43
1.6.3.2	E2 ubiquitin conjugating enzymes	43
1.6.3.3	E3 ubiquitin ligases	44
1.6.4	RING-finger proteins mediate ubiquitin ligase activity	47
1.6.5	The SCF-Ub ligase complex	50
1.6.5.1	Subunits of the SCF complex	50
1.6.5.2	Structure and function of the SCF components	51
1.6.5.2 (a)	Skp1	51
1.6.5.2 (b)	Cullin1/Cdc53	52
1.6.5.2 (c)	Hrt1/Rbx1/Roc1	52
1.6.5.2 (d)	F-box-containing proteins	53
	WD40 repeats	54
	Leucine rich repeats (LRR)	55
1.6.5.3	Mechanism of action of the SCF complex	58
1.6.5.3.1	The F-box hypothesis	58
1.6.5.3.2	Transfer of Ub residues to Lys side chains of the target protein	60
1.6.5.4	Substrates of the SCF	62

1.6.5.4.1	The hedgehog pathway	62
1.6.5.4.2	The Wnt/Wingless pathway	63
1.6.5.4.3	The NF- κ B pathway	66
1.6.6	The anaphase promoting complex (APC)/cyclosome ligase	66
1.6.7	The Cullin2/ElonginB/ElonginC (CBC) complex	67
1.6.8	Cul3-5 based ligases	68
1.6.9	Phosphorylation-dependent degradation signals	69
1.6.10	N-terminal ubiquitin as a degradation signal	70
1.6.11	Internalisation signals	71
1.6.12	De-ubiquitinating enzymes	74
1.6.13	The proteasome pathway	76
1.6.13.1	Structure and function of the 26S proteasome	76
1.6.13.2	Subcellular localisation of the proteasome	81
1.6.13.3	Ub-independent function of the proteasome	83
1.6.13.4	Inhibition of the proteasome	84
1.6.13.4 (a)	Non-specific inhibitors	84
	Peptide aldehydes	84
1.6.13.4 (b)	Proteasome-specific inhibitors	85
	Lactacystin	85
	Vinyl sulfone and boronic acids	85
	Epoxomicin	86
1.6.14	Functional diversity of the Ubiquitin pathway	87
1.6.14.1	Destructive role of ubiquitin	
1.6.14.1(a)	Implication of the Ub pathway in disease	87
1.6.14.2	Non-destructive role of ubiquitin in ribosome biogenesis	93
1.7	BACKGROUND TO THE PROJECT	95
1.8	PROPOSED STUDY	96
2	MATERIALS AND METHODS	97
2.1	GENERATION OF L-PERIAxin CONSTRUCTS FOR THE YEAST TWO-HYBRID SCREEN	97
2.1.1	PeriC1	99
2.1.2	PeriC2	100

2.1.3	PeriRA3	100
2.1.4	PeriR5	101
2.1.5	PeriA6	101
2.1.6	PeriA7	102
2.1.7	PeriC8	102
2.1.8	PeriC9	102
2.2	SEQUENCING OF THE PCR PRODUCTS	104
2.3	EXPRESSION OF PERIAXIN CONSTRUCTS	105
2.3.1	Fusion protein expression and extraction from yeast cells	105
2.3.2	Western Blotting	106
2.4	YEAST TRANSFORMATION IN THE LiAc/ss-DNA/PEG PROTOCOL	107
2.5	REPORTER GENE AUTOACTIVATION TESTS AND TRANSFORMATION EFFICIENCY CONTROLS	108
2.6	COLONY FILTER-LIFT ASSAY	209
2.7	RAT SCIATIC NERVE cDNA LIBRARY SCREEN IN THE YEAST TWO- HYBRID SCREEN	110
2.8	TESTING FOR SPECIFIC LIBRARY- “BAIT” INTERACTIONS	111
2.8.1	Isolation of plasmid from yeast	112
2.8.2	Isolation of yeast plasmid from bacteria and insert analysis	112
2.9	VERIFICATION OF INTERACTIONS BY BIOCHEMICAL METHODS	114
2.9.1	Generation, expression and purification of GST-fusion proteins of the interacting clones	114
2.9.1.1	Generation procedure	114
	Clone 11a	114
	Clone 26a	114
2.9.1.2	Expression of GST-fusion proteins	115
2.9.1.3	Purification of GST-fusion proteins	116
2.9.2	Pull down assay from sciatic nerve homogenate	116

2.9.3	Preparation of <i>in vitro</i> transcribed/translated L-periaxin	117
2.9.3.1(a)	<i>In vitro</i> transcription of L-periaxin	117
2.9.3.1(b)	<i>In vitro</i> translation of l-periaxin	118
2.9.3.2	Pull down assay using an <i>in vitro</i> transcription/translation product of L- periaxin	119
2.10	NORTHERN BLOTTING OF 26a	120
2.10.1	Construction of hybridisation probe for northern blot	120
2.10.2	Radioactive labelling of hybridisation probe	120
2.10.3	Preparation of RNA samples	120
2.10.4	Hybridisation process	121
2.11	ISOLATION OF FULL-LENGTH 26a (rFbx16) cDNA	121
2.12	GENERATION OF C-TERMINAL ANTIBODIES AGAINST CLONE 26a IN RABBITS	122
2.12.1	Preparation of KLH-coupled peptides for injection	122
2.12.2	Assessment of rabbit anti-serum by Western Blotting	122
2.12.3	Affinity purification of anti-serum	123
2.13	UBIQUITINATION EXPERIMENTS	124
2.13.1	Immunoprecipitation of ubiquitinated L-periaxin and β -catenin from P21 mouse sciatic nerve	124
2.13.2	Inhibition of the proteasomal pathway with epoxomicin to block L-periaxin degradation	125
2.14	TISSUE DISTRIBUTION OF 26a	126
2.15	TRANSGENESIS	127
2.15.1	Generation of rFbx16 Δ F transgenic construct	130
2.15.2	Purification of transgenic DNA for nuclear transfer	131
2.16	IMMUNOSTAINING OF SCIATIC NERVE SECTIONS	131
	APPENDIX I	132

3	RESULTS	134
3.1	PERIAXIN CONSTRUCTS PERIC1, PERIC2 AND PERIRA3 WERE EXPRESSED IN YEAST AS REVEALED BY WESTERN BLOTS	134
3.2	REPORTER GENES LACZ AND HIS3 WERE NOT AUTOACTIVATED BY PERIAXIN CONSTRUCTS	134
3.2.1	Transformation efficiency tests	137
3.3	ISOLATION AND HANDLING OF PUTATIVE PERIC1 POSITIVE INTERACTING LIBRARY CLONES	139
3.3.1	Assessment of interaction between the positive library clones and PeriC1, PeriC2 and PeriRA3	139
3.3.2	Clones 11a (8a) and 26a (13a) were chosen for further study	141
3.3.3	GST-fusions of clones 11a and 26a interacted with L-periaxin in sciatic nerve pull down assays	142
3.3.4	GST-11a and GST-26a interacted with an <i>in vitro</i> transcription/translation product of L-periaxin	144
3.3.5	Clone 11a interacts with a region of 170 aa of L-periaxin including the entire the acidic domain, whereas 26a requires a minimum of 85 residues, which comprises part of the acidic region of L-periaxin	146
3.4	FOCUSING ON CLONE 26a	148
3.4.1	The size of the mRNA of the full length 26a protein was determined by Northern Blotting	149
3.4.2	Full length 26a protein is the rat homologue of the mouse F-box-containing protein Fbl6/Fbx16	151
3.4.3	Alternative models of the 3D structure of rFbx16 based on crystallographic data from other F-box-containing proteins	155
3.4.4	rFbx16 mediates ubiquitination of L-periaxin in the sciatic nerve	160

3.4.5	The proteasome is involved in the turnover of L-periaxin in the sciatic nerve	163
3.4.6	rFbx16 is expressed in a variety of tissues	167
3.4.7	Investigation of the significance of L-periaxin ubiquitination by transgenesis	167
3.4.8	The C-terminal antibodies 26aC1 and 26aC2 did not immunostain sciatic nerve sections	167
	APPENDIX II	169
4	DISCUSSION	171
4.1	L-periaxin and the F-box hypothesis	171
4.1.1	rFbx16 is expressed in a variety of tissues and may associate with multiple substrates	172
4.1.2	Predicting the 3D structure of the LRR region of Fbx16: two possible models emerge	173
4.2	Conjugation of ubiquitin residues to L-periaxin	174
4.3	Investigation of the L-periaxin-rFbx16 interaction by transgenesis	175
4.4	L-periaxin, β -catenin and the ubiquitin/proteasome pathway: more than just a matter of elimination	176
4.4.1	β -catenin: a protein implicated in alternative F-box-mediated pathways of destruction	177
4.4.2	A hypothetical model for the ubiquitin-mediated regulation of L-periaxin, based on evidence for β -catenin	179
5	FUTURE WORK	183
6	REFERENCES	187

LIST OF FIGURES

FIGURE 1.	Adult rat sciatic nerve myelinated axon	4
FIGURE 2.	Peripheral myelin sheath formation	5
FIGURE 3.	Schematic diagram of an “unrolled” Schwann cell	6
FIGURE 4.	The Node of Ranvier in the peripheral nervous system	
FIGURE 5.	Ultrastructural and molecular properties of myelin	16
FIGURE 6.	The Schwann cell lineage	18
FIGURE 7.	Periaxin localisation shifts to the abaxonal membranes as the myelin sheath begins to mature	25
FIGURE 8.	The structure of the murine periaxin gene	27
FIGURE 9.	Domain structure of L- and S-periaxin	28
FIGURE 10.	The DRP2-L-periaxin- dystroglycan complex at the Schwann cell plasma membrane	32
FIGURE 11.	The yeast two-hybrid assay for detection of protein-protein interactions	37
FIGURE 12.	The ubiquitin/proteasome pathway of protein degradation	42
FIGURE 13.	RING-finger containing E3 ubiquitin ligases: the SCF, CBC and APC complexes	49
FIGURE 14.	Structure of the Leucine-rich repeats of porcine ribonuclease inhibitor	57
FIGURE 15.	Mechanism of action of HECT-domain and RING-finger ubiquitin ligases	61
FIGURE 16.	Substrates of the SCF complex	65
FIGURE 17.	Structure of the 26S proteasome	78
FIGURE 18.	Pathogenesis of Ubiquitin System-related diseases	89
FIGURE 19.	Full length L-periaxin and constructs used in yeast two-hybrid	98
FIGURE 20.	Structure of rFbx16 Δ F construct for transgenesis	129

FIGURE 21.	Expression of PeriC1, PeriC2 and PeriRA3 constructs in yeast strain Y190	136
FIGURE 22.	L-periaxin interacts with GST-fusions of clones 11a and 26a in sciatic nerve pull down assays	143
FIGURE 23.	GST-fusions of clones 26a (A) and 11a (B) interact specifically with L-periaxin generated by <i>in vitro</i> transcription/translation	145
FIGURE 24.	Yeast two-hybrid assay to investigate potential interactions of clones 11a and 26a with all L-periaxin constructs	147
FIGURE 25.	mRNA of clone 26a was detected in both brain and trigeminal nerve of P15 rat, by Northern Blotting	150
FIGURE 26.	Amino acid sequence alignment of the mouse (m) and rat (r) F-box-containing protein Fbx16	152
FIGURE 27.	Nucleotide and amino acid sequence of rFbx16	153
FIGURE 28.	Domain structure of clone 26a and rFbx16	154
FIGURE 29.	Clustal W alignment of the LRR region of rFbx16	156
FIGURE 30.	Proposed 3D structural model 1 (M1) of the LRR region of rFbx16	157
FIGURE 31.	Proposed 3D structural model 2 (M2) of the LRR region of rFbx16	158
FIGURE 32.	L-periaxin and β -catenin are ubiquitinated in sciatic nerve	162
FIGURE 33.	L-periaxin is stabilised in sciatic nerve upon inhibition of the proteasome by epoxomicin	164
FIGURE 34.	Effect of inhibition of the proteasome on the levels of L-periaxin in sciatic nerve	166
FIGURE 35.	Fbx16 is expressed in a variety of tissues	168
FIGURE 36.	(A) Cellular functions and regulation of β -catenin (B) Hypothetical model of the function and regulation of L-periaxin	182

LIST OF TABLES

Table 1.	The N-end rule	46
Table 2.	LRR subfamilies	56
Table 3.	Oligonucleotide primers for the generation of L-periaxin constructs	103
Table 4.	Oligonucleotide primers for clone 26a	115
Table 5.	Assessment of autoactivation of the reporter genes lacZ and HIS3 of PeriC1, PeriC2 and PeriRA3 periaxin constructs in the binding domain (BD) vector pODB8, in yeast strains CG1945 and Y190	135
Table 6.	Transformation efficiency of PeriC1 and rat sciatic nerve library cDNA co-transformed in yeast strains CG1945 and Y190.	138
Table 7.	Specific interactions of clones isolated from a rat sciatic cDNA library screen with periaxin constructs PeriC1, PeriC2 and PeriRA3 using the yeast two-hybrid system	140

ABBREVIATIONS

aa	amino acid
AD	activation domain
AMP	adenosine monophosphate
APC	adenomatous poliposis coli
APS	ammonium persulfate
3-AT	3-amino,1-2-4 triazole
BD	binding domain
bp	base pair
BSA	bovine serum albumin
cAMP	cyclic AMP
CDK	cyclin-dependent kinase
cDNA	complementary DNA
cfu	colony forming unit
CHX	cycloheximide
CMT	Charcot-Marie-Tooth
CNPase	2,'3'-cyclic nucleotide-3'- phosphodiesterase
CNS	central nervous system
Cx32	connexin-32
dATP	deoxyadenosine triphosphate
DEPC	diethyl pyrocarbonate
DMSO	dimethyl sulfoxide
DNA	deoxyribonucleic acid
DRP2	dystrophin-related protein 2
DSS	Dejerine-Sottas syndrome
DTT	dithiothreitol
EDTA	ethylene diaminetetra-acetic acid
ER	endoplasmic reticulum
ESCRT-1	endosomal sorting complex required for transport-1
FBX	F-box-containing protein
GalC	galactocerebroside
GAP43	growth- associated protein 43

GST	glutathione-S-transferase
HA	haemagglutinin
HECT	homology to E6-AP carboxy terminus
HNPP	hereditary neuropathy with liability to pressure palsy
HRP	horseradish peroxidase
IB	immunoblotting
Ig	immunoglobulin
IGP	imidazole glycerol phosphate
IP	immunoprecipitation
IPL	intraproduct line
kb	kilobase
kDa	kiloDalton
LB	Luria-Bertani medium
LiAc	lithium acetate
LRR	leucine-rich repeat
MAG	myelin-associated glycoprotein
MAPK	mitogen-activated protein kinase
MBP	myelin basic protein
MBS	m Maleimidobenzoyl-N-hydroxysuccinimide ester
MCS	multiple cloning site
MDL	major dense line
Mr	relative molecular mass
MVB	multivesicular body
MW	molecular weight
NCAM	neural cell adhesion molecule
NGFR	neural growth factor receptor
NLS	nuclear localisation signal
nNOS	neuronal nitric oxide synthase
PBS	phosphate-buffered saline
PCR	polymerase chain reaction
PDGFR	platelet- derived growth factor receptor
PDZ	PSD95/discs large/zona occludens

PEG	polyethylene glycol
PKA	protein kinase A
PLP	proteolipid protein
PMP22	peripheral myelin protein 22
PMSF	p-methane-sulfonic acid
PNS	peripheral nervous system
RACE	rapid amplification of cDNA ends
rcf	relative centrifugal force
RING	really interesting new gene
Rnase	ribonuclease
rpm	revolutions per minute
SAP95	synapse associated protein 95
SC	synthetic complete medium
SCF	Skp1/Cullin1/F-box protein
SD	synthetic dropout medium
SDS	sodium dodecyl sulfate
SDS-PAGE	SDS- polyacrylamide gel electrophoresis
Skp1	S phase kinase-associated protein
SOCS	suppressors of cytokine signalling
SS-DNA	single stranded DNA
TAE	40 mM Tris-acetate, 1 mM EDTA, pH8
TAT	tyrosine amino- transferase
TE	10 mM Tris, 1mM EDTA, pH8
TBE	22.5 mM Tris-borate, 1 mM EDTA
TCA	trichloro acetic acid
TEMED	N,N,N',N'-tertamethyl ethylenediamine
TNF	tumour necrosis factor
TrCP	transducin repeat containing protein
U	units
Ub	ubiquitin
Ubc	ubiquitin conjugating enzyme
Uch	ubiquitin C-terminal hydrolase

UFD

ubiquitin/fusion/degradation

X-gal

5-bromo-4-chloro-3-indolyl-D-galactoside

ABSTRACT

The morphological changes required for the ensheathment of peripheral nerve axons by Schwann cells are believed to be regulated by the cell cytoskeleton and its associated proteins. Control of the levels of these proteins is likely to be necessary for the assembly of compact myelin and the stability of the sheath.

L-periaxin was initially identified as a putative cytoskeleton-associated protein expressed by myelin-forming Schwann cells based upon its insolubility in non-ionic detergent. The pattern of developmental expression of L-periaxin and its shift in localisation from the adaxonal to abaxonal membranes of myelinating Schwann cells following their association with axons, implied a role in the stabilisation of the myelin sheath. In this work, an F-box containing protein termed Fbx16, was found to associate with the C-terminal acidic region of L-periaxin, in a search for binding partners of L-periaxin using the yeast two-hybrid method. The observed interaction was verified by *in vitro* pull down assays using mouse sciatic nerve homogenate and L-periaxin generated by *in vitro* transcription/ translation.

F-box proteins have been identified as components of a multi-enzyme complex termed SCF (Skp1/ Cullin1/F-box), which is responsible for the recruitment of substrates for ubiquitination and subsequent destruction. Fbx16 belongs to the leucine-rich repeat (LRR)-containing subfamily of F-box proteins. The C-terminal LRR region of the protein serves as the binding site for L-periaxin, whereas the F-box motif permits association with the core SCF complex. L-periaxin was detected as a ubiquitin conjugate in sciatic nerve explant cultures. Ubiquitination of the protein acts as a signal for degradation by the 26S proteasome, as revealed by stabilisation of L-periaxin upon inhibition of the proteasome by epoxomicin.

The participation of L-periaxin in a recently identified dystroglycan- dystrophin-related protein 2 (DRP2) complex, suggests an indirect role for Fbx16 in the structural and signalling functions of the cortical cytoskeleton. Regulation of the levels of L-periaxin by the ubiquitin/ proteasome pathway, mediated by Fbx16, is likely to be important for the stabilisation of the Schwann cell-axon unit.

ACKNOWLEDGEMENTS

I would like to acknowledge Professor Peter J Brophy for extensive supervision and valuable advice throughout the course of my experimental work and the composition of this thesis.

I am grateful to all the members of the PJB group for excellent demonstration of scientific techniques and assistance during my laboratory work. In particular, Stewart Gillespie and Diane Sherman for supervising my project and providing expert advice, Steven Tait for valuable comments and suggestions, and Linda Ferguson for excellent help with molecular biology techniques.

Thanks also go to my fellow PhD student, Anna Williams, with whom I've had very useful discussions and Felipe Court, who generated the 3D models included in this thesis. I would also like to thank Mary Davie for help with immunohistochemistry and Shona Melrose who provided expert assistance with several techniques.

Special thanks go to Richard Johnson (Dr J) who apart from being very helpful with laboratory work, has also been one of my good friends.

I would also like to acknowledge Graham Pettigrew, John Mason and Vince Moloney for their supervision, and the MRC for funding my project.

Finally and most importantly, I would like to express my gratitude to my family and close friends without whose continuous support this work would not have been possible.

Introduction

1. INTRODUCTION

1.1 INTRODUCTION

Protein-protein interactions are commonly the way in which the dynamic functions of proteins are manifested. An efficient way of ensuring that the correct interactions between proteins are formed is by controlling the levels of expression of these polypeptides in the appropriate location at the right time, so they can be readily available to their binding partners. Cells employ a highly selective mechanism to regulate their protein content, which involves the covalent modification of proteins to be eliminated by a small protein, termed ubiquitin. The process of attachment to ubiquitin, referred to as ubiquitination, is energy dependent and targets proteins for destruction by a self-compartmentalised protease system, the 26S proteasome.

Protein interactions are strongly implicated in the process of myelination resulting in the compaction of the myelin sheath. The adhesion of adjacent layers of the multi-lamellar sheath has been described to be largely accomplished by processes that involve the formation of protein complexes (Peters et al., 1970).

Stabilisation of the myelin sheath in the peripheral nervous system is influenced by the presence of L-periaxin protein expressed by myelin-forming Schwann cells (Gillespie et al., 1994). Its localisation to the periaxonal Schwann cell membranes, at the early stages of myelination, suggested a role in axon-glial communication and its possible binding partners have been sought among proteins associated with the axolemma or the Schwann cell cytoskeleton. Recently L-periaxin has been shown to interact with dystrophin-related protein 2 (DRP2) in the context of a dystroglycan-glycoprotein complex. It has been known for some time that the

expression of genes important for myelin assembly is regulated by Schwann cell contact with the basal lamina (Bunge et al., 1986). L-periaxin as part of the DRP2 complex, is required to support stabilisation of the myelin sheath in the later stages of the myelination process, as suggested by evidence from periaxin-deficient mice (Gillespie et al., 2000). L-periaxin associates with DRP2 through a highly basic domain localised near the N-terminus of the protein, downstream of a PDZ domain which is responsible for homodimerisation of the protein. This self-association of the protein is probably responsible for the clustering of the DRP2 complex in the plasma membrane of the Schwann cell (Sherman et al., 2001).

The object of this study was to identify other possible binding partners of L-periaxin by employing the yeast two-hybrid method (Fields and Song, 1989) using the C-terminal part of the protein, which comprises an acidic domain, as “bait”. Detection and subsequent characterisation of periaxin's interacting partners would provide clues to characterising its specific role in the Schwann cell and its involvement in peripheral nerve myelination.

1.2 MYELINATION IN THE PERIPHERAL NERVOUS SYSTEM

1.2.1 Myelinated fibres

1.2.1.1 Myelin and its formation

Myelin is a multilamellar structure with a high lipid to protein ratio (80:20 by weight), which serves as an insulator of nerve fibres and permits saltatory conduction of nerve impulses. Myelin is present in both the CNS and PNS and is elaborated by two different types of glial cells.

Oligodendrocytes are responsible for myelination in the CNS, whereas in the PNS myelin formation is accomplished by Schwann cells. In both cases, myelin is deposited by the repeated spiral wrapping of an extension of the plasma membrane of these cells around the axon (Kandel and Schwartz, 1985). The cytoplasm is extruded thus bringing adjacent cytoplasmic and adjacent extracellular membrane surfaces into apposition resulting in the formation of mature compact myelin sheath (Figures 1 and 2). However, Schwann cell -cytoplasm filled regions do persist in the periaxonal and adaxonal rim of the mature sheath, within the paranodal loops and in channels called Schmidt-Lanterman incisures (Figure 3) (Bunge et al., 1989(a)). The effect is imperfect myelin compaction due to the prevention of adjacent cytoplasmic membranes from fusing. The functional significance of the Schmidt-Lanterman incisures is not clear. It is known that they provide a pathway for protoplasmic connections between the inner and outer compartments of the Schwann cell and so they may serve as a route by which delivery of metabolic material to the distal regions of the sheath is accomplished (Thomas et al., 1984).

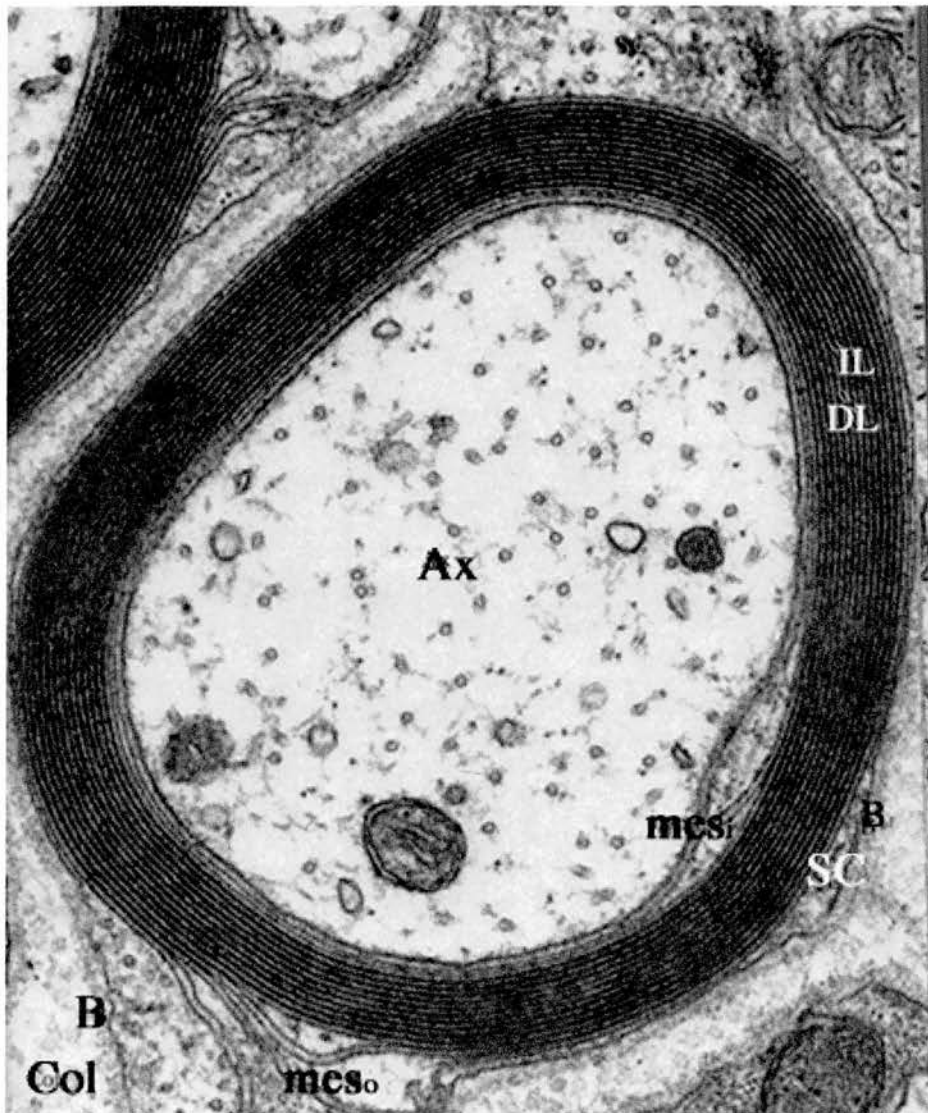


FIGURE 1. Adult rat sciatic nerve myelinated axon. The transversely sectioned axon (Ax), is surrounded by a myelin sheath formed from the spiraled Schwann cell (SC) membrane. The intraperiod (IL) and major dense lines (DL) of the sheath can be distinguished. The spiral of the lamellae starts at the internal mesaxon (mesi) on the inside of the sheath and ends at the outer mesaxon (meso) on the outside of the sheath. Outside the Schwann cell is a basal lamina (B) which is in contact with collagen fibres (Col). X100,000 (After Peters et al.,1970).

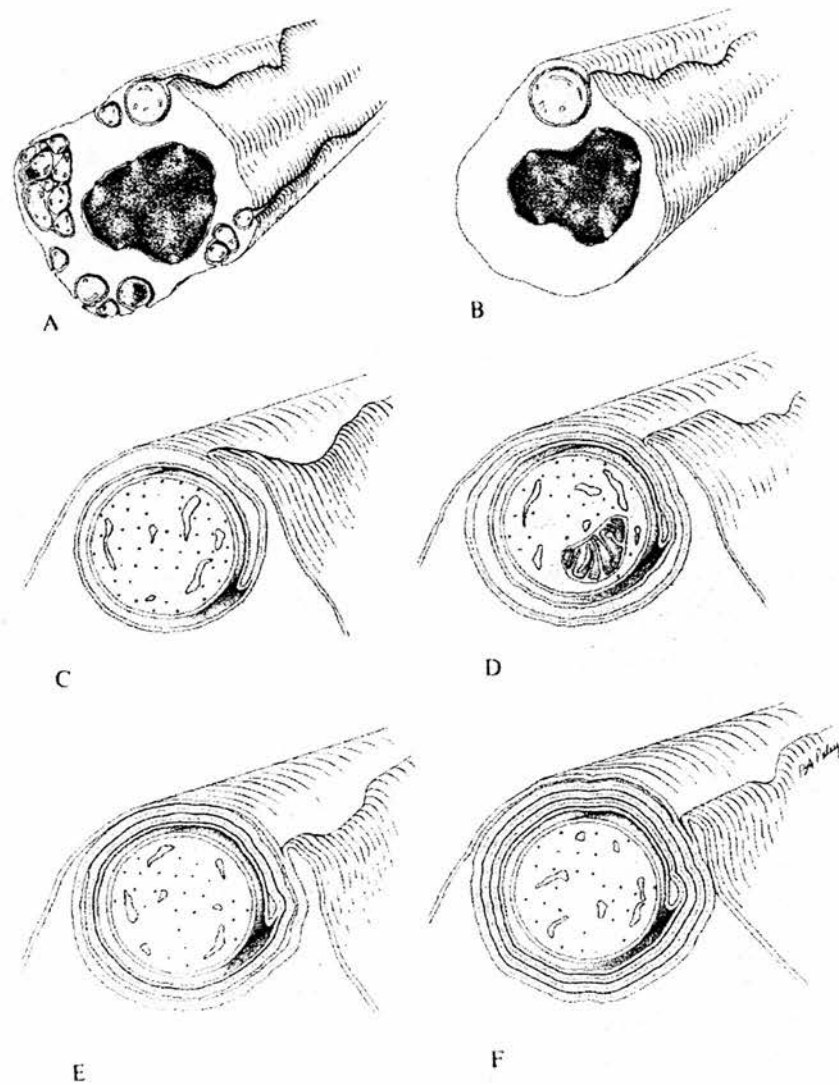


FIGURE 2. Peripheral myelin sheath formation. (A) Early in development a Schwann cell contains both bundles of small and individual larger axons. (B) Following an increase in Schwann cell numbers due to mitosis, each Schwann cell associates with a single axon. (C) The internal mesaxon is formed by the apposition of the enveloping processes. (D) The lips of the enveloping process extend to elongate the mesaxon and the intraperiod lines begin to form. (E) The major dense line results from the loss of the cytoplasm from the spiraling process. (F) Compaction of the sheath follows an increase in the number of turns of the spiral. (After Peters et al.,1970)

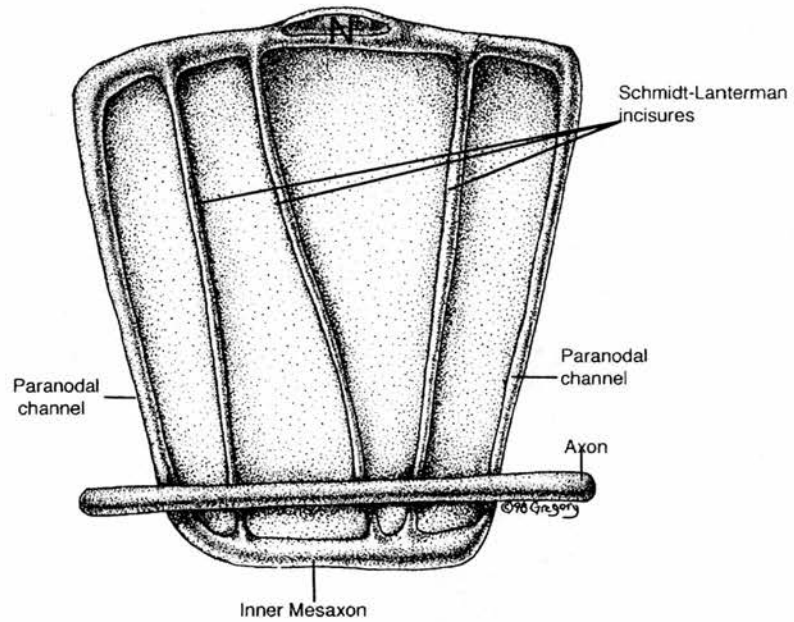


FIGURE 3. Schematic diagram of an “unrolled” Schwann cell. The myelin sheath of a myelinated nerve fibre has been "unrolled" to reveal the presence of cytoplasmic channels, referred to as Schmidt-Lanterman incisures, which traverse the compact myelin (N: Schwann cell nucleus) (Adapted from Zigmond et al., 1999).

Myelin sheaths are interrupted at regular intervals giving rise to a segmental appearance. These interruptions are the nodes of Ranvier (Ranvier, 1878), regions of bare axonal membrane exposed to the extracellular fluid, that exhibit electrical activity (Figure 4). The concentration of axonal sodium channels in these sites, and the accumulation of potassium channels in the juxtaparanodal and internodal regions, constitutes the basis of saltatory conduction of nerve impulses leading to a substantial increase in the velocity of conduction (Figure 4, lower panel)(Bunge and Fernandez-Valle, 1995). Segments of myelin between adjacent nodes are termed internodes. They appear as a result of a single myelin-forming Schwann cell establishing a 1:1 relationship with an individual axon. In mammalian fibres the internodal segments range in length from 200-250 μm to 1500 μm exhibiting a direct relationship between their length and the diameter of the axon. The larger the fibres, the longer the internodes they display (Young, 1942) (Thomas, 1955). The origin of the relationship between internodal length and axon diameter has been attributed to the stage of development at which myelin sheaths are acquired. Axons destined to have larger final diameters in the adult are myelinated first so they have longer internodes than smaller axons. The earlier onset of myelination in larger fibres is believed to fix the total number of Schwann cells along the length of the axon by inhibiting further cell division. Any subsequent increase in the length of the axon following the initial deposition of myelin segments involves only an increase in the length of existing internodes and not the addition of new ones (Thomas et al., 1984).

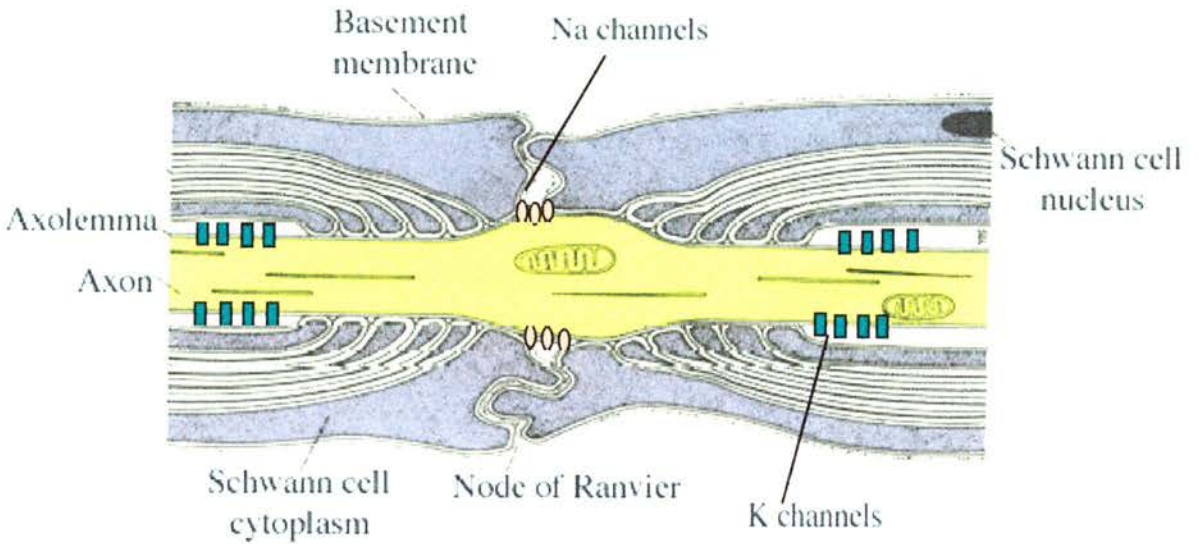
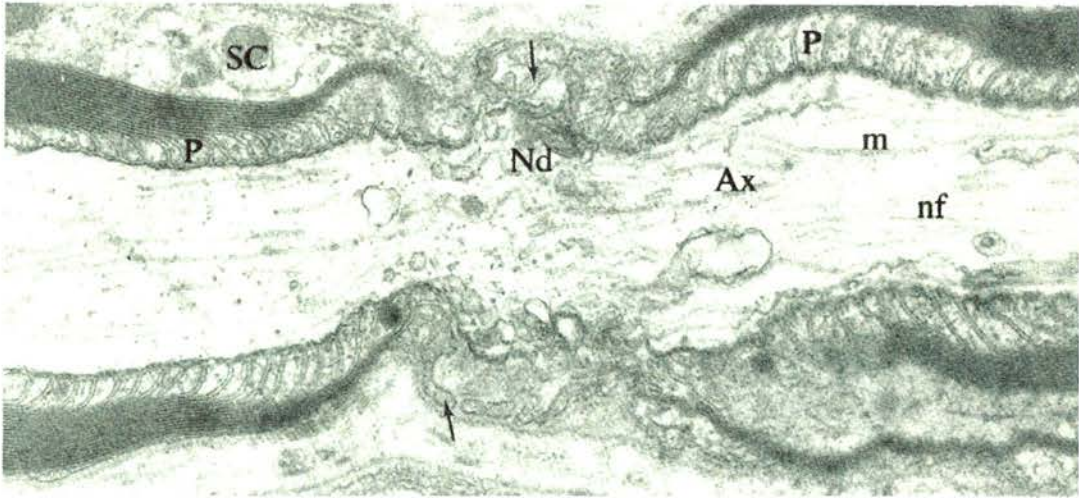


FIGURE 4. The Node of Ranvier in the peripheral nervous system. Longitudinal section of the nodal region of a myelinated axon of an adult rat sciatic nerve. **(upper panel)** The nodal region (Nd) of the axon (Ax) is flanked by pockets of paranodal cytoplasm (P) and it is covered by processes (arrows) from the Schwann cell (SC). The microtubules (m) and neurofilaments (nf) of the axon can be seen as well as the arrangement of the endoneurial collagen fibres (Col) X 110,000 (After Peters et al., 1970). **(lower panel)** Schematic diagram of the same node. Na channels are clustered in the nodal area, whereas K channels accumulate at the juxtapanodal region. This distribution allows saltatory conduction of action potentials to occur (Adapted from Snell, 1997).

The thickness of the myelin sheath has also been observed to be related to the thickness of the axon. Larger diameter axons possess thicker sheaths of myelin (Friede and Miyagishi, 1972). Although early in peripheral nerve myelination there is little correlation between these two parameters, a ratio is established later, during myelin sheath growth, that becomes relatively constant over a wide range of fibre diameters (Fraher, 1976) (Webster et al., 1987).

The myelin spiral terminates on the outside of the sheath at the external mesaxon and on the inside of the sheath at the internal mesaxon. In mature compact myelin, intraperiod lines are observed under the electron microscope where two areas of Schwann cell plasma membrane appose each other at the extracellular surfaces of the mesaxons, thus closing the 12-14 nm gap to 2.0-2.5 nm. These lines alternate with major dense lines which are produced by the fusion of the cytoplasmic or inner faces of the same pair of plasma membranes (Peters et al., 1970). The number of the major dense lines (and intraperiod lines) present in a myelin sheath corresponds to the number of times that a Schwann cell has encircled the axon. The fact that large diameter axons possess thicker myelin segments and thus a greater number of membrane turns has been performed, implies that axons may regulate the action of Schwann cells and influence the process of myelination (Bunge et al., 1986).

1.2.1.2 The structure and chemical composition of PNS myelin

The majority of the original observations concerning the composition of myelin were carried out on material obtained from white matter of the central nervous system due to the ease of its extraction without the presence of contaminating fractions. It was found that CNS myelin possessed a number of features that

distinguished it from other cellular membranes, such as a higher lipid to protein ratio, a large proportion of cholesterol and galactosphingolipid, the presence of relatively saturated long chain fatty acids and an apparently relatively simple protein composition (Thomas et al., 1984).

Subsequent studies of PNS myelin revealed differences in its constitution compared to the CNS myelin despite their apparent similarity in structure and function. It was discovered that the two types of myelin differ both in protein and lipid composition. PNS myelin contains a much larger proportion of sphingomyelin and is much richer in glycoprotein.

The major proteins of myelin were initially thought to be structural in nature but subsequent studies revealed additional roles for these proteins. The fact that they tend to be strongly conserved among the higher vertebrates implies their potential involvement in the formation and maintenance of the myelin sheath. Most of these proteins are known to exist as isoforms derived from alternative splicing (Braun, 1977) (Figure 5).

The major integral membrane protein of peripheral nerve myelin is the **P0 protein**, a member of the immunoglobulin superfamily, characterised as such due to the presence of an Ig-like domain. P0 accounts for over 50% of the total protein in compact myelin. It is a glycoprotein with a molecular mass of 28 kDa. It is thought to interact homotypically on apposed Schwann cell extracellular membrane surfaces at the intraperiod line, thus playing an important role in myelin compaction (D'Urso et al., 1990) (Filbin et al., 1990). It may also support the stabilisation of the major dense line via interactions of its highly charged intracellular portions with the phospholipid head-group of apposed membranes.

A group of small (12-22 kDa) peripheral membrane proteins localised in the major dense line, are the **myelin basic proteins (MBPs)**. They are involved in the process of the apposition of the cytoplasmic membrane regions that gives rise to the major dense line and they constitute 5-15% of the protein content (Lees and Brostoff, 1984). Their absence from shiverer mice indicates their importance in the formation of compact myelin. Shiverer mice are homozygous for a recessive mutation which results from deletion of five of the six exons of the MBP gene (Molineaux et al., 1986) (Montague et al., 1999). The animals display deficient and abnormal myelination. They experience tremors and convulsions and tend to have a short life span. The number of Schmidt-Lanterman incisures in shiverer mutants has been found to be more than double compared to that of normal PNS myelin sheaths, which suggests that MBPs may play a critical role in the process of compaction of the sheath (Gould et al., 1995).

Peripheral myelin protein 22 (PMP22) is a 22 kDa protein that contributes a further 2-5% of PNS myelin protein. Although its deduced amino acid sequence predicts a protein of 17 kDa, the presence of a single N-linked glycosylation site results in the increased Mr value of 22 kDa by SDS-PAGE. PMP22 is membrane-associated, with a rather complex structure comprising four transmembrane domains, two extracellular loops, one intracellular loop and two short intracellular tails which represent the N- and C- termini respectively. It is a very hydrophobic protein localised to compact myelin (Thomas et al., 1984). Its expression is dependent upon axonal contact and is affected by intracellular levels of cAMP. Elevation in intracellular cAMP levels leads to upregulation of *Pmp* gene expression in cultured Schwann cells (Spreyer et al., 1991) (Pareek et al., 1993).

Point mutations in the *Pmp* gene and gene dosage, as supported by transgenic mouse models result in peripheral neuropathies such as Charcot-Marie-Tooth type 1A (CMT1A), Dejerine-Sottas syndrome (DSS) and hereditary neuropathy with liability to pressure palsy (HNPP) (Lupski et al., 1991) (Roa et al., 1993) (Chance et al., 1993). The effects of these mutations have suggested that PMP22 plays a vital role in myelin formation and may also be involved in the regulation of the thickness and the maintenance of the myelin sheath (Lupski, 1999; Maef and Suter, 1999).

One of the minor but potentially important myelin proteins involved in the early events of myelination is **myelin-associated glycoprotein (MAG)** which exists in two isoforms of 67 and 72 kDa termed, respectively, S-MAG and L-MAG. MAG is present in both the CNS and PNS constituting about 0.1% of the total protein. In the PNS it is specifically localised to the periaxonal membranes, Schmidt-Lanterman incisures, paranodal loops and the outer mesaxon, but it is not present in compact myelin (Sternberger et al., 1979) (Trapp and Quarles, 1982). Immunocytochemical and biochemical approaches in Schwann cell–neuron co-cultures have revealed that MAG expression precedes the development of the myelin sheath and its removal from the Schwann cell membrane is necessary to allow myelin compaction, mediated by P0, to occur (Owens and Bunge, 1989). However, mice that lacked a functional MAG gene (*Mag* null) generated by homologous recombination, were able to form myelin in both the CNS and PNS displaying phenotypes with no significant abnormalities in young animals (Li et al., 1994) (Montag et al., 1994). At later stages of development, however, (8 months of age) animals appeared to exhibit a phenotype with axon and myelin degeneration in

30% of peripheral nerve fibres (Fruttiger et al., 1995). These observations lead to the assumption that MAG expression is not necessary in the initial stages of axonal ensheathment and spiralisation but is involved in the maintenance of the myelin sheath. The two major functions ascribed to MAG include maintenance of the structural integrity of periaxonal regions of the myelin sheath and mediation of intercellular interactions (Martini and Schachner, 1986) (Trapp et al., 1984b). MAG is also thought to be responsible for the formation and stabilisation of the 12-14 nm Schwann cell-cytoplasmic periaxonal collar (Trapp et al., 1984a).

Proteolipid protein (PLP) is the principal integral membrane protein of CNS myelin (50% of total protein) but contributes less than 1% to the PNS myelin protein content. Alternative splicing of the *Plp* gene gives rise to two isoforms; a 30 kDa isoform commonly referred to as PLP and a smaller isoform, DM-20, with a molecular mass of 26 kDa. DM-20 predominates in the PNS and is found in the cytoplasmic regions of the internode, the satellite cells of cranial, spinal and autonomic ganglia as well as ensheathing cells of the olfactory bulb (Campagnoni et al., 1992). Unlike DM-20, the larger PLP isoform is localised to the perinuclear regions of myelin-forming Schwann cells. Neither isoform has been observed to be present in compact myelin.

Protein P2, whose concentration appears to be highly variable among species (1% total myelin protein in rodents, 14% in humans), is a 15 kDa protein located in the major dense line. It is believed to play a significant role in fatty acid elongation or transport during myelination, as it is closely related to lipid-binding proteins (Narayanan et al., 1988).

More than 40 enzymes have been identified in CNS myelin including a **2',3'-cyclic-nucleotide phosphodiesterase (CNPase)**. It has been reported that the lipid and protein components of myelin have measurable turnover rates even during the period that follows active myelination (Benjamins and Smith, 1977). More recent studies have revealed that myelin membranes possess receptor and signal transduction activities in addition to related enzyme activities. The former category includes high-affinity muscarinic cholinergic receptors and G-proteins while the latter involves adenylate cyclase, phospholipases as well as enzymes that participate in phosphoinositide metabolism (Bernier et al., 1989) (Boulias and Moscarello, 1989) (Braun et al., 1990) (Golly et al., 1990). A further protein associated with uncompact myelin is **connexin-32 (Cx32)**. This is a gap junction protein whose structure resembles that of PMP22 featuring four transmembrane domains and intracellular carboxy and amino-termini (Peters et al., 1970). Although it appears to play an important part within myelinating Schwann cells, as its absence results in peripheral demyelinating neuropathy (CMT1X), further studies are required to establish its exact function in myelinating glia.

The adhesive glycoprotein **E-cadherin** has also been detected at the paranodal loops, inner and outer mesaxons and in Schmidt-Lanterman incisures (Bunge et al., 1989(b)) (Fannon et al., 1995) (Hall and Williams, 1970). It is a member of a superfamily of calcium-dependent proteins, present in adherens-type junctions, that are involved in tissue differentiation and structure. Their roles include cell recognition and segregation, morphogenic regulation and tumour suppression (Magee and Buxton, 1991) (Grunwald, 1993). E-cadherin has been reported to be absent in the Schwann cell-axon interface or between two Schwann cells. Instead,

it has been observed to mediate homophilic (autotypic) interactions between plasma membranes synthesised by a single Schwann cell (Fannon et al., 1995). Although it is not directly involved in the process of myelination, it has been shown to be necessary for the stabilisation of the structure of individual Schwann cells (Fannon et al., 1995).

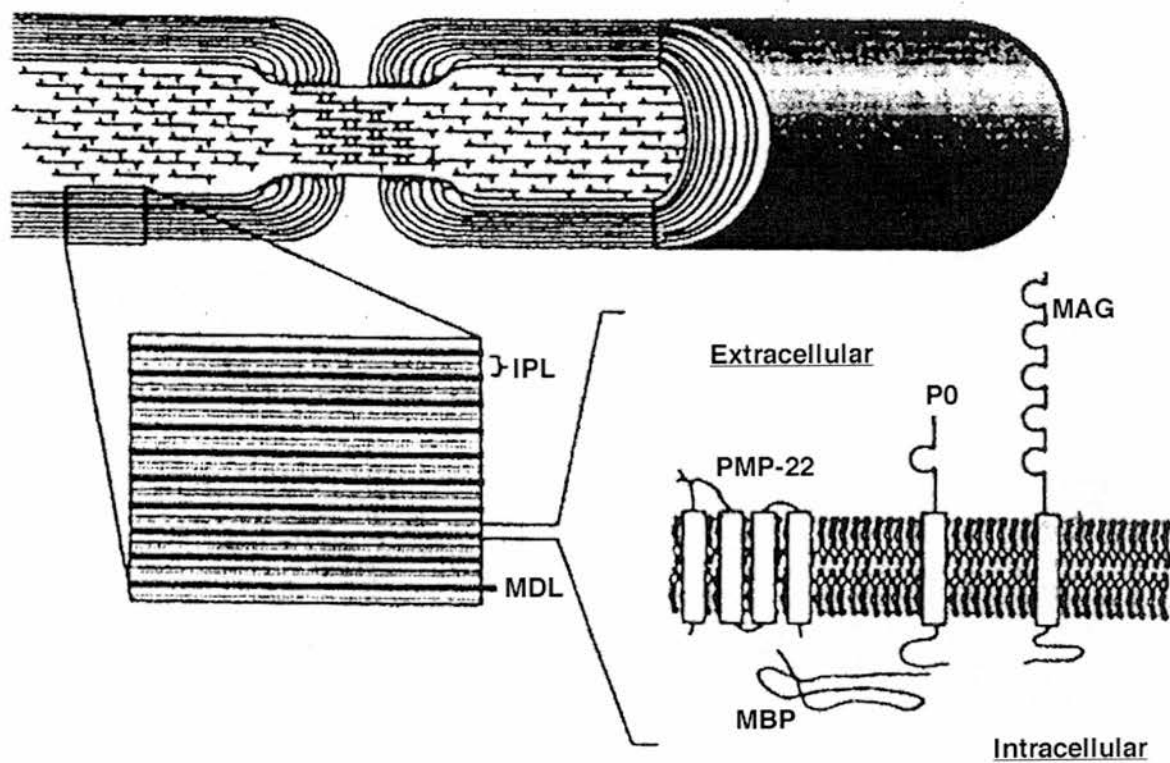


FIGURE 5. Ultrastructural and molecular properties of myelin. A cutaway view of the nodal region of a myelinated sheath shows the higher density of the axoplasmic neurofilaments at the node of Ranvier and displays the alternating layers of intraperiod (IPL) and major dense lines (MDL). The major dense line contains specific myelin proteins: MAG, myelin-associated glycoprotein; MBP, myelin basic protein; P0, protein zero, PMP-22, peripheral myelin protein 22 (After Shepherd, 1994).

1.3 ROLE OF THE SCHWANN CELL IN PERIPHERAL MYELINATION

Schwann cells associate with axons in the peripheral nervous system. They ensheath all peripheral nerve fibres, thus forming an interface between the neural tissue and the surrounding connective tissues. This arrangement provides a partial intervening basal lamina and ensures that the peripheral nerve contains considerable amounts of connective tissue that confer considerable mechanical strength. They exist in two types: myelin-forming Schwann cells that elaborate a myelin sheath around axons, and non-myelin-forming cells, which associate with smaller axons.

1.3.1 Embryological development of the Schwann cell

Both myelinating and ensheathing Schwann cell types arise from a common precursor. They are derived from the neural crest, a longitudinal cluster of ectodermal cells located near the dorsal edge of the embryonic neural tube (Jessen and Mirsky, 1992) and they appear at a very early stage during the development of peripheral nerve accompanying outgrowing bundles of axons.

The Schwann cell lineage involves the formation of two intermediates: the Schwann cell precursor, detected in rat at embryonic day 14 and 15 (E14 and E15) and in mouse at E12 and E13, and the immature Schwann cell found from E17 in rat (mouse E15). Differentiation of the immature cell type starts just after birth, with mature myelin-forming cells appearing before the non-myelinating type (Figure 6) (Jessen and Mirsky, 1999).

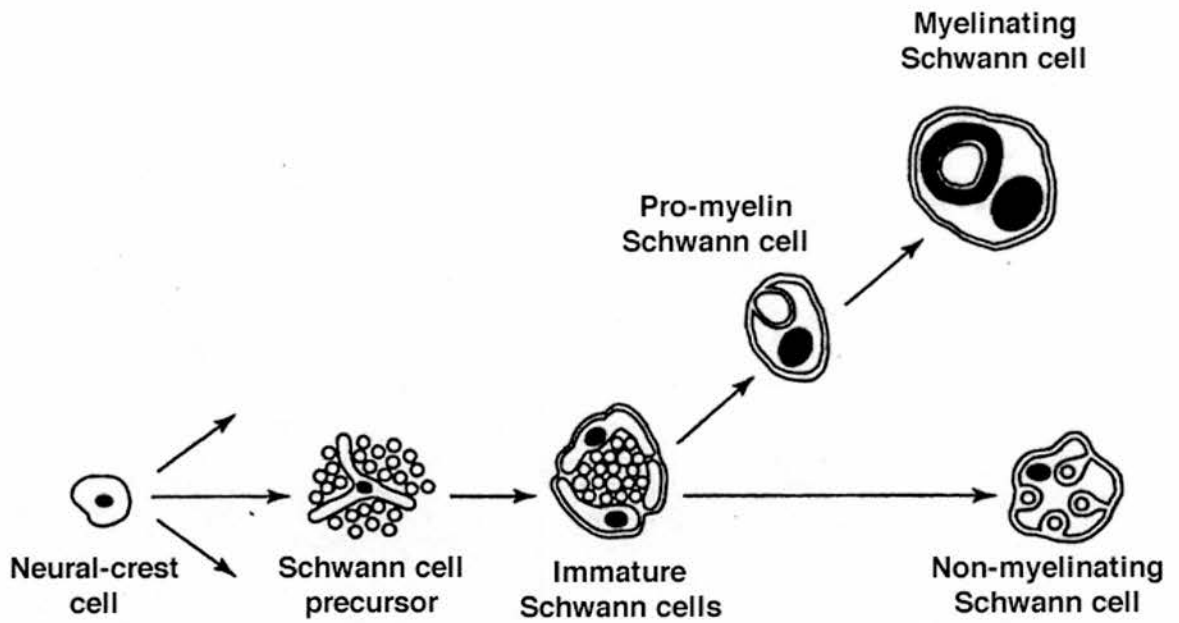


FIGURE 6. The Schwann cell lineage. Early migrating neural crest cells give rise to Schwann cell precursors, which subsequently form immature Schwann cells. These are able to differentiate into either myelin-forming or non-myelinating mature Schwann cells (After Jessen, 1999).

1.3.2 Determination of the Schwann cell phenotype

Signalling from axons is thought to be responsible for the differentiation of the neural crest cells to Schwann cell precursors, and those precursor cells to the myelin-forming and non-myelin forming phenotypes. One view supports the “lineage neutrality” of neural crest cells, according to which axonal contact is required to trigger their ability to support glial or neuronal differentiation (Mirsky and Jessen, 1996). Neuregulins represent alternatively spliced products of the same gene that are important candidates as Schwann cell lineage regulators. β -neuregulin has been considered as an axonal signal required for precursor survival. It is also believed to function as mitogen and survival factor for perinatal Schwann cells.

An alternative hypothesis supports the idea that crest cells have entered the glial lineage prior to their association with axons. This is based on the observation that migrating crest cells express P0, which is considered as a Schwann cell-specific protein, indicating that crest cells may be able to select the glial pathway very early in development (Mirsky and Jessen, 1996).

Myelin-forming Schwann cells express MAG, P0, MBP and PMP22 whereas ensheathing cells synthesise, instead, glial fibrillary acidic protein (GFAP), neural cell adhesion molecule (N-CAM), nerve growth factor receptor (NGFR), growth associated protein 43 (GAP-43) and L1, an immunoglobulin-related adhesion protein. Both subtypes express lipids including galactocerebroside (Martini and Schachner, 1986) (Mirsky et al., 1986) (Jessen and Mirsky, 1991).

1.3.3 Factors involved in Schwann cell proliferation and differentiation

Schwann cells potentially proliferate at least twice during their life-time: early in development in order to increase in number and ensheath the rapidly growing nerve fibre and subsequently after nerve injury. Schwann cell proliferation is influenced by a number of factors. These include axonal mitogens, components of the extracellular matrix (eg. fibronectin), soluble factors such as cAMP and agents that increase intracellular cAMP levels, glial growth factor as well as myelin itself. It has been suggested that a mitogen is released from myelin via lysosomal processing which follows the ingestion of myelin released during wallerian degeneration. Myelin that lacked MBPs was observed to be devoid of mitogenic activity (Baichwal and De Vries, 1991).

A number of transcription factors are believed to be involved in the differentiation of Schwann cells. The POU-domain factors Oct-6 (also known as Tst-1 and SCIP) and Egr-2 (Krox-20) are expressed in Schwann cells and play important roles in the development of the myelin-forming lineage. Inactivation of either Oct-6 or Egr-2 in mice, has been found to block the development of the Schwann cell at a pro-myelinating stage. Schwann cells that associate with large diameter axons, are able to envelop but not perform the spiralisation process, thus failing to generate myelin. This block in myelination observed in Oct-6 knock out mice is temporary, which implies a role of additional POU-containing transcription factors in Schwann cells that are able to replace the function of Oct-6 (Jessen and Mirsky, 1999).

The zinc-finger protein Egr-1 (Krox-24) and SOX-10, a member of the SRY-like HMG (high mobility group) domain class, are also considered as transcription

factors with a role in Schwann cell development. Egr-1 is expressed only by immature and non-myelin forming Schwann cells. Another transcription factor, Pax-3, may have a role in controlling gene expression in non-myelin forming Schwann cells, since it is able to activate GFAP, N-CAM, L1 and NGFR promoters. The leucine zipper transcription factor c-Jun is expressed by Schwann cells and its levels appear to rise, following disruption of axonal contact. In combination with SV40 T antigen, it represses P0 expression (Bharucha et al., 1994).

1.3.4 Axon-Schwann cell interactions determine the length of the myelin segment and induce the formation of a basal lamina

Interaction of axons with Schwann cells influences axonal diameter and also determines the length of the myelin internode. Experiments performed in tissue culture have demonstrated an increase in axon diameters in areas of the culture that contain Schwann cell ensheathment as opposed to adjacent areas in the same culture where axons are not ensheathed (Windebank et al., 1985).

The function of Schwann cells is largely dependent upon the formation of a basal lamina which is induced by axonal contact. When Schwann cell basal lamina assembly is prevented, the Schwann cells are unable to ensheath or myelinate axons (Bunge et al., 1982). Although the precise reason for this observation is unknown, it is believed that the presence of a basal lamina permits polarisation of the Schwann cell plasmalemma in a way that the abaxonal and adaxonal surfaces are restricted to contact with components of the extracellular matrix and the axon respectively. This polarisation, in conjunction with potential signaling to the cytoskeleton, is associated with cell shape changes that accompany ensheathment (Bunge et al., 1982). Neurons affect the production of a basal lamina through a

number of signals that regulate different stages in the synthesis, secretion and assembly of basal lamina constituents (laminin, type IV collagen and heparan sulfate proteoglycan) (Bunge et al., 1986) (Clark and Bunge, 1989).

1.3.5 Schwann cells and their precursors control neuronal survival and development

Trophic support from Schwann cells and their precursors is believed to be necessary for the survival of neurons. Loss of dorsal root ganglia (DRG) as well as sensory and motor neurons in *ErbB* knockout mice, that lack Schwann cell precursors and mature Schwann cells, was observed during the second half of embryonic development (Riethmacher et al., 1997). The number of DRG and motor neurons in these animals displayed an 80% reduction by E14 and E18, respectively. The absence of *ERBB3* protein in neurons themselves was not responsible for their depletion, as suggested by data obtained from chimeric mice. It has been proposed that DRG survival depends, initially, on glial-derived signals from Schwann cell precursors, and subsequently, once the axons have established contact with their targets, on signals originating from those targets. In the case of motor neurons, where cell death was observed after the neurons had reached their targets, it is possible that glial-derived and target-derived signals act simultaneously and not sequentially, as in DRG. It is also believed that the glial signal responsible for motor neuron survival is derived from immature Schwann cells (Jessen and Mirsky, 1999).

A single or a number of neuronal survival factors acting synergistically, may be required. Glial cell-line derived neurotrophic factor (GDNF), found in Schwann cell precursors and immature Schwann cells in embryonic nerves, is considered a good candidate for neuronal survival factor. Mice that lack GDNF lose

approximately 20% of their motor neurons by birth (Moore et al., 1996). Neurotrophin 3 (NT3) is thought to act as a trophic signal derived from Schwann cell precursors. It is expressed by Schwann cells at birth and by tissues associated with ganglia in the embryo. Experimental evidence suggests that NT3 acts to support DRG neurons before target innervation but there is no proof that the survival of early DRG neurons depends upon an NT3-containing signal from Schwann cell precursors (Jessen and Mirsky, 1999).

Myelinating Schwann cell-derived signals have been implicated in the regulation of axonal structure and function. The formation of the three types of nerve sheath that serve as protection barriers for axons, namely the epineurium, perineurium and endoneurium, is induced by Desert Hedgehog, a signalling molecule secreted by Schwann cells (Parmantier et al., 1999).

1.3.6 Schwann cells regulate their own survival via an autocrine mechanism

Following injury, Schwann cells distal to the site of assault are deprived of axonal contact but must survive in order to guide axonal re-growth and ensure nerve regeneration by providing the necessary trophic factors. Schwann cell survival in the absence of axons is accomplished by an autocrine loop which operates in mature Schwann cells but not their precursors. This autocrine system is likely to include a number of growth factors such as insulin-like growth factor 2 (IGF2), platelet-derived growth factor BB (PDGF-BB) and NT3 (Meier et al., 1999). It is not mitogenic for Schwann cells and unable to sustain precursor survival. Further experiments for the characterisation of this autocrine survival signal would be required.

1.4 PERIAXIN: A PROTEIN EXPRESSED BY MYELIN- FORMING SCHWANN CELLS

Axonal contact triggers Schwann cell differentiation but the morphological changes that take place to allow ensheathment and myelination to occur are probably regulated by the cell cytoskeleton and the proteins associated with it. In an attempt to identify Schwann cell cytoskeletal and cytoskeleton-associated proteins with expression and localisation patterns regulated developmentally during differentiation and myelination, periaxin was isolated and was subsequently detected in early post-natal nerve at the periaxonal membranes of myelin-forming Schwann cells (Gillespie et al., 1994).

After completion of the spiralisation process as the myelin sheath begins to mature the localisation of periaxin shifted to the abaxonal membranes (Figure 7). This implied involvement of the protein in the stabilisation of the mature sheath possibly by participating in membrane-protein interactions. Within the Schwann cell it was found in the periaxonal membranes, paranodal loops and the Schmidt-Lanterman incisures but it was absent from compact myelin (Gillespie et al., 1994). Expression of periaxin appeared to be under the control of axon-Schwann cell interactions, preceding that of the major myelin proteins P0, MBP and possibly even MAG (Salzer et al., 1980(b)) (Scherer et al., 1995).

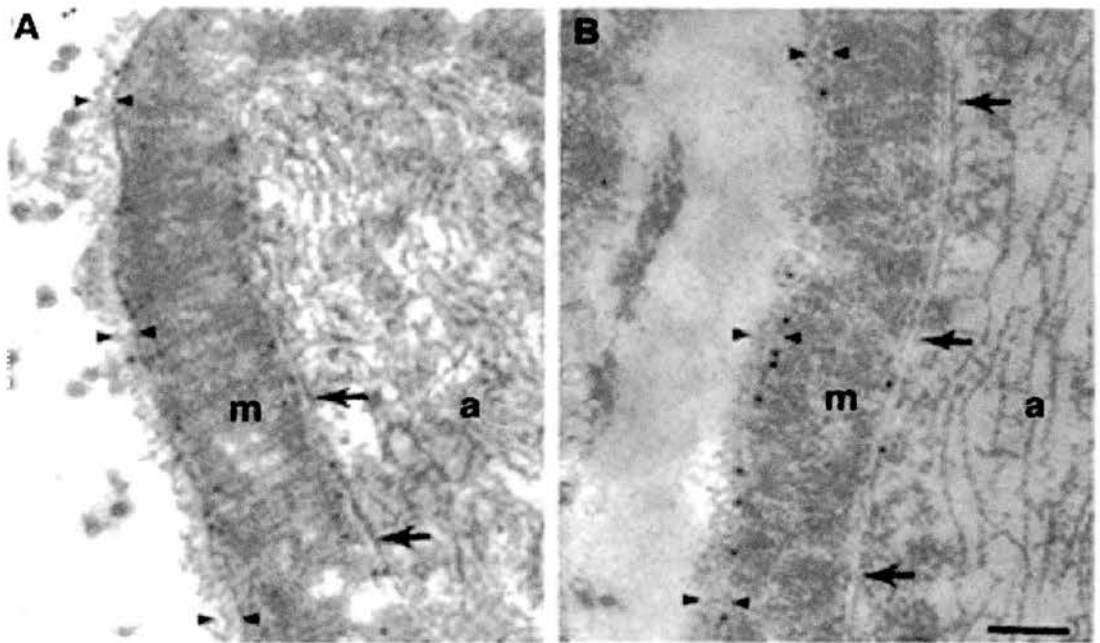


FIGURE 7. Periaxin localisation shifts to the abaxonal membranes as the myelin sheath begins to mature. (A) Longitudinal section of P3 sciatic nerve (initial stages of myelination). Immunoelectron microscopy reveals that the protein (gold particles) is abundantly detected in both the adaxonal and abaxonal membranes of the myelin sheath. (B) However, by P28 in a rat trigeminal nerve section, the protein appears to have shifted to the abaxonal membranes. Arrows indicate the axolemma at the interface of the axon (a) and the compact myelin sheath (m) which is surrounded by a basal lamina (between arrowheads) (After Scherer et al.,1995).

1.4.1 Periaxin isoforms and the structure of the periaxin gene

The structure of the murine periaxin gene is shown in Figure 8. It is composed of 7 exons interrupted by 6 introns and spans 20.6 kb. Two isoforms of periaxin (L-periaxin 147 kDa and S-periaxin 16 kDa) have been identified, encoded by 4.6 and 5.2 kb mRNAs respectively. The smaller isoform arises by a relatively rare alternative splicing event which involves the retention of intron 6. A large fusion exon is generated, which comprises exon 6, intron 6 and exon 7. This introduces an in-frame stop codon that encodes a 21 amino acid C-terminus unique to S-periaxin. Intron retention is dependent upon the presence of suboptimal splice sites at the 5' and 3' ends of the intron. These sequences differ from the consensus sequences that promote splicing and require enhancer elements in the downstream exon, termed exonic splice enhancers (ESEs), for splicing to occur (Dytrych, 1997).

1.4.2 Primary structure and developmental regulation of periaxin

L- and S- periaxin contain a single PDZ (PSD95/discs large/zona occludens) domain which is typically present in proteins that interact with the cytoplasmic tail of plasma membrane proteins and with the cortical cytoskeleton. This suggests that the L-isoform which is localised to the periaxonal membranes might be implicated in signal transduction pathways whereas the cytoplasmic distribution of the S-isoform implies the existence of other factors that affect PDZ-protein binding. L-periaxin, furthermore, contains a basic region near its N-terminus (amino acids 118-196), a region of a series of repeats (432-725 aa) and a highly acidic domain towards its C-terminus (1036-1163 aa). The domain structure of L- and S-periaxin is shown in Figure 9.

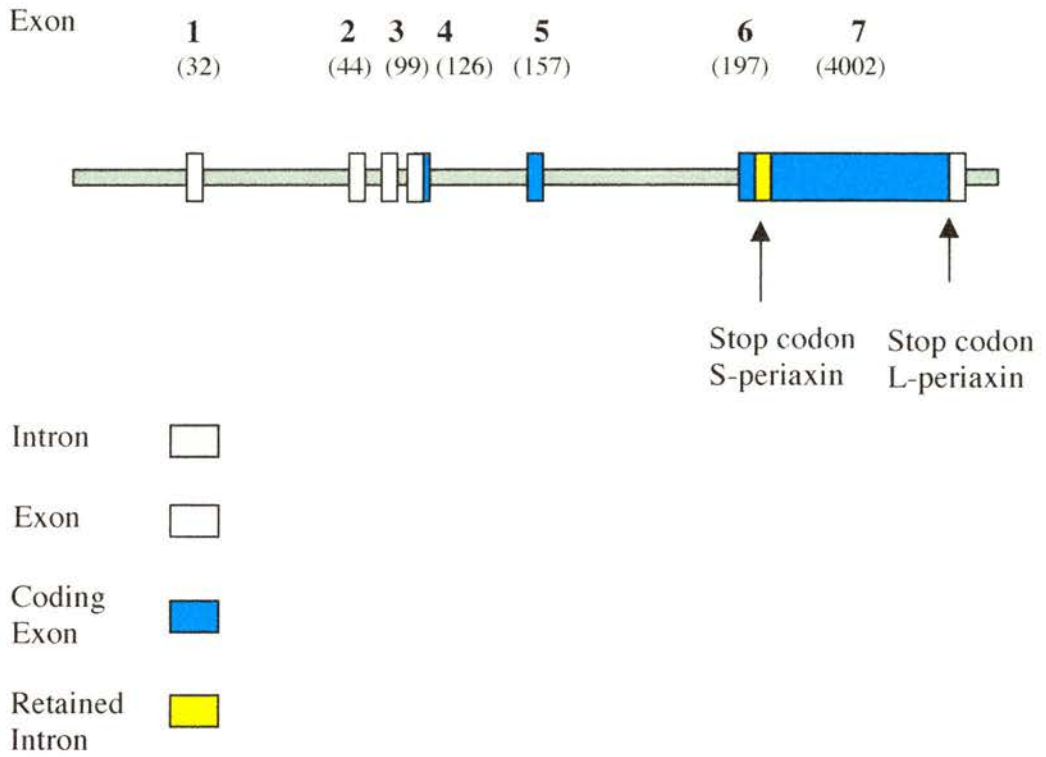


FIGURE 8. The structure of the murine periaxin gene. The murine periaxin gene comprises 7 exons (shown as solid vertical lines). Coding exons (**4,5, 6** and **7**) are indicated by light blue. Intron 6, retained in S-periaxin is indicated by yellow. Arrows point to the position of Stop codons for each isoform. Exon sizes (in kb) are shown in brackets.

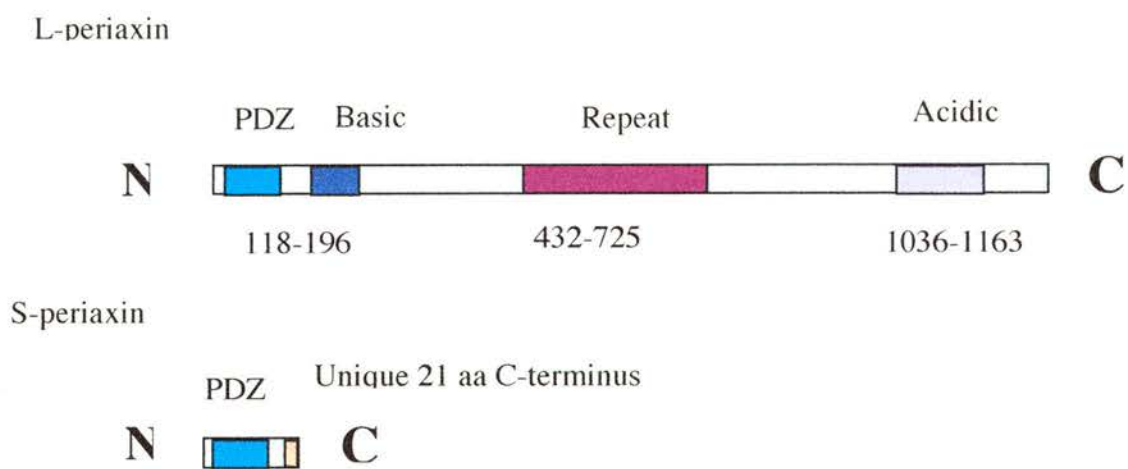


FIGURE 9. Domain structure of L- and S-periaxin. (Amino acid residues shown).

The basic domain is responsible for nuclear targeting of the protein which has been observed both *in vivo* and *in vitro* in embryonic Schwann cells. The nuclear localisation signal (NLS) of L-periaxin is tripartite (Sherman and Brophy, 2000). Nuclear expression is developmentally regulated and ceases after E17.5. The repeat region consists of a pentameric core (aliphatic non-polar: proline: glutamic acid or aspartic acid: aliphatic non-polar: variable; either alanine or glutamine), which is interrupted by a tripeptide spacer (leucine: proline: lysine). The function of this region is unclear (Sherman, 1998). It appears to be less flexible than the rest of the polypeptide and it has been suggested to act as a spacer that keeps the potentially functional basic and acidic domains separated (Gillespie et al., 1994). Acidic domains have been widely implicated in protein-protein interactions (Kobe and Deisenhofer, 1995a). Analysis of the primary structure by hydrophobicity plots has indicated the absence of any transmembrane domains which suggests that periaxin is not an integral membrane protein. Despite the presence of a single potential N-glycosylation site, the protein was not found to be glycosylated (Gillespie et al., 1994).

Multiple potential phosphorylation sites are also present whose role is currently being investigated. It appears to display a rather linear conformation, with very little secondary structure, which might point to a role in coupling cortical proteins to the cytoskeleton.

1.4.3 L-periaxin participates in a dystroglycan transmembrane complex

Dystroglycan associates with dystrophin (or its homologue utrophin), sarcoglycans, sarcospan, syntrophins and dystrobrevin to form the dystrophin glycoprotein complex (DGC) (Winder, 2001). In both skeletal muscle and the PNS,

the DGC links extracellular matrix molecules to the cytoskeleton. Dystrophin-related protein 2 (DRP2) is a member of the dystrophin family. It comprises two spectrin-like repeats, closer to the N-terminus, followed by a WW domain, two EF hands, a ZZ domain and two coiled-coil regions proximal to the C-terminus. The two spectrin-like repeats of DRP2 interact with the three basic subdomains of L-periaxin, BD1 (aa 116-145), BD2 (aa 146-176) and BD3 (aa 176-196) which have been characterised as components of the tripartite NLS of the protein (Sherman et al., 2001). DRP2 was also found to associate with β -Dystroglycan and hence localise to the Schwann cell plasma membrane. A complex that contains L-periaxin, DRP-2, α - and β - dystroglycan, utrophin and the truncated form of dystrophin, Dp116, was isolated from peripheral nerve lysates by immunoaffinity chromatography (Sherman et al., 2001). L-periaxin does not bind directly to Dp116 and utrophin, which is indicative of their participation in a distinct DGC. Association of L-periaxin with DRP2 is essential for the stability of the DRP2 complex (Figure 10). Homodimerisation of L-periaxin via its PDZ domain and interaction with DRP2 through the basic region, clusters the complex to the cortical cytoskeleton and stabilises the DRP2 complex. In the absence of L-periaxin, in Prx null mice, the majority of the DRP2 is lost and the remaining is not detectable in clusters but diffuse in the cytoplasm. The dependency of the correct localisation of DRP2 on L-periaxin suggests a role of the latter as a scaffold for the assembly of the complex. β -Dystroglycan, utrophin and Dp116 expression and localisation are independent of L-periaxin. Prx knockout mice seem to be able to form a myelin sheath, which is however unstable, leading to the development of a late-onset demyelinating neuropathy (Gillespie et al., 2000). Because myelin instability in Prx

null mice is observed following initial formation of the sheath, it is suggested that the L-periaxin-DRP2 complex is implicated in the regulation of terminal stages of the myelination process. L-periaxin translocates from the adaxonal to the abaxonal membrane of the Schwann cell at a later stage of myelination when the sheath begins to mature, at a position where it could associate with the cortical DRP2 complex and consequently influence the maturation of the sheath.

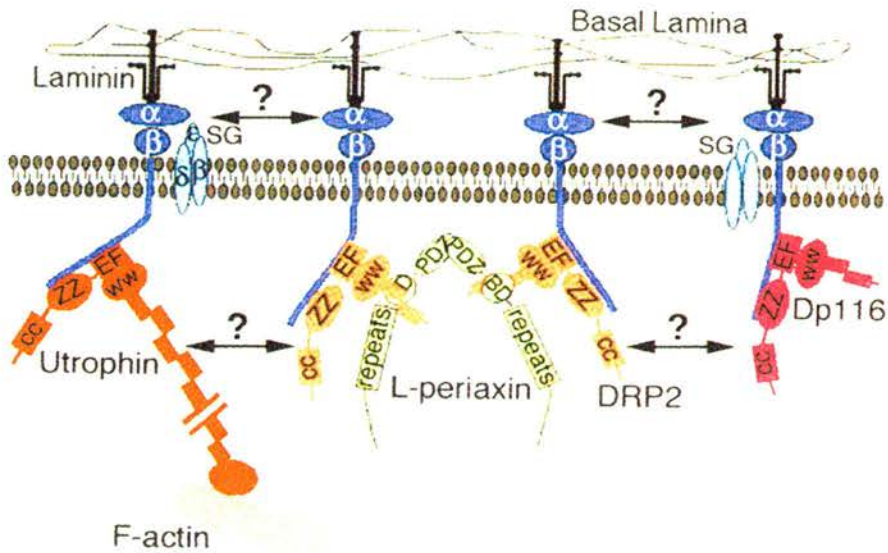


FIGURE 10. The DRP2-L-periaxin- dystroglycan complex at the Schwann cell plasma membrane. Periaxin associates via its basic domain (BD) with the spectrin-like repeats of DRP2 which also associates with β -dystroglycan. Clustering of DRP2 to the membrane could be a consequence of L-periaxin homodimerisation through its PDZ domain. SG, sarcoglycans, α and β dystroglycan (After Sherman, 2001).

1.4.4 Periaxin null mice display peripheral demyelination and neuropathic pain

The Prx gene was inactivated by homologous recombination in mice, in an effort to assess the effects of lack of periaxin on the formation and stabilisation of the PNS myelin. The Schwann cells of these mice were able to generate a myelin sheath in an apparently normal fashion. Light microscopy on peripheral nerves of 6-week old homozygous Prx^{-/-} mice, revealed focal thickenings referred to as tomacula and infoldings of internodal myelin. However, the levels of major myelin proteins such as P0, MAG and MBP were found normal when assessed by Western Blot on sciatic nerves from mutant mice, supporting the view that demyelination at this age was not extensive. The phenotype of the animals until up to 6 weeks of age also appeared normal, although they displayed a distinctive clasping of their hindlimbs when lifted by the tail, from about 4 to 6 weeks and some animals showed a slight tremor. Older mutant mice (6-9 months of age), however, displayed an unsteady gait and a difficulty to support themselves on their hindlimbs. Electron microscopy revealed extensive demyelination in sensory, motor and autonomic nerves. Disruption of the normal function of sensory nerves leads to the perception of neuropathic pain (Devor, 1989). Periaxin knockout mice display symptoms of mechanical allodynia and thermal hyperalgesia which could be reversed upon intrathecal administration of the selective N-methyl D-aspartate (NMDA) receptor antagonist, 3-([R]-2-carboxy-piperazin-4-yl)-propyl-1-phosphonic acid ([R]-CCP), indicating that some form of central change may be implicated in the Prx null phenotype that could be responsible for the manifestation of neuropathic pain (Gillespie et al., 2000).

1.4.5 Mutations in human periaxin are responsible for Dejerine- Sottas neuropathy (DSN) and Charcot-Marie-Tooth Disease 4F (CMT4F)

DSN and CMT are heterogeneous inherited peripheral myelinopathies. DSN results from dominant mutations in PMP22, P0, and EGR2, with recessive mutations in PMP22 also documented as cause for the disease (Hayasaka et al., 1993) (Roa et al., 1993). Loss- of- function mutations in human Prx result in sporadic and autosomal recessive DSN with phenotypes of reduced conduction velocities and onion bulb formations (Boerkoel et al., 2001).

CMT constitutes a group of inherited peripheral motor and sensory neuropathies. The clinical symptoms of the disease are manifested as chronic distal weakness with progressive muscular atrophy and sensory loss in distal extremities (Guilbot et al., 2001). Inheritance of CMT may be autosomal dominant, autosomal recessive (ARCMT), or X-linked. A non-sense mutation in human L-periaxin, which converts Arginine at position 196 into a STOP codon (R196X), gives rise to a truncated molecule that comprises only the PDZ and basic domains. This mutation is believed to be responsible for the onset of CMT 4F, a form of ARCMT, which maps to human chromosome 19q13 at the same locus where the human Prx gene is mapped (Guilbot et al., 2001). Non-sense frameshift mutations have been described, which delete the acidic domain of human L-periaxin (Boerkoel et al., 2001). A mutation in Cysteine 715, which converts it to a STOP codon (C715X) gives rise to L-periaxin that lacks the acidic domain and the rest of the C-terminus. Patients who are homozygous for this mutation, display an autosomal recessive demyelinating neuropathy similar to CMT 4F. The neuropathy has a very early onset and is strikingly sensory with a relatively mild motor weakness (A. Williams, personal communication). The phenotype of human demyelinating neuropathies

caused by Prx mutations is similar to the phenotype observed in the Prx null mice. Histopathology from the sural nerve obtained from a CMT4F patient revealed demyelination, onion bulb formation and the presence of supernumerary Schwann cells, which are features seen in the Prx null mice (Guilbot et al., 2001). This implies that these animals could prove valuable in the study of the molecular pathophysiology of disease. New candidate genes for other autosomal recessive forms of CMT may be identified by deduction of the rest of the components of the periaxin complex.

1.5 DETECTION OF SPECIFIC INTERACTIONS BETWEEN PROTEINS: THE YEAST-TWO HYBRID APPROACH

The yeast-two hybrid is a molecular genetic test for protein interactions used to identify proteins that interact with a protein of interest (Gietz et al., 1997). This assay relies on the modular domain structure of eukaryotic transcription factors, many of which comprise two physically distinct and separable domains: the DNA-binding domain and the transcriptional activation domain. The former localises the transcription factor to specific DNA sequences upstream of the genes to be regulated and the latter interacts with the RNA polymerase complex resulting in transcriptional initiation. The interaction between two candidate proteins is tested by producing a fusion protein that consists of the DNA binding domain coupled to the DNA sequence of a target protein ("bait") and a construct that comprises the activation domain fused to another protein ("prey" fusion protein). Interaction of the two fusion proteins will result in reconstitution of a functional transcription factor that will initiate the transcription of a reporter gene.

The yeast two-hybrid genetic system was devised to study interactions between proteins by taking advantage of the properties of the GAL4 protein of the yeast *Saccharomyces cerevisiae* (Fields and Song, 1989). This protein controls transcription of genes whose products are involved in the metabolism of galactose. GAL4 binds to an upstream activating sequence (UAS_G) and activates transcription of genes under the control of the GAL1 promoter in the presence of galactose. To generate hybrid proteins containing parts of the GAL4 protein, the GAL4 DNA binding domain is fused to a protein X and the GAL4 activation domain is fused to a protein Y. This permits the assessment of interaction between those two proteins. The activation of the reporter gene *lacZ* is an indicator of the formation of a protein-protein complex that brings the GAL4 domains in close proximity to allow transcription (Figure 11).

Another reporter gene present in yeast is *HIS3* whose expression permits growth on media that lack the amino acid histidine. This gene is normally under the control of the native yeast *HIS3* promoter. However, in yeast strain CG1945 the entire *HIS3* promoter has been replaced by the entire GAL1 promoter which links the activation of the *HIS3* gene to the UAS_G (Clontech Manual PT3024-1).

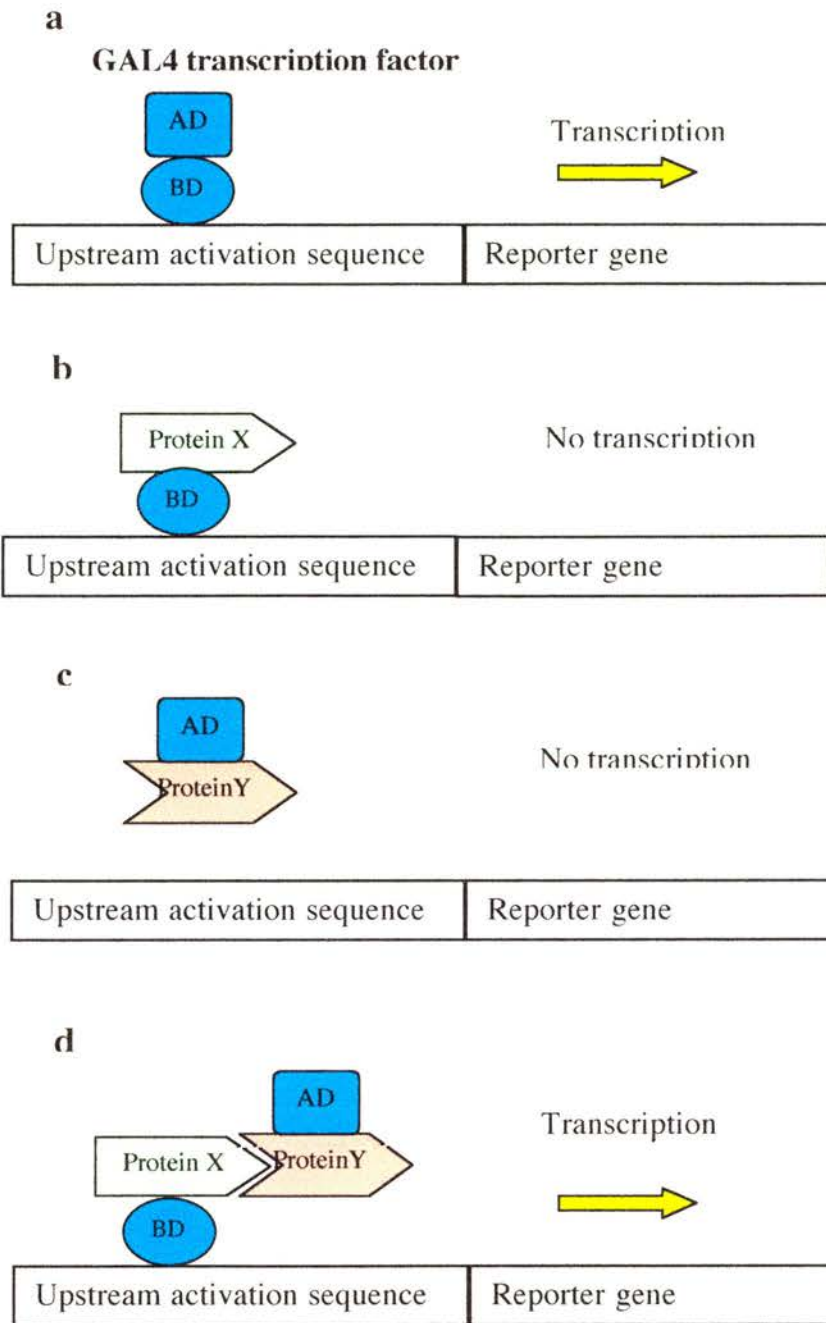


FIGURE 11. The yeast two-hybrid assay for detection of protein-protein interactions. (a) The native yeast transcription factor GAL4 binds to an upstream activation sequence in the nucleus and induces transcription of a reporter gene (BD: DNA binding domain, AD: transcription activation domain). Hybrid proteins containing either the DNA binding domain (b), or the transcriptional activation domain (c), are unable to induce transcription independently. (d) Interaction between hybrid proteins reconstitutes the activity of the native transcription factor and results in activation of the reporter gene.

1.6 INTRACELLULAR CONTROL OF PROTEIN ABUNDANCE

1.6.1 The ubiquitin pathway of protein degradation

Regulation of the abundance of cellular proteins is essential for cell survival and normal function. To overcome the dangerous effects of protein accumulation the cell employs various mechanisms that act to prevent aggregation, attempt refolding or promote degradation of abnormal proteins. A highly discriminative, energy dependent pathway operates in the cytoplasm to ensure removal of damaged proteins. This pathway, mediated by the protein ubiquitin, is a complex cascade of reactions that involve multi-enzyme complexes whose action is temporally and tightly controlled and plays an important part in a broad range of cellular processes. In addition to destroying damaged proteins, the pathway targets many naturally short-lived polypeptides and proteins that are involved in regulatory processes. Conjugation to ubiquitin, in the majority of cases, targets substrates for degradation by the 26S proteasome, an energy dependent self-compartmentalised protease (Hochstrasser, 1996). Ubiquitination of certain plasma membrane proteins has been found to be responsible for their internalisation and subsequent degradation by the lysosome (Hicke and Riezman, 1996). It is not yet known how the proteasomal and endocytic signals conferred by ubiquitin are distinguished (Thrower et al., 2000). It has been proposed that the length of the Ub-chain may be the determinant of such distinction. A minimum of four Ub residues in a chain is thought to be required for proteasomal recognition, whereas mono-ubiquitination is considered responsible for endocytosis (Hicke, 1999). However, the major ubiquitinated form of neuronal nitric oxide synthase (nNOS) was found to be a conjugate of one or only a few Ub molecules, and is still degraded by the

proteasome (Bender et al., 2000). Control of cellular protein levels also occurs via an unregulated vacuolar pathway that is mediated by lysosomes, endosomes and the endoplasmic reticulum.

The ubiquitin pathway of protein degradation is responsible for the turnover of key short-lived regulatory proteins that participate in processes as diverse as the cell cycle, cellular signalling in response to stress and extracellular signals, morphogenesis, the secretory pathway, DNA repair and organelle biosynthesis (Carrano and Pagano, 2001; Maniatis, 1999; Ulrich and Jentsch, 2000; Wiederkehr et al., 2000).

1.6.2 Discovery of an energy dependent proteolytic process mediated by ubiquitin

Ubiquitin (Ub) is a 76- amino acid protein that is highly conserved in organisms as diverse as yeast and humans. Its globular structure may serve to prevent it from proteolysis during the hydrolysis of its bound proteins (Bebington et al., 2001). The involvement of ubiquitin in protein degradation and the mechanism through which the process is accomplished, were discovered by Hershko and Ciechanover in a series of biochemical experiments in a cell free system from rabbit reticulocytes (Hershko et al., 1980). The energy requirement of intracellular protein degradation, in particular that of the enzyme tyrosine aminotransferase (TAT) in hepatoma cells, lead Hershko to the assumption that there was an unknown proteolytic system that utilised energy to ensure high selectivity in the mechanism of protein degradation, considering that proteolysis *per se* is an exergonic process (Hershko, 1996). Their approach was to reproduce ATP-dependent proteolytic degradation in a cell- free system that had already been described by Etlinger and Goldberg (Etlinger and Goldberg, 1977) and

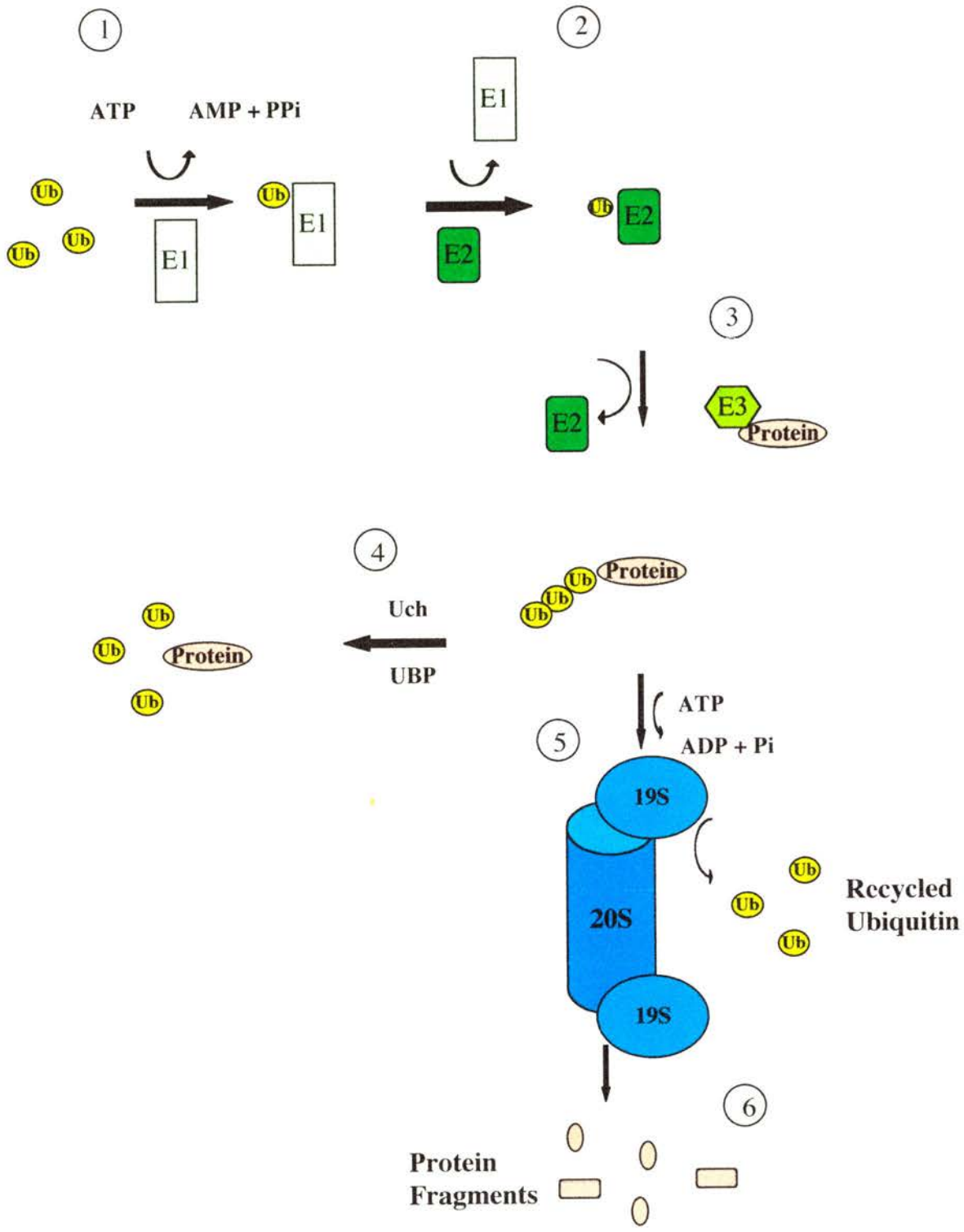
subsequently fractionate such a system to deduce the function of its components. Using lysozyme as an artificial substrate for *in-vitro* proteolysis, Hershko and co-workers deduced that several molecules of ubiquitin form conjugates with the substrate polypeptide. In their original model, proposed in 1980, conjugation of ubiquitin was accomplished via the action of a protein amide synthetase. The protein-Ub conjugate was screened by a "correction" amidase prior to degradation by a cytoplasmic endopeptidase. An isopeptidase was responsible for recycling Ub molecules removed from the substrate.

This model has since been modified but the basic principles remain the same. According to the current information available, the pathway comprises two distinct steps and requires the co-ordinated action of three classes of enzymes. First, the target protein is modified by the covalent attachment of ubiquitin molecules and subsequently degraded by the 26S proteasome complex (Coux et al., 1996). Ubiquitin is activated through the formation of a thiolester bond between its C-terminus and the active site cysteine residue of a ubiquitin activating enzyme (E1). It is subsequently transferred to a ubiquitin-conjugating enzyme (E2) which is either capable of relaying ubiquitin to the substrate by itself, or requires the participation of a ubiquitin ligase enzyme (E3) (Hershko and Ciechanover, 1998; Hershko et al., 2000). Association with the substrate is accomplished by the formation of an isopeptide bond between the C-terminus of ubiquitin (Gly 76) and lysine residues either on the target protein or on the last Ub residue of a protein-bound multi-ubiquitin chain. The presence of ubiquitin residues on the substrate serves as a cue for its recognition by the 26S proteasome whose role is to remove the ubiquitin tag and degrade the target protein. Prior to its association with the

proteasome, the protein-Ub conjugate is monitored by a class of thiol proteases that recognise the C-terminus of ubiquitin. These enzymes form two groups: ubiquitin-carboxy-terminal hydrolases (Uch) and Ub-specific proteases (UBPs). Their role is to remove Ub moieties from incorrectly targeted polypeptides (Figure 12).

It is clear that E1, E2 and E3 perform the function originally ascribed to protein amide synthetase, the endopeptidase required for degradation is in fact the proteasome. A “correction” amidase and the isopeptidase needed for Ub recycling are members of the Uch/UBP family. The specific role of each of the distinct components of the ubiquitin/ proteasome pathway will be discussed next.

FIGURE 12. The ubiquitin/proteasome pathway of protein degradation. (1) Ubiquitin is activated by the formation of a thiolester bond with an E1 enzyme, that requires ATP. (2) Ubiquitin is subsequently ligated to an E2 conjugating enzyme, in an energy independent manner, releasing E1. (3) A class of enzymes termed E3 ubiquitin ligases, mediates the transfer of ubiquitin residues from E2 to the substrate protein. (4) Ubiquitin C-terminal hydrolases (Uch) and ubiquitin specific proteases (UBP) remove ubiquitin moieties from erroneously tagged proteins, in a “proof-reading” mechanism that ensures degradation of appropriate substrates. (5) Degradation substrates are targeted to the proteasome to be destroyed in an energy-dependent mechanism. The Ub tag is removed by proteases of the 19S subunit, and recycled. (6) The 20S core of the 26S proteasome cleaves the substrate which is released in small peptide fragments or individual amino acids that are re-used for protein synthesis.



1.6.3 Components of the ubiquitination machinery

1.6.3.1 E1 ubiquitin activating enzyme

Initiation of the ubiquitination cascade depends on ubiquitin activation. This is accomplished via its interaction with an activating enzyme (E1) in a reaction that requires energy in the form of ATP. Reactive Ub is then passed on to a carrier protein (E2). Eukaryotic genomes encode one or at least only a few ubiquitin activating enzymes (Joazeiro and Weissman, 2000). E1 enzymes from different species appear to be highly conserved. The majority possesses a Gly-X-Gly-XX-Gly motif (where X indicates any amino acid) (McGrath et al., 1991).

1.6.3.2 E2 ubiquitin conjugating enzymes

Activated Ub is bound to a ubiquitin-conjugating enzyme (Ubc) in an energy independent manner, to be subsequently transferred on to the target protein. Association with the substrate occurs, most commonly, through the mediation of an E3 enzyme complex. However, the direct interaction of E2 with the target protein has also been reported. Such associations have been detected using protein-protein interaction screening methods and their physiological role remains unclear. An example of a protein tagged by ubiquitin in the absence of a ligase is Huntingtin which is ubiquitinated by E2-25 kDa (Kalchman et al., 1996). A large number of ubiquitin conjugating enzymes have been identified (13 genes encode E2-like enzymes in yeast *S. cerevisiae*) (Hershko and Ciechanover, 1998).

E2 enzymes have been isolated that perform overlapping functions, such as Ubc2/Rad6 in *S. cerevisiae* that is required for both DNA repair and the proteolysis of N-end rule substrates (see section 1.6.3.3). Diverse functions are also performed by Ubc4 and Ubc5 whose action is needed for the elimination of a number of

abnormal and normal short-lived proteins (Hochstrasser, 1996). Specific roles of E2 enzymes have also been described. A mutation in the *Drosophila bendless* gene which encodes an E2 enzyme, results in impairment of synaptic connectivity during development, whereas disruption of the murine UbcM4 gene (homologous to yeast Ubc4/Ubc5) is responsible for impairment of the placenta's formation (Harbers et al., 1996; Muralidhar and Thomas, 1993). All E2 enzymes can be inactivated by mutating the active Cys residue that is used for conjugation to Ub (Ciechanover, 1998). The identity of E2s and their cognate E3s determines the stringency of their interactions. Several E2s, such as Ubc4, are able to associate with more than one E3 enzyme. Conversely, some E3s may interact with several E2s. The identification of membrane-associated E2s implied their possible involvement in degradation of abnormal or virus-targeted ER proteins.

1.6.3.3 E3 ubiquitin ligases

E3 ubiquitin ligases mediate the critical step of substrate recruitment to the pathway. They may either bind the substrate directly or via the intervention of an adapter molecule. The mechanism of Ub transfer to the substrate also differs among various E3 enzymes. They either bind Ub by forming a thiolester bond prior to its transfer to the substrate or facilitate direct transfer of Ub from E2 to the target by tightly binding E2 and the substrate protein.

To describe the different modes of action of the E3 family of Ub ligases, the following definition has been proposed by Hershko and Ciechanover. They define E3 as an enzyme that binds specific protein substrates, either directly or indirectly and promotes the transfer of ubiquitin, directly or indirectly, from a thiolester intermediate to amide linkages with proteins or poly-ubiquitin chains (Hershko and

Ciechanover, 1998). According to this definition, the known E3s may be classified in four families: I. Ligases that recognise substrates following the **N-end rule** according to which the metabolic stability of a protein depends on the identity of its N-terminal residue. The N-end rule pathway operates in organisms as diverse as yeast and mammals and is also functional in bacteria despite the absence of the ubiquitination machinery (Varshavsky, 1997). It relies on the existence of N-degrons, which are a set of degradation signals. They comprise a destabilising N-terminal residue and an internal lysine which serves as the site of formation of the Ub chain (Varshavsky, 1996). N-terminal destabilising residues form three groups: primary, secondary and tertiary (Table 1).

Primary destabilising residues (N-d^p) are active upon direct binding to a ubiquitin ligase enzyme (E3). They are subdivided into Type 1 (N-d^{p1}) and Type 2 (N-d^{p2}) according to the type of E3 binding site they recognise. Type 1 residues are basic (arginine, lysine, histidine) whereas Type 2 includes bulky hydrophobic amino acids (phenylalanine, leucine, tryptophan, tyrosine, isoleucine).

Secondary destabilising residues (N-d^s), require association with Arg-tRNA-protein transferase to confer their activity. These residues are arginine and lysine in *E. coli*, aspartic acid and glutamic acid in *S. cerevisiae*, aspartic acid, glutamic acid and cysteine in mammalian cells.

Tertiary destabilising residues (N-d^t) are asparagine and glutamine, whose activity depends on accessibility to N-terminal amidohydrolase.

The pathway operates in both the cytosol and the nucleus and results in protein level regulation through the action of the 26S proteasome.

Primary destabilising residues	Secondary destabilising residues	Tertiary destabilising residues
<u>TYPE 1</u> D, E, R, K, H	D, E	N, Q
<u>TYPE 2</u> L, F, Y, I, W		

Table 1. The N-end rule. Primary, secondary and tertiary destabilising residues according to the N-end rule pathway (single-letter abbreviations of amino acids shown).

The first E3 discovered, (E3 α) is a 200 kDa protein that binds N-end rule protein substrates bearing a Type I (basic) or Type II (bulky hydrophobic) N-terminal amino acid residue, via its two distinct binding sites. 2. A second type of E3 ligases contains what is described as a HECT (**H**omology to **E6-AP C**arboxy **T**erminus) domain. This is a region of approximately 350 amino acids homologous to E6-associated protein (E6-AP), an E3 type enzyme recruited by the human papilloma virus E6 oncoprotein to induce degradation of the tumour suppressor p53 (Cummings et al., 1999). A large family of HECT domain-containing proteins has been identified in many eukaryotic organisms (Huibregtse et al., 1995). All HECT domain proteins contain a conserved active site Cys residue for conjugation to Ub, near the carboxy-terminus and display highly variable amino-terminal regions which are the sites involved in the recognition of specific substrates. Ub is transferred from E2 to the HECT motif of the ligase and subsequently to the target protein. HECT- domain proteins are usually large polypeptides (90-200 kDa) whose N-terminal domains appear to display substrate binding sites. The majority

of HECT-containing proteins possess a C2 domain at the N-terminus which is implicated in Ca^{+2} -dependent phospholipid binding (Hoppe et al., 2000). The HECT region is located at the C-terminus of the protein. The presence of WW domains allows binding to proteins containing proline-rich (PPXY) motifs. 3. A ubiquitin ligase activity specifically associated with cell-cycle regulatory proteins has been ascribed to a large (~ 1500 kDa) multi-subunit complex termed the cyclosome or anaphase-promoting complex (APC) (see section 1.6.6). 4. The fourth class of E3s comprises multi-subunit complexes, the majority of which appear to depend on phosphorylation of the substrate.

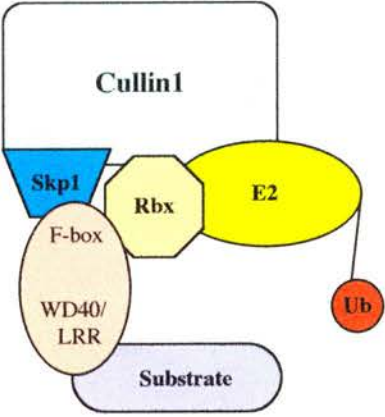
1.6.4 RING-finger proteins mediate ubiquitin ligase activity

The discovery of a novel motif termed the RING finger has changed the original classification of E3 enzymes. RING (**R**eally **I**nteresting **N**ew **G**ene) fingers are defined by the occurrence of a total of eight cysteine and histidine residues that encase two structurally essential zinc ions. The consensus sequence of a RING finger motif is the following: Cys-X(2)-Cys-X(9-39)-Cys-X(1-3)-His-X(2-3)-Cys/His-X(2)-Cys-X(4-48)-Cys-X(2)-Cys, where X represents any amino acid. Ring fingers are subdivided into two categories; RING-HC and RING-H2 depending on the presence of a Cys or a His at the fifth co-ordination site (underlined), respectively (Joazeiro and Weissman, 2000). They were originally thought to play a role in mediating dimerisation of several proteins. It was later deduced that they were also involved in mediation of protein degradation according to the N-end rule and the process of transferring Ub both to heterologous substrates and themselves (Freemont, 2000; Joazeiro and Weissman, 2000) (Jackson et al., 2000).

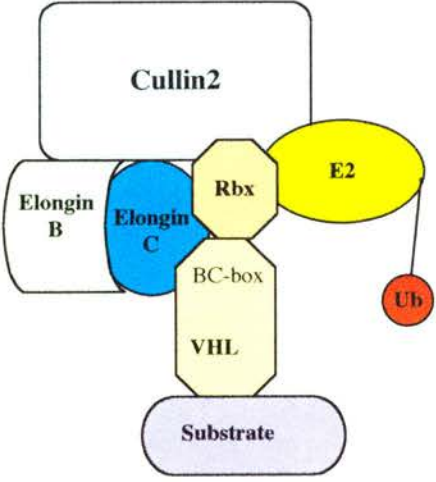
The identification of a RING finger domain in Apc11, an essential anaphase promoting complex (APC) component that controls the anaphase-to-metaphase transition and destruction of cyclin B to allow exit from mitosis, suggested its association with control of cellular protein levels by ubiquitination. This view was further supported by studies that identified a small noncanonical RING finger protein, Rbx1 (also referred to as Roc1 and Hrt1) as an integral component of both VHL-containing and SCF complexes that were shown to possess E3 activity (Chen et al., 2000). The current view supports the division of E3 ligases in two groups based on the presence of either the HECT domain or a complex that includes cullin and a RING-H2 subunit. The latter group defines a superfamily of four types of complexes, namely the SCF (Cul1-based), the CBC (Cul2-based) also referred to as VHL-like, the APC/cyclosome and a putative Cul3-5 based ligase (Tyers and Jorgensen, 2000) (Figure 13). A new class of ubiquitin ligases has been identified recently, which comprises a U-box motif. The prototype U-box protein, Ufd2, was identified in yeast as a factor believed to be required for the assembly of poly-ubiquitin chains, acting in concert with E1, E2 and E3. The U-box is a ~ 70 aa domain which displays 3D structural similarities to the RING finger motif. U-box containing proteins have been observed to function as E3s in E2-dependent ubiquitination (Hatakeyama et al., 2001). The U-box protein CHIP associates with the chaperones Hsp90 and Hsp70 to induce ubiquitination of the glucocorticoid receptor and immature cystic fibrosis transmembrane regulator (CFTR), respectively.

FIGURE 13. RING-finger containing E3 ubiquitin ligases: the SCF, CBC and APC complexes. The RING-finger type of E3 ubiquitin ligases are multicomponent enzymes that mediate the transfer of Ub molecules to substrates. The SCF, VBC and APC subtypes consist of a core that comprises cullin/Apc2, a RING-finger protein (Rbx/Apc11) and a protein that facilitates the association of the core with the adaptor-substrate complex, namely Skp1/ElonginBC/Apc1. The substrate is recruited by an adaptor protein (F-box/VHL-like/Ccd20) that displays binding sites for both the target protein and the Skp1/ElonginBC/Apc1 component of the complex.

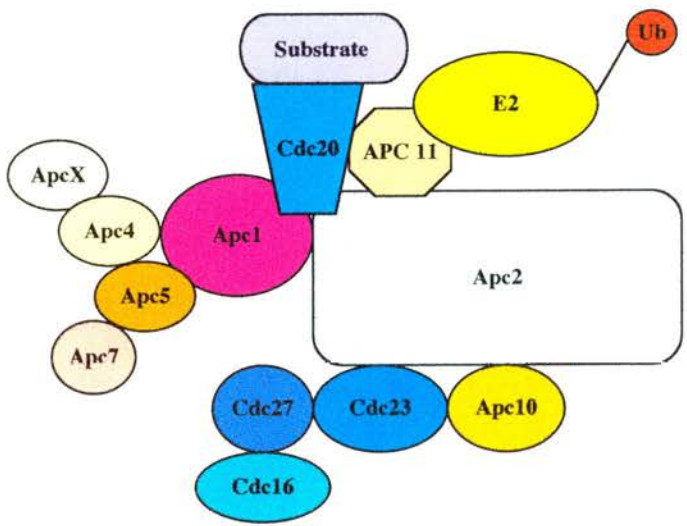
SCF complex



CBC complex



APC/C complex



1.6.5 The SCF ubiquitin ligase complex

The first SCF-mediated pathway was identified in yeast *S. cerevisiae* through analysis of the G1 to S-phase transition. Initiation of DNA synthesis (S-phase) in yeast requires the action of cyclin-dependent kinase (Cdk) which is inhibited by Sic1. Destruction of Sic1 is essential to allow DNA replication to proceed. This is dependent on phosphorylation of the inhibitor by G1 cyclin-Cdk kinases in late G1 phase and requires the action of the E2 enzyme, Cdc4 (Craig and Tyers, 1999). Schwob and coworkers demonstrated that budding yeast *cdc4^{ts}*, *cdc34^{ts}* and *cdc53^{ts}* mutants failed to enter S-phase due to inability to destroy Sic1 (Schwob et al., 1994). The components of the SCF pathway were discovered and characterised in a number of studies performed in several laboratories.

1.6.5.1 Subunits of the SCF complex

Assembly of four distinct subunits gives rise to the heterotetrameric structure of the SCF ubiquitin ligase. The “core” component consists of Cullin1 (or its yeast homologue Cdc53), Skp1 and the RING-finger protein Rbx1/ROC1 (Hrt1 in yeast). The substrate is targeted by an F-box-containing protein (eg. Cdc4) which is linked to the rest of the complex via association with Skp1. The role of Cull1 and Rbx1 is to recruit the ubiquitin conjugating enzyme (E2).

All known SCF subunits are highly conserved throughout eukaryotes (Deshaies, 1999). Substitution of Cdc53, ySKP1 and HRT1 with their respective human homologues CUL1, hSKP1 and RBX1/ROC1 in yeast results in assembly of an active SCF ligase which supports the view of functional conservation of these proteins (Bai et al., 1996) (Skowyra et al., 1999).

1.6.5.2 Structure and function of the SCF components

1.6.5.2 (a) Skp1

Skp1 has been found to associate directly to both Cull1/Cdc53 and a number of F-box proteins (Skowyra et al., 1997) (Yam et al., 1999). The human homologue comprises two domains, based on sequence comparisons and deletion analyses: an N-terminal domain of approximately 110 amino acids that is related to Elongin C and a ~53 aa unique C-terminal region. A 30 aa insertion within the N-terminal domain of the yeast Skp1 (ySkp1) does not seem to play a significant functional role, as *skp* temperature sensitive mutants are complemented by hSKP1.

Yeast two-hybrid assays have revealed that amino acids 1-91 in hSkp1 bind to hCull1, whereas association with the F-box protein Skp2 was accomplished via residues 37-163 and 1-65 with an efficiency of 15 and 20% respectively, compared to the full length hSkp1 (Ng et al., 1998). It is apparent that the first 91 amino acid residues of hSkp1 contain binding determinants for both Cullin and the F-box motif. The ability of ySkp1 to bind to both Cdc4 and Cdc53, lead to the assumption that its main function is to link the cullin and F-box components of the SCF. However, the assembly of a functional SCF that comprises the F-box protein Grr1 in insect cells in the absence of hSkp1 (Skowyra et al., 1997) and the association of a mutant Skp2, that has lost its ability to bind hSkp1, with hCull1 (Lisztwan et al., 1998) suggest an alternative role for hSkp1. It is possible that it acts to mediate the optimal position of the cullin and F box components in order to facilitate the transfer of Ub from E2 to the substrate (Deshaies, 1999).



1.6.5.2 (b) Cullin1/Cdc53

Cullin1/Cdc53 associates with Skp1 through the first 219 amino acids of its N-terminus, as revealed by yeast two-hybrid and GST pull-down assays (Michel and Xiong, 1998). It also contains an internal domain responsible for the interaction with yCdc34 (E2) and Hrt1. At least five different cullins (Cul1, Cul2, Cul3, Cul4(A&B) and Cul5) have been identified in mammalian cells to interact with Rbx1 (Kamura et al., 1999), although Cul5 preferentially interacts with the Rbx1/ROCI homologue, ROC2 (Chen et al., 2000). Cul2-Cul5 do not bind to Skp1 in the yeast two-hybrid screen (Michel and Xiong, 1998). N-terminal deletion mutants of Cul1 abolish interaction with Skp1 but binding to Cdc34 and Hrt1 remains unaffected. The region involved in recruiting the E2-RING-domain subunit is referred to as the cullin homology (CH) domain and displays similarities to the APC/C component Apc2 (Zachariae et al., 1998). The C-terminus of Cul1 is the most conserved region among cullins but its function remains largely unknown (Deshaies, 1999). It has been found to serve as the attachment site for Rub1, a ubiquitin-related protein (Patton et al., 1998).

1.6.5.2 (c) Hrt1/Rbx1/Roc1

Hrt1/Rbx1/Roc1 is a small protein (~121 amino acids) that consists of a 53 aa N-terminal domain and the RING-finger-containing carboxy terminus which spans approximately 67 amino acids (Deshaies, 1999). Its ability to bind Cdc53/hCul1 directly (Ohta et al., 1999) (Seol et al., 1999), stabilises the yCdc34-Cdc53 interaction (Skowyra et al., 1999) and bind Cdc53/Cul1 at regions that overlap yCdc34 binding, suggests a role of Hrt1 in linking yCdc34 to the CH domain of cullin by directly binding to both proteins. Mutation of the conserved Cys and His

residues of the RING finger motif results in abrogation of ubiquitin ligase activity *in vitro* (Kamura et al., 1999), but binding to cullin still occurs, which implies the involvement of the RING motif in recruitment of E2 to the complex.

1.6.5.2 (d) F-box –containing proteins

F-box proteins are the specificity-determinants of the SCF subtype of E3 ubiquitin ligases. They comprise two essential domains: the F-box motif for association with the core E3 ligase complex, via binding to Skp1, and a protein-protein interaction motif for recruitment of substrates for ubiquitination. Particular SCF complexes are designated by their associated F-box components (eg. SCF, ^{cdc4} SCF ^{β-TrCP}).

The F-box motif consists of approximately 50 amino acids and is usually found at the N-terminus of the protein. It was identified as a region of homology among Cdc2, Met30, β-TrCP, Scon2 and MD2 but its implication in inter-protein associations was recognised on the basis of its presence in cyclin F (hence the name F-box) (Bai et al., 1996). An intact F-box is necessary for association with Skp1 as confirmed by mutagenesis studies, but may not be sufficient as indicated by the inability of the minimal F-box of Grr1 to bind ySkp2 in a yeast two-hybrid assay (Li and Johnston, 1997). In accordance with this finding, a mutation of two residues near the C-terminus of Skp2 (away from the F-box region), abolished binding to both human cyclin A (as anticipated) and Skp1 (Lisztwan et al., 1998). Taken together, these observations suggest that the stability of F-box-Skp1 interactions may be dependent on sequences lying outside the F-box. The consensus sequence derived from the alignment of 234 sequences indicates that there are very few invariant positions which makes the detection of the F-box motif

particularly difficult. The most conserved residue in the F-box sequence is a proline preceded usually by a leucine, found in the N-terminal region of the protein. This bipetide was identified as essential for binding of Cdc4 to γ Skp1 (Bai et al., 1996), it was, however, not required for Skp2-hSkp1 interaction (Yam et al., 1999).

The C-terminus of the protein is occupied by the protein interaction motif that is responsible for substrate recognition. Two such motifs present in the majority of the F-box proteins so far characterised, are Tryptophan-Aspartic acid (WD40) repeats and Leucine-rich repeats (LRR). The presence of a particular protein interacting domain, other than the F-box, determines the nomenclature of the protein.

F-box proteins containing WD repeats are classified as FBXW (previously Fbw). The occurrence of leucine-rich repeats in F-box proteins is indicated by FBXL (previously Fbl) whereas FBXO (previously Fbx) denotes a protein with either another or no protein binding motif (Cenciarelli et al., 1999) (Winston et al., 1999a). WD40 repeats and leucine-rich repeat regions constitute members of a group of domains that are able to associate with phosphoSerine/Threonine (pSer/Thr) modules and phosphorylated sequence motifs. Other members of the group include WW domains, 14-3-3 proteins and forkhead-associated (FHA) domains (Yaffe and Elia, 2001).

WD40 repeats

WD40 domains display a β -propeller structure analogous to that of clathrin (ter Haar et al., 2000) that allows binding of linear polypeptide motifs within the grooves formed by adjacent propellers. The WD40 domain of the F-box protein β -

TrCP (Transducin repeat Containing Protein) recognises the following consensus sequence DpSGXXpS in both I κ B α and β -catenin (Winston et al., 1999b).

Leucine-rich repeats (LRR)

Leucine-rich repeat proteins constitute a superfamily that can be divided into at least six subfamilies, based on differences in the length and the consensus sequence of the repeats (Table 2) (Kajava, 1998). The crystal structure of ribonuclease inhibitor (RI), a protein made up entirely of leucine-rich repeats, revealed that LRRs correspond to structural units giving rise to a β -sheet and an α -helix (Kobe and Deisenhofer, 1995b). These units are arranged so that the sheets and helices are parallel to a common axis, with the β -strands lining the inner circumference and the α -helices flanking the outer surface of a horseshoe-shaped molecule. The concave face of the structure is exposed to the solvent and serves as the surface of interaction between the LRR-containing protein and its substrate. The non-globular (horseshoe) shape of the molecule increases the area available for interaction, whereas the exposure of the β -sheet-lined concave face to the solvent, possibly renders this structure a protein-binding motif (Figure 14). Amino acid substitutions within the beta-strand permit alterations in specificity by modification of the surface area. This flexibility is indicative of a role of LRRs not only in recognising specific substrates but also in adjusting to the requirements of a specific interaction (Kobe and Deisenhofer, 1995b). RI displays 16 LRRs and belongs to the subfamily that contains repeats of 28-29 residues, whereas the most common size of a consensus sequence is 24 residues.

A member of the cysteine-containing subfamily, namely Grr1, mediates the ubiquitination of G1 cyclins Cln1 and Cln2. It displays an unusually high density

of cationic charges in the inner circumference of its LRR region. These positively charged residues are thought to be involved in binding to phosphorylated substrates (Hsiung et al., 2001). It is believed that a single LRR does not fold into a defined structure but a number of such motifs are required to jointly form a module (Krantz et al., 1991). The number of repeats within a single domain is thought to modulate the function of the LRR. All the LRR-containing proteins identified so far are involved in protein-protein interactions (Kobe and Deisenhofer, 1994).

LRR subfamily	Length (residue)	Range (residues)	Consensus sequence
Typical	24	(20-27)	LxxLxxLxLxxNxLxx LpxxoFxx
RI-like	28-29	(28-29)	xxx <u>LxxLxLxxN/CxLx</u> xxgoxxLxxoLxx
Cysteine Containing	26	(25-27)	C/LxxLxxLxLxxCxxI TDxxoxxLa/gxx
Plant Specific	24	(23-25)	LxxLxxLxLxxNxL/s GxIPxxLGx
SDS22-like	22	(21-23)	LxxLxxLxLxxNr/KIrr/ KKIEN/GLEx
Bacteria	20	(20-22)	PxxLxxLxVxxNxLxx LPD/EL

Table 2. LRR subfamilies. The LRR superfamily is grouped in six classes based on repeat consensus sequences. Bold and uppercase letters indicate, respectively, more than 70% and 40% occurrence of the residue in a certain position. Lowercase letters indicate more than 30% identity (x: any amino acid, o: non-polar amino acid). Underlined is the constant part of the repeat sequence (Adapted from Kajava, 1998).

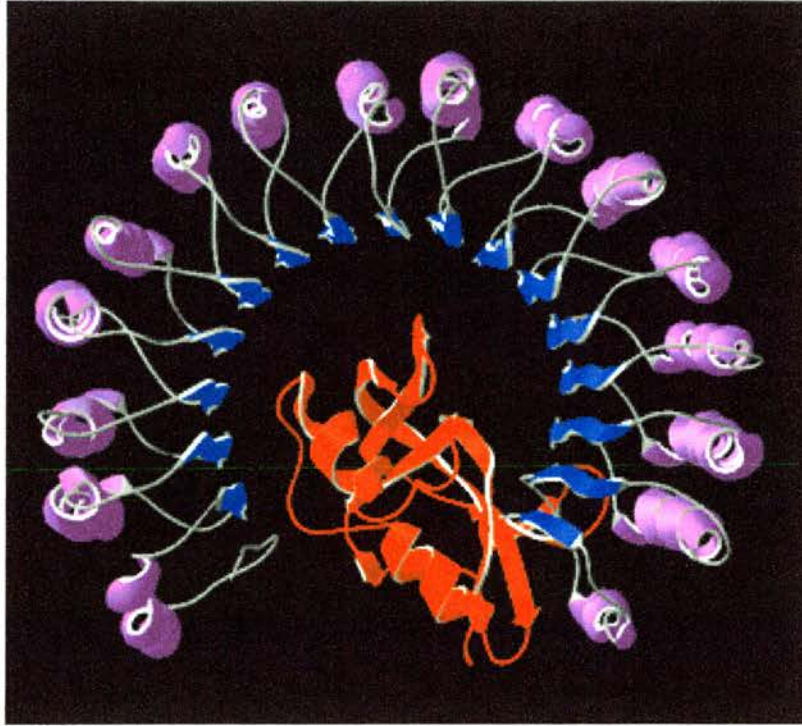


FIGURE 14. Crystal structure of the LRR-containing protein Ribonuclease Inhibitor (RI). The association of RI with its substrate ribonuclease A (shown in red) is facilitated by the distinct arrangement of the LRRs to form a horseshoe-like structure. RI is a protein entirely made of LRRs. Each repeat comprises a β -sheet (blue) associated with an α -helix (purple).

1.6.5.3 Mechanism of action of the SCF complex

1.6.5.3.1 The F-box hypothesis

Evidence from a number of studies suggests that F-box proteins recruit phosphorylated substrates to the SCF complex (Hsiung et al., 2001) (Latres et al., 1999) (Skowyra et al., 1997). However, it has been unclear whether phosphorylation is essential only for the recognition of the SCF substrates by the F-box proteins, or it plays a role in the process of the ubiquitination reaction itself. It is possible that phosphorylation induces a conformational change in the substrate to reveal preferred ubiquitination sites (Montagnoli et al., 1999). A new strategy devised to target non-SCF substrates for ubiquitination via engineering of the F-box component, has provided insight into the phosphorylation requirements of the target proteins. Physiologically stable cellular proteins can be destined for destruction through association with an F-box protein that has been engineered to bear binding determinants for the desired protein. Targeted proteolysis experiments have demonstrated that substrate recognition is dependent on F-box binding alone and does not require phosphorylation. Hence degradation via the SCF complex might depend exclusively on substrate binding to the F-box component (Zhou et al., 2000). The recent finding that the F-box protein Ebi mediates ubiquitination of unphosphorylated β -catenin, supports the view of a phosphorylation-independent substrate recognition manner of particular F-box proteins (Matsuzawa and Reed, 2001). Phosphorylated β -catenin is recognised by the F-box protein FWD1/ β -TrCP/Slimb (see section 1.6.5.4.2), which facilitates its ubiquitination by the SCF complex. The identification of two distinct, although structurally related F-box proteins, which mediate the ubiquitination of the same substrate by binding to

different sites on the target protein, provides evidence against the previously expressed view that a particular substrate may associate with a single F-box protein.

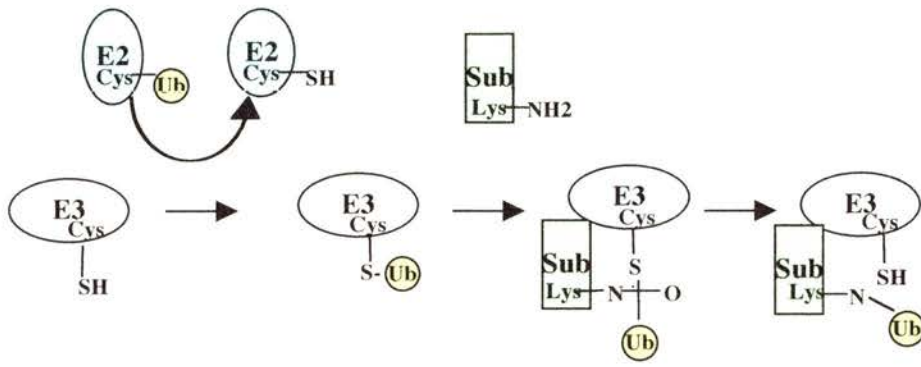
The F-box subunit may not always bind the protein targeted for ubiquitination directly. The HIV protein Vpu contains a recognition motif found also in $\text{I}\kappa\text{B}$ and β -catenin that directs binding to β -TrCP and mediates their destruction. In the case of Vpu, the motif does not act to target the protein for degradation but facilitates destruction of its bound CD4 receptor (Margottin et al., 1998). Substrate binding may also be enhanced by the formation of functional homo- or heterodimers of F-box proteins (Suzuki et al., 2000; Wolf et al., 1999), whose potential role in catalysis is not known. According to **“The F-box Hypothesis”** a large number of F-box proteins present in the cell mediates the destruction of an even larger number of substrates through association with Skp1 in multiple degradation pathways (Bai et al., 1996). It suggests that Skp1 is responsible for the turnover of all SCF targets via its interaction with different F-box proteins bearing specific substrates. The notion that numerous F-box proteins utilise the same core SCF complex poses a problem of maintaining an equilibrium between the F-box component and the limiting amount of core complex. This is possibly overcome by the regulated turnover of F-box proteins in an SCF- dependent manner. Regulation of multiple F-box proteins via auto-ubiquitination has been documented to occur following release of their substrates from the complex (Zhou and Howley, 1998) (Mathias et al., 1999) (Galan and Peter, 1999).

1.6.5.3.2 Transfer of Ub residues to Lys side chains of the target protein

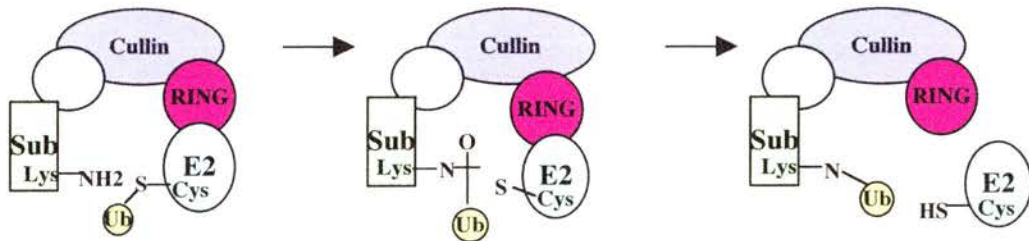
Recruited substrates are tagged with ubiquitin via the action of the cullin/RING-H2 heterodimer. The mechanism of transfer on Ub moieties in the SCF complex appears to be different from HECT- domain mediated ubiquitination (Figure 15). Whereas HECT domains of E3 enzymes bind Ub through a C-terminal Cys residue and subsequently pass it on to the substrate, in the case of SCF treatment of Cdc53/Hrt1 with the alkylating agent N-ethylmaleimide (NEM) that inactivates sulfhydryls had no effect on the auto-ubiquitination of yeast Cdc34 (Seol et al., 1999). This was indicative of the operation of a mechanism that does not involve a core complex Cys residue. It has been proposed that the cullin/RING-H2 conjugate triggers a conformational change in ubiquitin-bearing E2 (E2-Ub) that results in reduction of the energy barrier for the formation of the oxyanionic intermediate generated during the transition state of Ub transfer from the catalytic cysteine of E2 to the ϵ -amino group of a substrate Lys side chain (Seol et al., 1999). The application of such a conformational switch would ensure that E2 enzymes specifically ubiquitinate SCF-bound targets and not random cellular proteins that they might encounter given their substantial excess compared with SCF complexes. It also suggests that the efficiency of the core SCF can be controlled and reach its maximal level upon encountering the F-box protein- bound target, since a Ub moiety is directly transferred from E2 to the substrate (Deshaies, 1999).

FIGURE 15. Mechanism of action of HECT-domain and RING-finger ubiquitin ligases. The HECT domains of E3 enzymes bind Ub through a C-terminal Cys residue and subsequently pass it on to a Lys side chain of the substrate, whereas the cullin/RING-H2 conjugate mediates a direct transfer of Ub from E2 to the target protein, in a mechanism that does not involve prior association of Ub with the ligase (Adapted from Zachariae, 1999).

HECT-domain ligases



Cullin-RING finger ligases



1.6.5.4 Substrates of the SCF

Proteins regulated via the SCF pathway represent a broad range of polypeptides involved in a wide variety of processes including control of cyclin-dependent kinase (CDK) activity in the cell cycle, signal transduction cascades, transcriptional activation and DNA replication. A number of transcription factors, tumour suppressors and oncoproteins are regulated selectively by the SCF machinery. The best characterised systems that depend on SCF-mediated ubiquitination include the hedgehog, wnt/wingless and NF- κ B pathways all of which depend on the action of the same F-box protein, namely β -TrCP or its *Drosophila* homologue Slimb (supernumerary limbs) (Figure 16).

1.6.5.4.1 *The hedgehog pathway*

The hedgehog (Hh) pathway in *Drosophila* controls the development of limbs and the formation of the anterior-posterior axis in wing and leg imaginal discs, by regulating the expression of *wingless* (*wg*) and *decapentaplegic* (*dpp*) genes (Hammerschmidt et al., 1997). Ectopic Hg signalling results in mutants with duplicated wings and legs. In the absence of Hh signal, the transcription regulator Cubitus interruptus (Ci), a 155 kDa microtubule-associated protein, undergoes proteolytic processing to yield a 74 kDa N-terminal protein that lacks the cytoplasmic tethering domain. This truncated polypeptide is released from the microtubule complex and translocates to the nucleus where it functions as a transcriptional repressor of *wg* and *dpp* genes. This processing of Ci is ubiquitin-dependent, mediated by the F-box/WD40 protein Slimb and requires phosphorylation of the substrate by protein kinase A (PKA) (Craig and Tyers, 1999). The 155 kDa form of Ci accumulates in the presence of Hh signalling. It

translocates to the nucleus by an unknown mechanism that permits its release from the microtubule complex, and acts as a transcriptional activator of downstream genes (Maniatis, 1999).

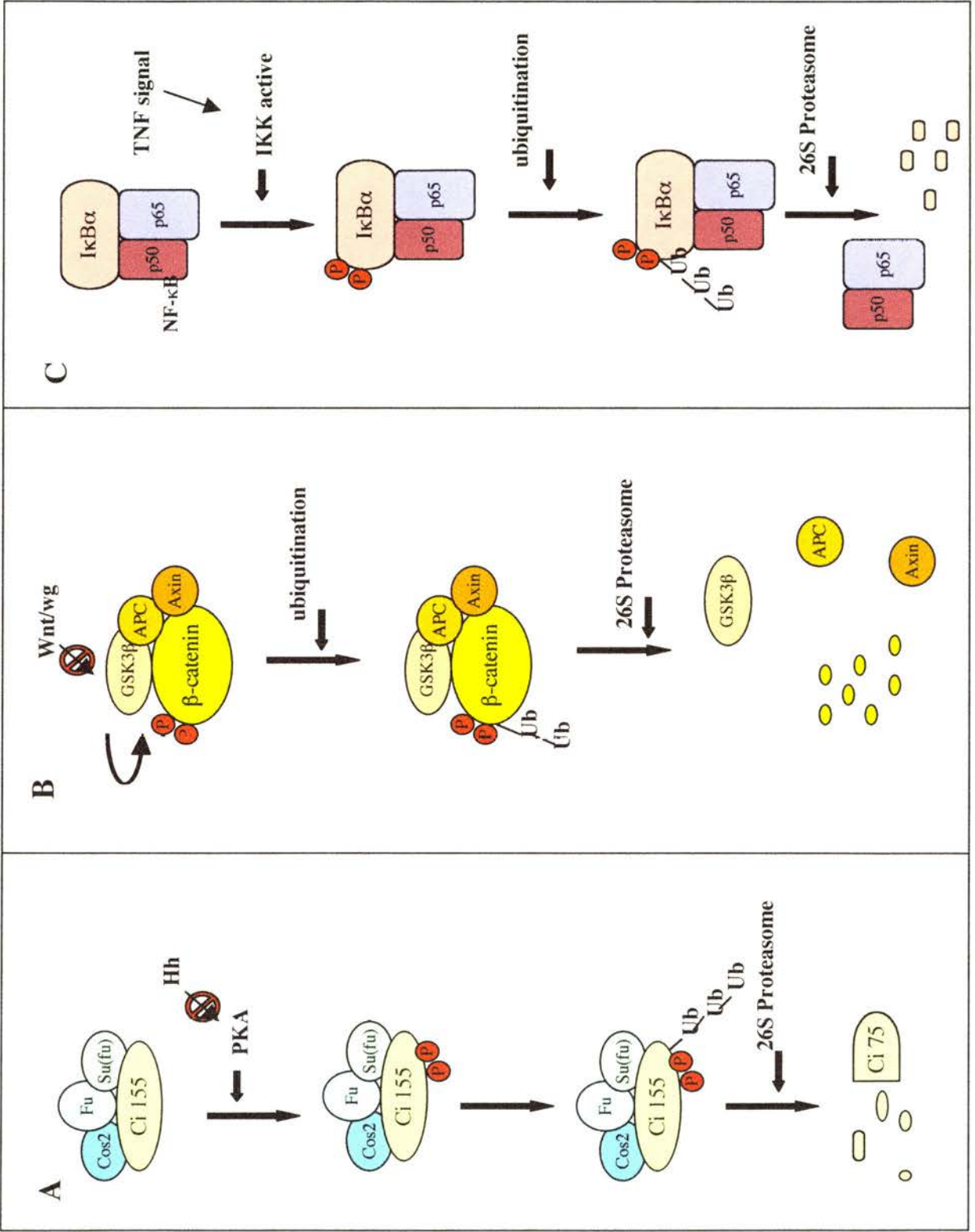
1.6.5.4.2 *The Wnt/Wingless pathway*

The Wnt/Wingless pathway plays a central role in development and organogenesis. It regulates processes as diverse as segmental pattern formation, CNS patterning and asymmetric cell divisions (Wodarz and Nusse, 1998). In *Drosophila* and *Xenopus* it controls segmental pattern formation and dorsal axis determination, respectively (Jiang and Struhl, 1998). The *Drosophila* Wg ligand stimulates a signal transduction cascade that targets the transcription factor Armadillo (Arm) which lies downstream of the wingless receptor and the serine kinase Zeste-White 3 (ZW3). The *Xenopus* and mammalian homologues of Wg, Arm and ZW3, are Wnt-1, β -catenin and glycogen synthase kinase 3 β (GSK 3 β), respectively (Orford et al., 1997). In mammals β -catenin plays a significant role in cell-cell adhesion and growth factor signal transduction. It exists as membrane-associated through its interaction with E-cadherin and α -catenin that leads to the formation of the adherens junction and it is also found in a cytoplasmic pool which is important for signalling (Gumbiner, 1995). The mammalian Wnt signalling cascade is initiated through binding of the Wnt-1 ligand by the cell surface receptor Frizzled. This interaction causes inhibition of GSK 3 β which fails to phosphorylate β -catenin. As a result the cytoplasmic levels of the protein increase and excess hypophosphorylated β -catenin translocates to the nucleus where it associates with T cell factor/ lymphocyte enhancer binding factor (TCF/LEF) transcription factors and modulates expression of their target genes (Huber et al., 1996). One of these

genes was identified as the proto-oncogene c-myc (Pennisi, 1998). β -catenin also associates with the adenomatous poliposis coli (APC) tumour suppressor gene product. De-regulation of APC, β -catenin, and E-cadherin expression, leads to elevated levels of cytoplasmic β -catenin which increase the transcriptional activity of TCF/LEF, resulting in tumour formation in a variety of tissues (Sadot et al., 2000).

In the absence of Wnt-1 signalling, active GSK 3 β phosphorylates β -catenin in a reaction that occurs in a complex comprising APC and Axin/conductin (Munemitsu et al., 1995). The phosphorylated N-terminal six amino acid region (DSGIHS) of β -catenin is recognised by the F-box protein β -TrCP which links beta catenin to the core SCF complex for ubiquitination and subsequent degradation (Orford et al., 1997) (Latres et al., 1999).

FIGURE 16. Substrates of the SCF complex. (A) The hedgehog pathway. Hedgehog (Hh) signalling inhibits the action of PKA whose function is to phosphorylate the Cubitus interruptus (Ci) 155 component of a transcriptional regulator. Phosphorylated Ci 155 is tagged with Ub and partially degraded by the proteasome to yield a functional 75 kDa product that acts as a transcription repressor. **(B) The Wnt/Wingless pathway.** In the absence of Wnt/wg signalling, β -catenin in a complex with APC and axin, is phosphorylated by GSK 3 β and subsequently ubiquitinated and degraded by the 26S proteasome. Accumulation of cytoplasmic β -catenin results in nuclear translocation and leads to elevated expression of oncogenes, with the consequent formation of tumours in a variety of tissues. **(C) The NF- κ B pathway.** The nuclear factor κ B (NF- κ B) exists as a heterodimer of p50 and p65 subunits, sequestered in the cytoplasm by binding to the inhibitor I κ B α . Phosphorylation of I κ B α by the kinase IKK, upon tumour necrosis factor (TNF) signalling, results in I κ B α ubiquitination and degradation. Released NF- κ B translocates to the nucleus to exert its transcriptional activity.



1.6.5.4.3 The NF- κ B pathway

NF- κ B (nuclear factor κ B) is a member of the Rel family of transcription factors that control expression of genes involved in the inflammatory, immune and stress responses (Maniatis, 1999) (Baeuerle and Baltimore, 1996). NF- κ B1, the best characterised type comprises two subunits, namely p50 and p65 (RelA). The smaller subunit, p50, is the processed N-terminal fragment of a 105 kDa precursor molecule, via limited ubiquitin-dependent proteolysis (Palombella et al., 1994) (Coux and Goldberg, 1998). The p50/p65 heterodimer is sequestered in the cytoplasm by association with the inhibitor I κ B α which masks the nuclear localisation signal of the complex and abolishes its ability to bind DNA (Arenzana-Seisdedos et al., 1995). Extracellular signals such as tumour necrosis factor- α (TNF- α), lead to the activation of an I κ B-kinase complex (IKK) that phosphorylates I κ B α on residues Ser-32 and Ser-36 of its N-terminal DSGLDS region, which is very similar to the β -catenin phosphorylation site. The phosphorylated domain is directly recognised by the F-box protein β TrCP (Yaron et al., 1997). This modification targets the protein for destruction in the Ub/proteasome pathway. Degradation occurs while I κ B α is still bound to the NF- κ B complex (Chen et al., 1995) (Alkalay et al., 1995). Released NF- κ B is able to translocate to the nucleus and exert its transcriptional activity (Orian et al., 1995) (Yaron et al., 1998).

1.6.6 The anaphase promoting complex (APC) / cyclosome ligase

The APC was the first multi-subunit ubiquitin ligase described. It contains the cullin homologue Apc2, associated with a RING-H2 finger protein, Apc11, which is similar to Rbx1. Its activation requires the action of two classes of WD repeat-

containing proteins; Cdc20/Fizzy and Cdh1/Hct1/Fizzy-related (Zachariae and Nasmyth, 1999). The proteins targeted for destruction by the APC display one of the following destruction signals: the nine-residue destruction box (D-box) or a transposable seven-residue motif, the KEN box. The D-box is present in all substrates that use the Cdc2 adapter and some Cdh1-associated substrates whereas the KEN-box is found exclusively linked to Cdh1. This adapter is not only able to target D-box and KEN-box substrates but also Cdc20 itself. APC-mediated ubiquitination appears to be dependent on phosphorylation of the complex but not necessarily of its substrates (Jackson et al., 2000).

1.6.7 The Cullin2/ Elongin B/ Elongin C (CBC) complex

The CBC ubiquitin ligase shares striking structural similarities with the SCF complex. It is composed of a core that contains Cullin (Cul2) associated with the RING finger protein Rbx1, the Skp1 homologue Elongin C, as part of the Elongin BC heterodimer, and a SOCS (Suppressors Of Cytokine Signalling) box-containing protein equivalent to but distinct from F-box proteins (Deshaies, 1999).

The association of Elongin B and Elongin C, referred to as the Elongin BC complex, was identified initially as a positive regulator of the RNA polymerase II elongation factor Elongin A, and subsequently as part of the von Hippel Lindau (VHL) tumour suppressor complex, where it functions in tumour suppression and negative regulation of hypoxia-inducible genes (Kamura et al., 1998). Elongin B is a 118 aa protein that contains an N-terminal ubiquitin homology (UbH) domain (84 aa) that is fused to a 34 aa C-terminal tail of Elongin C, which comprises 112 amino acids and is similar to Skp1 (Bai et al., 1996). The Elongin BC complex has been reported to interact with the SOCS box motif found in proteins that belong to

the SOCS, ras, WD40 repeat, SPRY domain and ankyrin repeat families. The SOCS box is an ~50 aa motif composed of two blocks of conserved sequence, separated by 2-10 non-conserved residues. The N-terminal conserved domain (~12 aa) is a consensus BC box. SOCS box proteins are modular, comprising a SOCS-box motif at the extreme C-terminus and either an SH2, Ras-like, WD40 repeat, ankyrin repeat or SPRY domain at the extreme N-terminus (Kamura et al., 1998). SOCS box –containing proteins act as the substrate recruiting component of the complex. A known substrate –selecting protein that participates in the formation of a CBC ligase, is VHL. Association of VHL with the core CBC to form a complex termed CBC^{VHL} or VBC, occurs via the BC box present in VHL.

Rbx1 acts as the mediator of the E2-E3 interaction and also associates with Elongin C (Kamura et al., 1999).

An additional component of the CBC that has no corresponding subunit in the SCF complex, is Elongin B which is believed to function as an adaptor by binding VHL, Elongin C and Cul2. Its precise function remains elusive. The CBC complex has been observed to bind to and regulate the activity and stability of multiple proteins including kinases involved in the Jak/ STAT pathway (Kamizono et al., 2001).

1.6.8 Cul3-5 based ubiquitin ligases

Cul3-5 based E3s have not been well characterised yet. It is not currently known whether they conform to the theme that applies to the rest of the superfamily members. It is believed that they possibly involve an Skp1-like subunit that associates with both the Cullin and a receptor which recruits the (phosphorylated?) substrate. A RING-H2 component is most probably the mediator of E2 binding to the ligase complex (Deshaies, 1999).

1.6.9 Phosphorylation –dependent degradation signals

Post-translational modification of a protein by phosphorylation could serve to target it for ubiquitination. Sequences in polypeptides rich in proline, glutamic acid, serine and threonine, referred to as PEST (in single letter abbreviation) have been found to function as signals for degradation (Rechsteiner and Rogers, 1996). Phosphorylation of the yeast G1 cyclin Cln3 at a PEST region is necessary for its destruction (Yaglom et al., 1995). The sequence SSSTDSTP at positions 99-106 of the transcriptional activator Gcn4, a PEST-like motif, acts as a signal for its degradation. Gcn4 in yeast controls expression of genes involved in the synthesis of amino acids and purines (Kornitzer et al., 1994). Targeting could also occur through phosphorylation of a residue that lies outside the PEST motif as is the case for cyclin D1 (Diehl et al., 1997).

A short E3 binding segment present in $\text{I}\kappa\text{B}\alpha$ (DSGLDS), and β -catenin (DSGIHS), depends on phosphorylation of the two Ser residues for binding to the ubiquitin ligase complex (Laney and Hochstrasser, 1999).

Phosphorylation of a target protein by a kinase appears to be essential for recognition of the substrate by a specific ubiquitin ligase. It is also evident that different ubiquitin ligases recognise distinct patterns of phosphorylation as well as additional motifs on target proteins (Hershko and Ciechanover, 1998). WW domains of ubiquitin ligases are able to recognise proline-rich sequences or phosphoserine and phosphothreonine containing elements (XPPXY or PY) present in their substrates. Rsp5 ubiquitin ligase (the yeast homologue of mammalian Nedd4 which was found to interact with an epithelial sodium channel), recognises via its WW domain, the heptapeptide sequence SPTSPSY present in the C-

terminus of its target, the large subunit of yeast RNA polymerase II (Rpb1) (Laney and Hochstrasser, 1999).

A functional connection between phosphorylation and ubiquitination was also evident in the case of the proto-oncogene encoded signal- transducing transcription factor c-Jun, a member of the AP-1 family. Signal transduction through c-Jun is dependent upon phosphorylation by mitogen-activated protein kinase (MAPK)-type enzymes. MAPK phosphorylation of c-Jun causes an increase in its transactivating potential and DNA-binding activity and occurs in sites proximal to a 27 amino acid region found at the amino- terminus of the protein, termed the δ domain (Treier et al., 1994). The δ domain is required for both polyubiquitination and degradation of c-Jun and its absence from v-Jun renders it stable. It has been demonstrated that phosphorylation of c-Jun in vivo resulted in its stabilisation by suppression of ubiquitination (Musti et al., 1997). Fusion of the 67 N-terminal amino acid region of c-Jun that includes the δ domain, to β -galactosidase, an otherwise stable protein, resulted in its rapid turnover. The ability of this motif to mediate ubiquitination and degradation of a previously stable heterologous protein, classifies it as a necessary and sufficient transferable degradation signal (Treier et al., 1994).

1.6.10 N-terminal ubiquitin as a degradation signal

Ubiquitin chains attached to a polypeptide at specific lysine residues serve as a recognition cue for the proteasome and lead to destruction of the tagged protein. Non-removable ubiquitin residues found at the N-termini of polypeptides function as primary degradation signals. Proteins that bear DNA-encoded linear Ub adducts in their N-termini are degraded by a Ub/proteasome-dependent system termed the

UFD pathway (**Ub**iquitin/**F**usion/**D**egradation) (Johnson et al., 1995). The targeting of a protein by the UFD pathway results in the formation of a multiubiquitin chain on the non-removable Ub moiety, a modification necessary for subsequent recognition by the proteasome.

The action of a ubiquitin conjugating enzyme (E2) is not essential in the UFD unlike the N-end rule pathway. Physiological substrates for the UFD pathway are largely unknown but may include proteins that bear Ub-like domains (eg Elongin B). It is also possible that targeting by UFD depends on recognition of Ub residues within a post-translationally added multi-ubiquitin chain, a hypothesis which excludes the presence of Ub-like domains on potential substrates (Johnson et al., 1995). The identification of yeast Rad23, a conditionally short-lived protein that comprises a Ub-like N-terminal region as a physiological substrate for UFD, favours the view that Ub-like N-terminal domains of other proteins may act as degradation signals. The Ub-like region of Rad23 is implicated in its role in UV-damaged DNA repair which implies that its metabolic instability is related to its function. This could be the case for other Ub-like domain bearing proteins (Varshavsky, 1997).

1.6.11 Internalisation signals

Ubiquitination of a number of cell surface receptors, activated by tyrosine kinase-dependent phosphorylation, has been observed to occur upon binding of specific ligands (Bonifacino and Weissman, 1998). Ligand-dependent ubiquitination of T-cell antigen receptor (TCR), platelet -derived growth factor receptor (PDGFR) β and c-Met receptors has been documented (Cenciarelli et al., 1992) (Jeffers et al., 1997) (Mori et al., 1995). In the case of c-Met, inhibition of

the proteasome blocked degradation of the protein, which implied a role of this protease in the turnover of the receptor. TCR and PDGFR β , on the other hand, are stabilised by treatment with the lysosome inhibitors monensin and ammonium chloride (Bonifacino and Weissman, 1998). When the proteasomal pathway is not employed, conjugation of ubiquitin to membrane receptor and transporter proteins has been found to mediate their endocytosis and subsequent degradation in the lysosome (vacuole in yeast). The association between ligand-induced ubiquitination and endocytosis of membrane proteins has been studied in the yeast G-protein coupled receptor Ste2, which binds the pheromone α -factor. Binding to α -factor results in internalisation and rapid degradation of the receptor. The cytoplasmic tail of Ste2 contains a region that is regulated by serine phosphorylation, SINNDAKSS, identified as essential for both endocytosis and ubiquitination of the protein (Wu and Haber, 1996).

The consensus sequence DAKTI, reminiscent of the last five residues of SINNDAKSS, found in the linker region which connects the two homologous transmembrane regions of Ste6 transporter, is necessary for its ubiquitination and internalisation. The linker region of Ste6 comprises an N-terminal acidic stretch termed the A-box and a C-terminal basic region called the B-box, collectively referred to as the D-box (“destabilisation-box”). DAKTI is found within the A-box region of Ste6 and can act as a ubiquitination signal in heterologous proteins only as part of the entire D-box motif. It is thus necessary but not sufficient to mediate ubiquitination and endocytosis (Kolling and Losko, 1997).

Internalisation of the uracil permease Fur4 is associated with ubiquitination and vacuolar degradation. Mutants defective in internalisation, accumulate as

ubiquitin conjugates. A point mutation in the D-box (“destruction box”) of Fur4 results in its inability to be degraded, as does the mutation of serine to alanine in the N-terminal PEST region of the transporter.

The way in which ubiquitin mediates endocytosis is not clear. It has been suggested that ubiquitin could bind to components of the internalisation machinery such as clathrin in mammalian cells or the actin cytoskeleton in yeast (Bonifacino and Weissman, 1998). It has also been proposed that the process involves proteolysis of the cytosolic tail of the substrate (Hershko and Ciechanover, 1998). A third way in which ubiquitin could facilitate internalisation of plasma membrane proteins is by affecting the location of a protein within the plasma membrane. Ubiquitin-induced translocation of a protein to a region of the membrane that forms an early endosome is possible either via multimerisation of the receptor or by utilising Ub as a localisation signal (Hicke, 1999).

Unlike polyubiquitination, which acts as a signal for proteasomal degradation, endocytosis appears to rely on conjugation of either a single Ub molecule or two residues linked to Lys63 of ubiquitin itself. It has recently been demonstrated that mono-ubiquitination is not only important for receptor internalisation, but also for endosomal sorting (Katzmann et al., 2001).

Protein sorting and cell surface receptor downregulation in the multivesicular body (MVB) pathway involves ubiquitin as a signal required for entry in the pathway. MVB is also important for delivery of hydrolases to the lysosome. A conserved component of the endosomal machinery termed ESCRT-1 (Endosomal Sorting Complex Required for Transport), recognises ubiquitinated MVB substrates and functions in both yeast and mammalian cells to transport these

substrates into budding late endosomal vesicles that will form an MVB. Subsequent fusion of the mature MVB with the lysosome will result in delivery of internal vesicles and their cargoes to the lysosomal lumen for destruction. ESCRT-1 is able to bind Ub via its Vps23 component, which comprises a Ubc-like domain. It has been suggested but not proven, that this interaction is direct.

Ubiquitin-tagged receptors are targeted to the vacuole following internalisation in yeast. In mammalian cells, however, ligand-induced and constitutive endocytosis are often followed by re-cycling or dissociation from the ligand and re-location at the cell surface. It is not known whether these recycling processes coincide with cycles of ubiquitination and de-ubiquitination of the target plasma membrane proteins.

1.6.12 De-ubiquitinating enzymes

Release of ubiquitin from its adducts is essential for two processes: Ubiquitin biosynthesis and the degradation pathway. Ubiquitin is synthesised either as a linear polyubiquitin precursor or as an N-terminal fusion of two ribosomal proteins and acts as a chaperone that targets them to the ribosomal complex. In the former case individual Ub molecules are released from the chain by specific enzymatic cleavage between the fused residues that renders them available for conjugation to the substrate protein. The last ubiquitin residue in the precursor chain contains an additional C-terminal amino acid that must be removed in order to expose the active C-terminal glycine. In the second type of precursor, ubiquitin is cleaved from the ribosomal complex after incorporation of the proteins it is fused with (Ciechanover, 1998).

In the process of degradation, ubiquitin has to be released from mis-targeted proteins in the “proof-reading” mechanism of the pathway, from the lysine side chains of the substrate upon encounter with the proteasome and from the end proteolytic products. Multi-ubiquitin chains removed from substrates must also be disassembled to recycle Ub molecules. Cleavage of Ub residues, in any case, is performed by either of the two classes of thiol proteases that recognise the C-terminal region of Ub. Ubiquitin C-terminal hydrolases (Uch) and Ubiquitin-specific proteases (UBP) (Hochstrasser, 1996).

Uch proteases are ~25 kDa enzymes, which play a role in the post-translational processing of Ub precursor molecules and mediate Ub release from adducts with amines and thiol groups.

UBPs are larger enzymes (~100 kDa), involved in the cleavage of Ub from cellular proteins or free poly-ubiquitin chains (Ciechanover, 1998). UBPs exist either as free enzymes or associated with the 19S component of the proteasome and may function in an energy dependent or independent manner. De-ubiquitinating enzymes may act to inhibit or promote proteolysis. Binding of a UBP specifically to a protein that bears a degradation signal results in inhibition of proteolysis by preventing the assembly of a multi-Ub chain (Varshavsky, 1997). Inhibition of protein degradation is also accomplished by removal of the Ub tag from incorrectly targeted polypeptides.

Acceleration of proteolysis is mediated by release of Ub from inactive precursors or terminal proteolytic products thus ensuring re-use of Ub moieties. De-ubiquitinating enzymes promote the function of the proteasome by catalysing the disassembly of multi-Ub chains which could bind to the proteasome and inhibit

its action, or by modifying the chains to render them easily recognisable by the 26S proteasome.

1.6.13 The proteasomal pathway

Proteolysis is an essential cellular process but could also prove dangerous unless spatially and temporally regulated. To control protein breakdown, the cells have devised a strategy referred to as compartmentalisation whereby the proteolytic action is restricted to specific sites, accessible only by polypeptides that bare a degradation signal (Baumeister et al., 1998). A degradation compartment can be a membrane-defined organelle, (e.g. the lysosome) or a self-assembled complex of unrelated proteolytic subunits that form a barrel-shaped structure. Subunit assembly in the latter case, termed self or auto-compartmentalisation, yields molecular destruction tools with greater flexibility than lysosomes (Lupas et al., 1997). These proteases display localisation signals that allow them to perform their function in various cellular locations in both the cytosol and the nucleus whenever their action is required. A paradigm of this type of protein regulation is the proteasome.

1.6.13.1 Structure and function of the 26S proteasome

The proteasome is the most abundant protease in the cytosol, accounting for approximately 1% of the total cellular protein content (Hirsch and Ploegh, 2000). It comprises a catalytic core, referred to as the 20S subunit, linked to a regulatory structure termed the 19S cap that binds to both ends of the 20S component to form the intact 26S proteasome complex (Figure 17).

The 20S proteasome is a cylindrical structure of 11 nm in diameter and 15 nm in length (Lupas et al., 1997). It comprises two different types of subunits, namely

α and β with distinct structural and functional roles that are further divided in seven subfamilies. Each 20S complex contains seven different α and seven different β subunits, arranged in the following order $\alpha 1-7 \beta 1-7 \beta 1-7 \alpha 1-7$, so that the α components form the outer rings and the β subunits the inner rings of the four stacked- ring structure (Hirsch and Ploegh, 2000) (Coux et al., 1996). Both α and β -type subunits belong to a family of N-terminal (Ntn) hydrolases that consist of two central antiparallel β -sheets flanked on either side by α -helices. The active site cleft is formed by an aperture at one end of the structure (Lowe et al., 1995).

The α subunits are more conserved both within and among species and are capable of forming rings, unlike β subunits whose assembly requires the prior formation of α rings. They possess a nuclear localisation signal (NLS) and thus control the nuclear action of the intact proteasome. Their role includes the generation of a physical barrier that controls the access of substrates to the catalytic core and association with the 19S and 11S modifiers of proteolytic activity of the complex. Despite the fact that they are catalytically inactive, they are necessary for the stabilisation of the two-ring structure of the β chains.

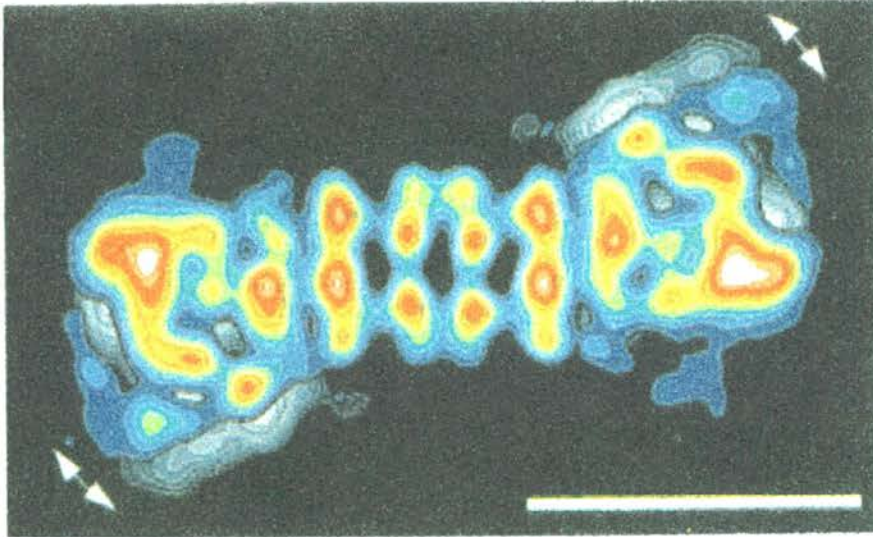


FIGURE 17. Structure of the 26S proteasome. Electron microscopic image of negatively stained specimens of the *Drosophila melanogaster* 26S proteasome. It comprises a catalytic core of four seven-membered stacked rings ($\alpha_7\beta_7\beta_7\alpha_7$), termed the 20S subunit, linked to a regulatory structure, the 19S cap, on either side. Two superimposed states of the 26S complex (one in grey and one in colour) are shown, indicating the flexibility in the linkage of the 19S caps to the 20S core. (White arrows indicate direction of motion, scale bar is 20 nm) (After Baumeister, 1998).

The β subunits are generated by cleavage of an N-terminal pro-sequence to reveal an active terminal threonine residue. The crystal structure of the 20S proteasome has revealed a distance of 28 Å between the active Thr sites of adjacent β subunits which suggests that the length of the generated proteolytic products could be approximately 8 amino acid residues. They are involved directly in peptide hydrolysis and can display peptidase activity even when expressed in the absence of α subunits (Coux et al., 1996). Adjacent pairs of identical β subunits, located on different β rings, give rise to six proteolytic sites. Each pair exhibits one of the following three distinct catalytic activities: a trypsin-like activity which cleaves after basic residues, a chymotrypsin-like one that cleaves after large hydrophobic residues and a post-glutamyl peptidyl hydrolytic (PGPH)-like one with a preference for acidic residues (Coux et al., 1996) (Ciechanover, 1998). In vertebrates, the presence of three additional interferon- γ (IFN- γ) inducible β subunits (LMP2, LMP7 and MECL1), may alter the peptidase activity of the proteasome (Hirsch and Ploegh, 2000). The exchange of three proteasomal subunits, namely X, Y and Z for the IFN- γ inducible β subunits LMP2, LMP7 and MECL1, respectively, leads to stimulation of trypsin-like and chymotrypsin-like activities, whereas the PGPH-like activity is reduced. These subunit exchanges, as well as point mutations in constitutive β chains are also thought to have given rise to two less characterised activities of the proteasome; BrAAP activity, which is targeted to branched-chain amino acids and SNAAP activity, that cleaves after small neutral residues (Meng et al., 1999).

To generate the complete 26S proteasome complex, the 20S core associates via its α subunits with a large regulatory complex that comprises at least 18

proteins whose molecular weights range from 25 to 110 kDa, in an ATP-dependent fashion. This complex, termed the 19S cap or proteasomal activator 700 (PA700), is responsible for selective degradation of ubiquitinated proteins and the activation of the peptidase activities of the 20S component. It comprises a Ub-chain binding site and a number of ATPases. It also displays isopeptidase activity for removal of Ub chains from degradation substrates prior to their entry into the catalytic complex.

Substrate recognition by the 26S proteasome is possibly accomplished by the interaction of particular 19S subunits with the multi-Ub chains of target proteins. It has been demonstrated that ubiquitin ligase-bound substrates interact directly with subunits of the 19S particle. Yeast Ubr1 and Ufd4 that constitute components of E3 ubiquitin ligases employed in the N-end rule and UFD pathway, respectively, have been found to associate with Rnp2, Rpt1, Rpt6 and exclusively Rpt6, respectively (Xie and Varshavsky, 2000). A model of delivery of substrates to the proteasome proposed by Xie and Varshavsky, predicts interaction of E2-E3 complexes with target proteins recognised by the presence of specific degrons, subsequent ubiquitination and delivery of the bound substrate to chaperone-like proteins of the 19S component of the 26S proteasome for degradation (Xie and Varshavsky, 2000).

The precise mechanisms of entry of substrates into the catalytic core and exit from the proteasome are not completely understood. The differences displayed by the bacterial *Thermoplasma acidophilum* and the yeast proteasomes as far as entry into the catalytic compartment is concerned, do not permit the deduction of a general mechanism. The *T. acidophilum* proteasome contains two entry sites at the

ends of the cylinder which are in contact with the seven α subunits. These pores are absent from the yeast proteasome, which appears to require rearrangement of the α subunits in order to allow entry of the substrate. Such rearrangements may occur following association with the 19S cap which would provide the necessary ATPase activity. The interface between α and β rings in the yeast proteasome, unlike its bacterial counterpart, exhibits narrow side orifices coated with polar residues, which lead to the active Thr sites of the β subunits. ATP-dependent rearrangement of these residues leads to generation of openings of approximately 10 Å in diameter which may serve as passage pores for unfolded protein substrates (Hershko and Ciechanover, 1998).

Another activator of the 20S that does not require ATP to exert its effect is the 11S or proteasomal activator 28 (PA28), a ring-shaped hexamer comprising alternating α and β subunits, that binds 20S on either or both ends. Association of 20S with two 11S particles leads to the formation of a complex that unlike the 26S proteasome, degrades only peptides and not intact ubiquitinated proteins. This is indicative of a role in processing 26S-generated proteolytic fragments into smaller peptides that can be recognised as epitopes by the class I MHC complex (Ciechanover, 1998). In support of this view, a proteolytic complex that consists of 20S bound to both 19S and 11S on either side, has been reported, that is able to perform proteolysis of intact Ub-tagged proteins and subsequent trimming of the resulting peptides (Hendil et al., 1998).

1.6.13.2 Subcellular localisation of the proteasome

Proteasomes are found dispersed in the cytosol or associated with ER membranes and the centrosome. The NLS signal present in α rings of the 20S

particle, is responsible for the nuclear distribution of the 26S complex. Fractionation studies have revealed the localisation of proteasomes at the nuclear envelope (Enenkel et al., 1998). Such diversity in the intracellular distribution of the proteasome could be the result of the action of modulators (e.g. the 19S or 11S particles) to serve as adapters that link the proteasome with subcellular compartments. An alternative mechanism would involve the implication of IFN- γ -inducible β subunits. However, both models contain drawbacks. In the former, a negative point is the complexity of the existence of multiple adapters for different types of association. In the latter, the presence of IFN- γ -inducible β subunits exclusively in vertebrates would fail to explain subcellular distribution in other types of organisms.

Hirsch and Ploegh suggest a model that arises by analogy to the association of the ribosome with the ER membranes. Proteasomes have been documented to associate with both soluble and membrane-bound proteins. Ubiquitination of membrane proteins occurs while the substrates are still embedded in the membrane. Subsequent interaction of the Ub-tagged polypeptide with the proteasome could result in anchoring the protease complex to the membrane and thus altering its subcellular localisation. Release of the proteasome from the membrane-bound complex and return to the pool of free proteasomes would follow substrate degradation (Hirsch and Ploegh, 2000). The same principle would apply for substrates bound to other organelles such as the centrosome or the cytoskeleton.

Proteasomes are absent from the ER lumen but their association with the ER membrane suggests a role in turnover of ER-resident polypeptides. ER-localised chaperones probably function to recognise partially folded or mis-folded proteins

and transport them to sites where their cytosolically exposed regions could be tagged by Ub molecules. These regions act to recruit the proteasome to the ER membrane. Interaction of the substrate with the proteasome results in removal of the protein from the ER membrane through, possibly, a protein-conducting channel. According to this view, which resembles the co-translational translocation of polypeptides accomplished by the ribosome, the proteasome is indirectly linked to the membrane in a process referred to as “co-degradational translocation” (Hirsch and Ploegh, 2000).

1.6.13.3 Ub-independent function of the proteasome

The proteasome was identified by its association with the ubiquitin pathway of protein degradation, as the protease responsible for the destruction of ubiquitinated polypeptides. However, it is also able to function in the regulation of proteins that do not bear Ub tags.

This process, that is also ATP-dependent, has been observed in the cases of casein, albumin and the oncoprotein c-Jun, to be reduced by several –fold but still operate despite the absence of Ub. The latter is also rapidly degraded in a Ub-dependent manner *in vivo*. The enzyme ornithine decarboxylase involved in polyamine biosynthesis, is regulated by the 26S proteasome in a Ub-independent fashion, presumably due to the exposure of a cryptic degradation signal found at its C-terminus that is revealed upon interaction with antizyme and serves as a recognition cue for the proteasome (Coux et al., 1996). Ubiquitin-independent degradation via the proteasome may exist for other unidentified cellular proteins.

1.6.13.4 Inhibition of the proteasome

The discovery of a number of inhibitors of the proteasome has been proven a very powerful research tool in the study of its structure and function as well as its participation in the ubiquitin-mediated degradation of specific proteins. Additionally, these molecules have a potential role in medicine and biotechnology. Their ability to mediate the turnover of transcription factors by blocking the proteasomal degradation pathway, may lead to regulation of a number of genetic diseases. Their application in cancer therapy is also a possibility but careful assessment of potential toxic effects would be necessary.

1.6.13.4 (a) Non-specific inhibitors

Peptide aldehydes

The first inhibitors to be identified, were the peptide aldehydes, N-acetyl-Leu-Leu-norleucinal (ALLN) and N-acetyl-Leu-Leu-methional (ALLM) which were found to covalently and irreversibly modify the Thr active site of β subunits, thus blocking the degradation of the majority of cellular proteins. Peptide aldehyde inhibitors subsequently identified, include Carbobenzyl-(Cbz)-Leu-Leu-norvalinal (MG-132) and Cbz-Leu-Leu-norvalinal (MG-155) which act to suppress the chymotrypsin-like activity of the proteasome (Lee and Goldberg, 1998). Cbz-Ile-Glu-(O-t-Bu)-Ala-leucinal (PSI) is another aldehyde inhibitor that is able to block the activity of the 26S proteasome without affecting the ATPase or isopeptidase activities.

Peptide aldehydes are described as reversible inhibitors because their removal restores proteolytic activity and they generally do not affect cell viability for 10-20 hours (Lee and Goldberg, 1996). However, their action was not specifically

targeted to the proteasome, since at higher concentrations they were observed to inhibit lysosomal cysteine proteases and calpains (Hershko and Ciechanover, 1998) (Lee and Goldberg, 1998).

1.6.13.4 (b) Proteasome-specific inhibitors

Proteasome inhibitors that are much more specific than peptide aldehydes in the sense that they target only a few non-proteasomal peptidases or act exclusively to inhibit the proteasome, are classified in this group. Such inhibitors include lactacystin, carbobenzyl-Leu-Leu-Leu-vinyl sulfone (Cbz-L₃VS), peptide boronic acids and epoxomicin (Fenteany et al., 1994) (Bogyo et al., 1997) (Meng et al., 1999).

Lactacystin

Lactacystin is a *Streptomyces* metabolite that inhibits cell- cell progression and induces de-differentiation in Neuro 2A murine neuroblastoma cell line (Dick et al., 1996). Hydrolysis of lactacystin gives rise to its active analogue *clasto*-lactacystin β -lactone which can readily penetrate cells. β -lactone acts as a pseudosubstrate that binds to the hydroxyl groups on the active site Thr of the β subunits and inactivates irreversibly the chymotrypsin and trypsin-like activities of the proteasome. Despite its apparent specificity for the proteasome, lactacystin also inhibits cathepsin A and tripeptidyl peptidase II (Geier et al., 1999).

Vinyl sulfone and boronic acids

Similar to that of lactacystin, is the action of Cbz- L₃VS. It covalently modifies the N-terminal active site Thr of β subunits. Its action is irreversible and affects all three characterised peptidase activities of the proteasome. It is also able to inhibit non-proteasomal proteases such as cathepsin S (Lee and Goldberg, 1998).

A class of proteasome inhibitors that contain an inhibitory boronate group linked to a natural or synthetic peptide sequence [Cbz-Leu-Leu-Leu-B(OH)₂], are able to reversibly attach to proteasomal catalytically active sites. Although their activity rate is approximately 100 times slower compared to peptide aldehydes, they display higher specificity for proteasomal proteases.

Epoxomicin

Epoxomicin is a natural α,β' -epoxyketone product, isolated from an *Actinomycetes* strain, which displayed anti-tumor activity against murine B16 melanoma tumors. It has been found to covalently bind to the IFN- γ -inducible β subunits LMP7 and MECL1 as well as their normal counterparts Y and Z subunits of the 20S proteasome. It inhibits primarily the chymotrypsin-like activity but it also affects the trypsin- like and PGPH-like at 100- and 1000-fold slower rates, respectively (Meng et al., 1999).

Epoxomicin is cell permeable and can inhibit proteasomal activity potently, selectively and irreversibly. It has been reported to inhibit the chymotrypsin-like activity 80-fold faster than lactacystin and 4-fold faster than *clasto*-lactacystin β -lactone. It targets the proteasome highly specifically, since it does not inhibit any of the known non-proteasomal proteases affected by other peptide-based inhibitors. At concentrations up to 50 μ M, it remains unreactive against trypsin, chymotrypsin, cathepsin B, papain and calpain. Epoxomicin is described as a unique molecular probe, which possesses the versatility to investigate the function of the proteasome in normal and pathological processes (Meng et al., 1999).

1.6.14 Functional diversity of the ubiquitin pathway

The ubiquitin pathway is employed in a wide range of cellular processes, including the cell cycle, cellular response to stress and extracellular signals, modulation of cell surface receptors, ion channels, DNA repair, differentiation and development, organelle biogenesis, the immune and inflammatory responses and apoptosis. Defects in the pathway have been implicated in the pathogenesis of a number of inherited and acquired diseases, which is hardly surprising, given the variety of substrates and processes associated with the ubiquitination cascade (Ciechanover, 1998). Conjugation to Ub may serve the regulation of protein levels by specific degradation but it could also function to promote protein synthesis. Ubiquitin has been described to act as a chaperone to facilitate organelle biosynthesis (Finley et al., 1989).

In the following section, the diversity of the cellular role of ubiquitin will be demonstrated focusing on its involvement in the pathogenesis of a number of diseases. A distinction between the destructive and non-destructive functions of the ubiquitin system will also be presented.

1.6.14.1 Destructive role of Ub

1.6.14.1 (a) Implication of the Ub pathway in disease

Cell survival and differentiation depend on spatial and temporal regulation of protein levels and defects in relevant control mechanisms, lead to manifestation of pathological states. Aberrations in the ubiquitin system of protein turnover, give rise to alterations in the steady-state levels of substrate proteins, thus resulting in the onset of either of two types of diseases. In the first type, pathology is due to accelerated degradation of a substrate, whereas decreased turnover rates of target

proteins are characteristics of the second type. This second type includes diseases that arise by mutations in either the enzymes involved in the system, or in recognition motifs on substrate proteins (Figure 18) (Hershko et al., 2000). Gain-of-function mutations result in accelerated degradation, whereas loss-of-function ones, lead to stabilisation of target polypeptides.

The degradation of p53 tumour suppressor, mediated by E6-AP ubiquitin ligase, is accelerated via its association with the human papilloma virus (HPV) E6 protein. E6 renders p53 recognisable by the ligase. The level of p53 is extremely low in uterine cervical carcinomas, which suggests that the virus uses the removal of the tumour suppressor as a means to transform cells.

Mutations in E6-AP that prevent association with its unidentified native substrate(s) (p53 is not a native substrate for E6-AP), result in their accumulation which appears to be toxic for the developing brain. Built-up of protein due to malfunction in E6-AP, is responsible for a pathological state described as Angelman's syndrome. It is a rare inherited disorder demonstrated by seizures, mental retardation and abnormal gait.

Pathogenesis of Ubiquitin System- Related Diseases

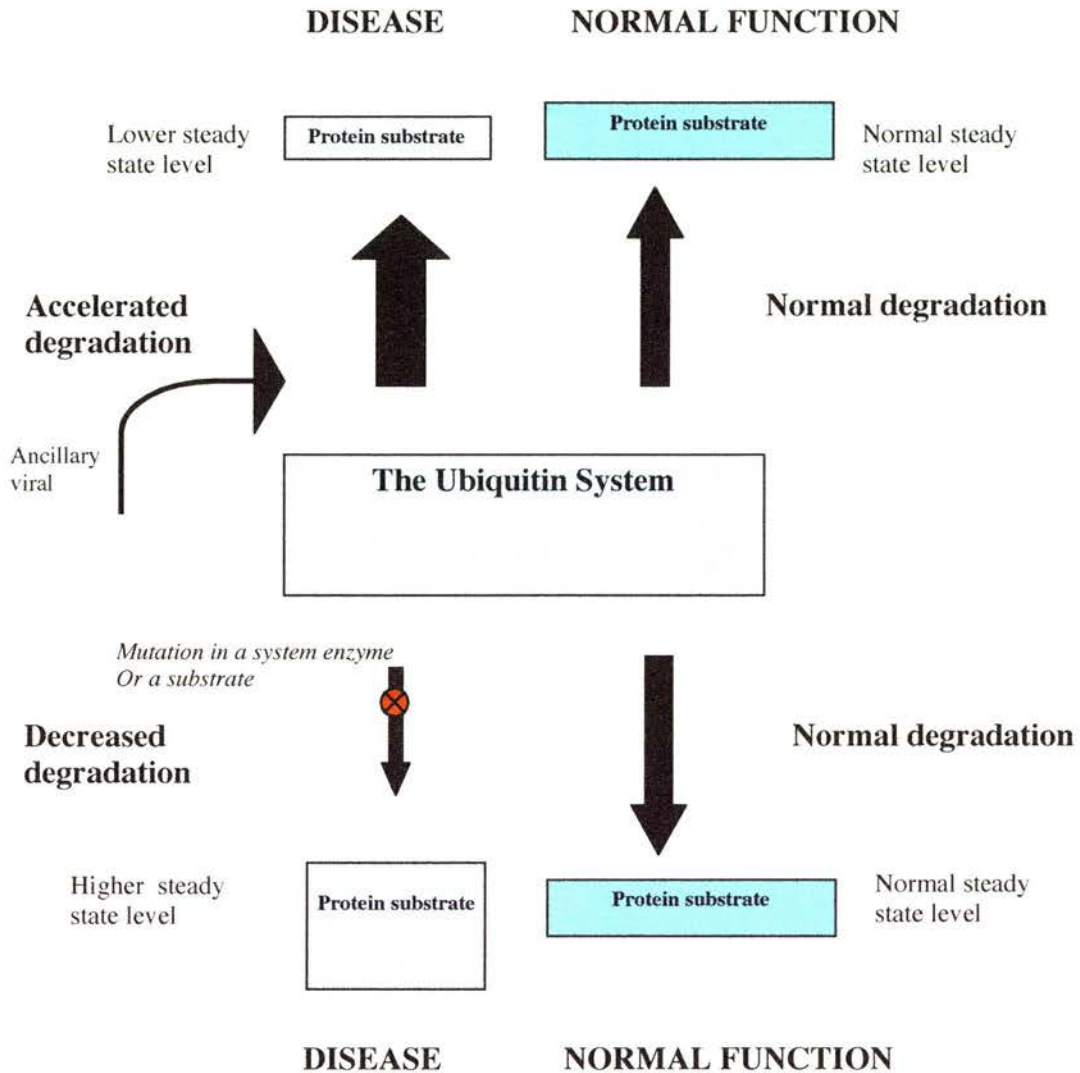


FIGURE 18. Pathogenesis of Ubiquitin System-related diseases. De-regulation of the function of the ubiquitin system of protein degradation is responsible for the manifestation of two types of disease: pathological states may arise either due to increased degradation of a protein, or owing to accumulation of a substrate protein, as a result of a decrease in its degradation rate (Adapted from Hershko, 2000).

Decreased rates of protein degradation as a result of mutations in recognition motifs on target proteins, have been observed in the cases of β -catenin and ENaC.

β -catenin is involved in signal transduction and differentiation of the colorectal epithelium. Mutation in the phosphorylation-targeting sequence of β -catenin which links it to the ubiquitin ligase complex, is responsible for stabilisation and accumulation of the protein. Uncontrolled activity of β -catenin is associated with colorectal carcinomas and malignant melanomas. Stabilisation of β -catenin may also be caused by mutations in adenomatous poliposis coli, a member of the degradation complex.

The amiloride-sensitive epithelial sodium channel (ENaC), is involved in sodium transport in kidney and other epithelia and it also regulates blood pressure. It is a heterotrimer of $\alpha\beta\gamma$ subunits, each containing two proline rich (PY) sequences. These sequences mediate binding to Nedd4 ubiquitin ligase at the WW domain. Deletion of PY motifs from β or γ subunits, gives rise to a pathological state termed Liddle's syndrome in which accumulation of the channel is the cause of hypertension owing to excessive re-absorption of sodium and water (Staub et al., 1996).

Immunohistochemical studies in many neurological disorders such as Alzheimer's (AD), Parkinson's (PD) and Lewy body diseases, amyotrophic lateral sclerosis (ALS) Creutzfeld-Jacob disease (CJD), Huntington's Disease (HD) and Spinocerebellar Ataxias (SCA), have revealed the presence of ubiquitin conjugates in both cytoplasmic inclusion bodies and in structures associated with the endosome/lysosome (Arnold et al., 1998). It is not possible to conclude with certainty the precise role of ubiquitin in the pathology of these diseases.

Aggregation of ubiquitinated proteins could be due to cell-specific defects in either an enzyme involved in the pathway (e.g. a ligase), in a recognition motif of the substrate itself (e.g. phosphorylation site), or incorrect assembly of the proteasomal machinery. In any case, protein accumulation is responsible for the pathology and eventual death of specific neuronal populations.

Inclusions result either from the self-tendency of unfolded proteins to associate and form insoluble aggregates or in a more complicated process that involves the transport of smaller aggregates along microtubules in a dynein-dependent retrograde manner, to form larger structures termed aggresomes (Johnston et al., 1998). Aggresomes are membrane-free cellular structures, formed when the cell's capacity to degrade misfolded proteins is exceeded. They contain ubiquitinated proteins, heat-shock proteins (hsp), ubiquitin-conjugating enzymes and proteasomes (Kopito, 2000). The presence of proteasomes in these structures indicates that aggresomes may be sites of proteolysis. An alternative view is that proteasomes are trapped within aggresomes, by polypeptides that are refractory to proteolysis, thus possibly reducing the overall capacity of the cells to degrade proteins (Sherman and Goldberg, 2001). Sequestering of unfolded proteins in the aggresome may serve to prevent their association with other cellular constituents and risk disruption of various cellular processes.

In polyglutamine-repeat containing proteins in HD and SCA, there is evidence to suggest that the extended polyglutamine sequence hinders degradation by the 26S proteasome through interactions with other molecules that prevent entry of the substrate in the 20S catalytic complex. Partial degradation releases smaller fragments with deleterious polyglutamine domains (Wellington et al., 1998).

Aggregation and abnormal association of mutant huntingtin with other cell proteins, results in impaired neuronal function and subsequent cell death. HD patients experience extensive neuronal loss in the striatum and cerebral cortex that is demonstrated by a reduction in brain size at the later stages of the disease.

Patients with another major neurological disorder, Parkinson's disease, display inclusions of α -synuclein, termed Lewy bodies, in their substantia nigra. These inclusions contain large amounts of ubiquitin and proteasomes which suggest that α -synuclein may be ubiquitinated, either prior to or following aggregation. The identification of parkin, a protein whose mutation results in one form of hereditary PD, as a ubiquitin ligase, classifies it as a candidate for α -synuclein ubiquitination (Sherman and Goldberg, 2001).

Heritable peripheral neuropathies caused by an increase in PMP22 expression, appear to be associated with the accumulation of the protein in aggresomes (Notterpek et al., 1999). Duplication of a 1.5 Mb region in human chromosome 17, that includes the PMP22 gene, results in a group of peripheral neuropathies collectively referred to as Charcot-Marie-Tooth type 1A (CMT1A) disease. In normal individuals, PMP22 is rapidly turned over in the Schwann cells. It has been suggested that the cell regulates specifically the levels of PMP22 via the ubiquitin/proteasome pathway. However, overexpression of the protein could overload the degradation machinery of the cell, leading to intracellular accumulation of PMP22. Inhibition of the proteasome with the inhibitor lactacystin, resulted in accumulation of ubiquitinated PMP22 in aggresomes. The possible implication of ubiquitinated protein aggregates in peripheral neuropathies

remains unclear. It is still not known whether ubiquitinated proteins undergo degradation in inclusion bodies or accumulate associated with proteasomes.

1.6.14.2 Non-destructive role of Ub in ribosome biogenesis

Ubiquitin has been established as a major regulator of protein turnover. An alternative role of the protein has been proposed, that involves its reversible association with a substrate in order to regulate its function without affecting its metabolic stability. Association with Ub has been observed to promote the formation of cellular components, whereby ubiquitin acts in a chaperone-like manner. One such example is the biogenesis of the ribosome.

Natural gene fusions give rise to linear ubiquitin adducts that are post-translationally processed to yield free ubiquitin molecules. In yeast *S. cerevisiae*, the hybrid proteins UBI1, UBI2 and UBI3 consist of Ub fused to amino acid “tail” sequences. These “tails” have been identified as ribosomal proteins whose association with Ub promotes ribosome biogenesis. The Ub moiety of UBI1-UBI3 possibly functions to transiently stabilise the tails and facilitate their incorporation into the nascent ribosomes. This is probably accomplished by increasing the rate of transport to and association with the ribosome, thus reducing the degradation rate of newly synthesised UBI1-UBI3, while transported to the ribosome (Finley et al., 1989).

In intact yeast ribosomes, ubiquitin is ligated to the L28 component of the large ribosomal subunit. Heavily ubiquitinated ribosomes have been found to be active in translation, *in vitro*. The ubiquitination of L28 is cell cycle dependent. It exhibits an increase during S phase and it declines in G₀ and G₁. Considering the fact that L28 is a stable protein, ubiquitination in this case plays a non-proteolytic role

(Spence et al., 2000). The multi-ubiquitin chain that is conjugated on L28 is formed by ligation of the C-terminus of one Ub residue on Lys63 of the previously linked ubiquitin. Ligation on Lys48 gives rise to chains that are preferentially recognised and degraded by the proteasome. This variant multiubiquitin chain (Lys63- linked) has been found to be necessary for the correct function of the translation machinery of the cell.

The ubiK63R yeast mutant, where lysine 63 has been substituted by an arginine, displays hypersensitivity to the translation inhibitors anisomycin and trichodermin, that target the peptidyl transferase centre, where L28 is located. This is indicative of a role of ubiquitinated L28 in the elongation phase of protein synthesis (Spence et al., 2000). The precise mechanism of such a role remains to be elucidated.

Potential new functions of ubiquitin are currently being investigated and it is assumed that the signal-recognising components of the pathway are much more numerous than previously appreciated. The interpretation of ubiquitin-based signalling, thus, may be critically influenced by the properties of the factors being involved in the pathway.

1.7 BACKGROUND TO THE PROJECT

L-periaxin was identified as a cytoskeleton-associated protein localised in the periaxonal membranes of Schwann cells. Its pattern of developmental expression and shift in localisation from the adaxonal to abaxonal membranes of myelin-forming Schwann cells, following their association with axons, implied a role in the stabilisation of the myelin sheath. This potential role was further supported by studies performed on mice that lacked a functional Prx gene (Prx^{-/-}). Prx-deficient mice appeared to form a normal myelin sheath, which was, however, unstable, leading to demyelination and the observation of clinical symptoms associated with neuropathic pain.

The recently identified participation of L-periaxin in a DRP2-dystroglycan complex implicated L-periaxin in the regulation of the terminal stages of the myelination process. L-periaxin associates with the DRP2-dystroglycan complex via a highly basic N-terminal domain, which also contains a NLS signal that is responsible for targeting the protein to the nucleus in embryonic Schwann cells. A PDZ domain, found upstream of the basic region, serves in mediating homodimerisation of the protein, which is believed to contribute to the stability of the DRP2-dystroglycan complex.

The protein also comprises a region of repeats and a highly acidic region proximal to the C-terminus. Acidic regions have been described as protein interaction motifs, therefore the potential role of the C-terminal acidic domain of L-periaxin was sought. Mutations in human L-periaxin are responsible for the manifestations of DNS and CMT4F neuropathies. Furthermore, a recently identified mutation that results in a truncated version of L-periaxin, which lacks the

C-terminus (including the acidic domain), is responsible for the early onset of autosomal recessive demyelinating peripheral neuropathy similar to CMT 4F (A. Williams, personal communication). This development increased the possibility of an important functional role of the C-terminal region of the protein, which was investigated.

1.8 PROPOSED STUDY

In an attempt to identify a potential functional role for the acidic domain and the C-terminus of L-periaxin, the possibility of their involvement in protein-protein interactions was assessed. The yeast-two hybrid genetic assay was employed in conjunction with biochemical methods, in order to identify and subsequently verify the association of L-periaxin with peripheral nerve proteins. The significance of the observed *in vitro* interaction was addressed by investigating the physiological role of the identified L-periaxin binding partner.

The effect of mutation of the interacting protein in the level of expression and localisation of L-periaxin, as well as the morphology of the Schwann cell and the process of myelination, was also considered. The generation of a transgenic mouse which over-expressed a mutant version of a positively interacting clone (dominant negative) was attempted in order to address the previously mentioned issues in a whole animal system.

Materials and Methods

2. MATERIALS AND METHODS

2.1 GENERATION OF L-PERIAXIN CONSTRUCTS FOR THE YEAST TWO-HYBRID SCREEN

Binding partners of L-periaxin were sought by applying the yeast two- hybrid technique described earlier (section 1.5). Truncated constructs of L-periaxin, to be used as “baits”, were generated as follows (Figure 19). PeriC1 (762-1383 aa) contained the region 37 amino acid residues after the repeat domain up to the C-terminus of the protein (623 aa). PeriC2 (996-1383 aa) consisted of the C-terminal 389 amino acids. PeriRA3 (700-1081 aa) encompassed a region of 370 residues between the end of the repeat region and the beginning of the acidic domain. Smaller constructs were also created in an attempt to deduce the minimal region of periaxin employed in interactions with library clones. PeriR5 contained 283 residues (712-995 aa) and PeriA6 encompassed 170 amino acids (996-1165 aa) which included the end of the repeat region and the whole of the acidic domain, respectively. PeriA7 (996-1080 aa) was a truncated version of PeriA6 which lacked the last 85 amino acids of the acidic domain. The 216 C-terminal amino acids of L-periaxin were used in PeriC8, whereas PeriC9 encompassed the extreme C-terminus of the protein (54 aa). All constructs were generated by PCR reactions using full length rat L-periaxin in pSPORT vector as template and were confirmed by sequencing. The oligonucleotide primer pairs used in each reaction are displayed in Table 3.

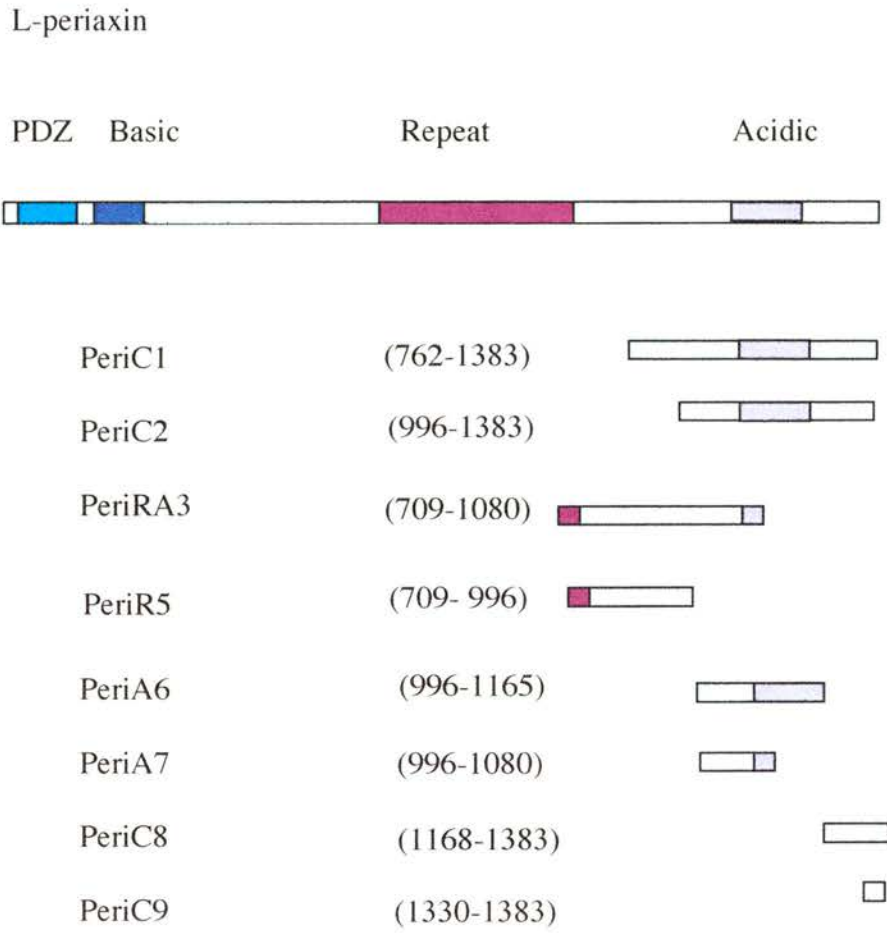


FIGURE 19. Full length L-periaxin and constructs used in yeast two-hybrid.
(Amino acid residues shown).

2.1.1 *PeriC1*

To generate PeriC1, full length L-periaxin in pSPORT was used as template in a PCR reaction with primers SV1-p300 to amplify a 735 bp product which possessed an EcoRI restriction site at the 5' end. The PCR reaction mix (50 μ l) consisted of 2 μ l template (200 ng), 5 μ l 2 mM dNTPs, 5 μ l 5 μ M primers, 5 μ l Dynazyme Buffer x10, sterile Milli Q water and 0.5 U Dynazyme thermostable DNA polymerase. A negative (no template) control reaction was also performed. The conditions used were: denaturation at 94 °C for 1 min, annealing at 55 °C for 1 min and extension at 72 °C for 30 s for 5 cycles, followed by 26 cycles of 94 °C for 40 s, 55 °C for 1 min and 72 °C for 30 s. The final stage comprised 1 cycle of denaturation at 94 °C for 40 s, annealing at 55 °C for 1 min and elongation at 72 °C for 5 min.

The SV1-p300 PCR product was digested with EcoRI and XhoI (Gibco BRL). The PCR product (22 μ l) was incubated with 3 μ l Buffer H (Mannheim Boehringer BCL), and 15 U of each enzyme (1.5 μ l) in a final volume of 30 μ l with Milli Q at 37 °C overnight. It was subsequently run on a 2% agarose TBE gel to resolve two fragments of 438 and 297 bp respectively. The 438 bp fragment was used to ligate to periaxin in pSPORT that had previously been digested with the same restriction enzymes. This gave rise to a periaxin construct that lacked the initial 2553 bp of the protein. This was digested with the restriction enzymes EcoRI and BglII. For this purpose, 2 μ l mini-prep DNA were used in a digestion reaction with 2 μ l React 3 buffer (Gibco BRL) and 10 U of each enzyme (1 μ l) to a total volume of 20 μ l with Milli Q water. The double digests were run on a 1% agarose gel in TAE and purified using the QIAEX kit for agarose gel extraction (Qiagen) according to the manufacturer's instructions. They were subsequently ligated into the cloning vector

pODB8 between the EcoRI and BamHI restriction sites of its multiple cloning site (MCS). For the ligation reaction, 4 µl of each of the vector and insert DNA were used with 1 µl ligation buffer (Fermentas MBI) and 1 U T₄ DNA Ligase (1 µl) (Fermentas MBI). The ligation was possible because BamHI and BglII are described as compatible enzymes, i.e. they yield complementary sticky ends (G ↓GATC↑ C for BamHI and A ↓GATC↑ T for BglII). pODB8 contains the binding domain region of GAL4 (147 bp) and includes the TRP1 gene which permits growth of the host yeast cells in media lacking the amino acid tryptophan.

2.1.2 *Peri C2*

The construction of PeriC2 required a PCR reaction with primers SV2-CSG2 under the same conditions as for PeriC1 described earlier. A 752 bp product was digested, in a total volume of 35 µl, with 2 µl React 3 buffer, 15 U EcoRI (1.5 µl), 3.5 µl Milli Q for 1.5 h at 37 °C, followed by addition of 2 µl React 3 buffer, 15 U StuI (1.5 µl), 1.5 µl Milli Q and incubation at 37 °C overnight. The double digest gave rise to two fragments of 500 and 189 bp, respectively. The latter fragment was ligated to periAxin in pSPORT, previously digested with EcoRI/ StuI. A construct of the C-terminal 1167 bp of the protein was formed which was subsequently ligated into the GAL4 binding domain vector pODB8, as described for PeriC1.

2.1.3 *PeriRA3*

PeriRA3 was generated by PCR with primers SV3F-SV3R. To amplify a 1.1 kb fragment, the following conditions were required: 5 cycles of denaturation at 94°C for 1min, annealing at 58°C for 1 min and extension at 72 °C for 4 min. This was followed by 28 cycles of 94 °C for 40 s, 58 °C for 1 min and 72 °C for 4 min. The final cycle involved denaturation at 94 °C for 40 s, annealing at 58 °C for 1 min and

extension at 72 °C for 5 min. The product contained an EcoRI and a BamHI restriction site at the 5' and 3' end respectively, which allowed ligation into the cloning vectors pSPORT and pODB8, after they were digested with the same enzymes. For this purpose, 25 µl purified (QIAEX) PCR product were digested with 3.5 µl REact 3 buffer and 15 U each enzyme (1.5 µl) in a total volume of 35 µl with Milli Q. The reason for generating a construct in pSPORT was to use it in sequencing reactions, as this vector contains the sequencing primer T7.

2.1.4 *PeriR5*

PeriR5 comprised 283 aa between positions 712 and 995. It was generated as a PCR product using primers SV3F and SV5R under the same conditions as for *PeriRA3*. The product contained an EcoRI site at the 5' end and a 3' end BamHI site which were used to ligate into the cloning vector pODB8.

2.1.5 *PeriA6*

PeriA6 was generated using primers SV2F2 and SV4R. To amplify a region comprising 170 aa (positions 996-1165) including the acidic domain of the protein, a PCR reaction was carried out under the following conditions: denaturation at 94 °C for 1 min, annealing at 60 °C for 30 s and extension at 72 °C for 1 min (5 cycles). The next stage consisted of 28 cycles of denaturation at 94 °C for 40 s, annealing at 60 °C for 30 s and extension at 72 °C for 1 min. The final cycle was performed at 94 °C for 40 s, 60 °C for 30 s and 72 °C for 2 min. The product was cloned into pODB8 between the EcoRI and BamHI sites of its MCS region.

2.1.6 *PeriA7*

PeriA7 was constructed using primers SV2F2 and SV3R under the same PCR conditions as for *PeriA6*. It was designed to encompass 85 amino acids between positions 996 and 1080. It was cloned into pODB8 between *EcoRI* and *BamHI*.

2.1.7 *PeriC8*

PeriC8 comprised the 216 C-terminal amino acids of L-periaxin (residues 1168-1383). It was generated as a PCR product with primers SV6F and DLS24 under the same conditions described for *PeriA6*. It was also cloned in pODB8 between the *EcoRI* and *BamHI* sites of the vector.

2.1.8 *PeriC9*

The extreme C-terminus of L-periaxin (54 aa) was amplified in a PCR reaction with primers SV7F and DLS24 (PCR conditions as described for *PeriA6*). The product contained an *EcoRI* site at its 5' end and a *BamHI* site at the 3' end. It was cloned into the GAL4 binding domain vector pODB8.

Maps of the plasmids used for the generation of the GAL4 hybrid proteins are shown in APPENDIX I (p.133).

Primer	Sequence (5' to 3')	Restriction Site (underlined)
SV1	<u>GGAATTC</u> ATTGAGGTTCCAGACAAACT	EcoRI
P300	ACAGCCCAAAGATGGC	
SV2	<u>GGAATTC</u> ATGCCCAAGCTGAAGATGCCA	EcoRI
CSG2	TATCCCTTCCTTGGCCTTTGC	
SV3F	<u>GGAATTC</u> CCCAAAGTGCCAGAGATGAAG	EcoRI
SV3R	<u>CGGGATC</u> CTTATAATGAGGACACCCACTGCGC	BamHI STOP codon
SV2F 2	<u>AGGAATTC</u> CCAAGCTGAAGATGCCA	EcoRI
SV2R2	<u>AAGCTT</u> ATCAGATGGCAGCAGCCTG	HindIII, STOP codon
SV4R	<u>CGGGATC</u> CTTACTGTTTCACCAGCCTGGGCTT	BamHI, STOP codon
SV5R	<u>CGGGATC</u> CTTACTTCACCTTCCCGTC	BamHI, STOP codon
SV6F	<u>CCGGAATTC</u> GAGGGCGGGTTAAAGCTGAA	EcoRI
SV7F	<u>CCGGAATTC</u> AAGTTCCGCTTTCCTTAGGGT	EcoRI
DLS24	ATAGTTTAGCGGCCGCAGATCTTCA GATGGCAGCAGCCTGGG	NotI, BglII, STOP codon

Table 3. Oligonucleotide primers for the generation of L-periaxin constructs. Restriction sites are underlined and the presence of a STOP codon is indicated.

2.2 SEQUENCING OF THE PCR PRODUCTS

The PCR products for constructs PeriC1, periC2 and PeriRA3, in the cloning vector pSPORT, were sequenced in a manual sequencing reaction with the T7 promoter primer. Sequencing of all other constructs was performed using the automated sequencing service at the Department of Biochemistry, University of Dundee, UK.

In the manual sequencing reaction, 1 μg plasmid DNA was denatured with 2 μl 2M NaOH in a final volume of 8 μl , for 10 min at room temperature. The sample was subsequently precipitated with 3 μl 3M sodium acetate pH 5.5, 7 μl Milli Q water and 60 μl absolute ethanol at $-70\text{ }^{\circ}\text{C}$ for 20 min. The DNA was then centrifuged at $4\text{ }^{\circ}\text{C}$ for 30 min at 13,000 rpm and the pellet was washed with 200 μl 70% ethanol. Following a 5 min centrifugation, the pellet was vacuum dried for 5 min and re-suspended in 5 μl distilled water. The denatured DNA sample was annealed to T7 sequencing primer (1 μl , 5 μM) with the addition of 1 μl annealing buffer and incubation at $37\text{ }^{\circ}\text{C}$ for 20 min followed by 10 min at room temperature. The annealed template was labelled in a 4-min incubation at room temperature with 3 μl labelling mix. This consisted of 1.5 μl Label Mix A, 1 μl T7 DNA polymerase diluted 1:4 v/v with dilution buffer, and 0.5 μl [α - ^{35}S] dATP. The reaction was terminated by the addition of 2.3 μl of the labelling mix to each of 4 tubes containing 1.3 μl of A, G, T, C termination mixes, that had been pre-warmed at $39\text{ }^{\circ}\text{C}$ for 4 min. After a 5 -min incubation at $39\text{ }^{\circ}\text{C}$, 2.5 μl of STOP buffer were added to each of the 4 tubes and the samples were placed on ice or stored at $-20\text{ }^{\circ}\text{C}$ overnight, prior to electrophoresis. All the reagents for labelling were provided in the Pharmacia T7 labelling kit. Electrophoresis of the labelled DNA samples was performed on a

sequencing gel that consisted of 6% acrylamide: bisacrylamide, 42% urea, 0.005% TEMED, 0.0025% APS in TBE. Aliquots of DNA (1.8 μ l) were pre-heated at 80 °C for 3 min and then loaded on the gel and run at 60 W for approximately 3.5 h. The gel was subsequently embedded into a fixative solution (5% methanol, 5% acetic acid) for 30 min and dried onto 3 MM Whatman paper under vacuum for 1 h at 80 °C. The dried gel was exposed to X-ray film (Agfa Curix RP-1 Plus) for 48 h at room temperature. It was developed for 3 min using Kodak X-ray developer and fixed for 2 min with Kodak Industrex fixer.

2.3 EXPRESSION OF PERIAXIN CONSTRUCTS

2.3.1 Fusion protein expression and extraction from yeast cells

The constructs were used to transform yeast strains CG1945 and Y190 as described in the LiAc/SS-DNA/PEG transformation protocol (Gietz and Sciesti, 1995) (see section 2.4). Colonies (3) of approximately 1-2 mm in size were allowed to grow in 9.4 ml synthetic dropout (SD) medium that lacked the amino acid tryptophan (-T) with 0.4 ml 50% glucose, for 48 h at 30 °C, 210 rpm. The yeast cultures were spun at 3,000 rcf for 5 min and the cell pellet was re-suspended in 50 ml YPAD medium, supplemented with 25% Glucose (final concentration). The culture was allowed to grow at 30 °C, 210 rpm until the OD₆₀₀ was approximately 0.6. At this point, the culture was harvested in pre-chilled Sorvall 50 ml tubes, half way filled with ice and spun at 1,000 rpm, at 4 °C for 5 min in a Sorvall RC 5B centrifuge. The supernatant was discarded and the pellet was re-suspended in 50 ml ice cold H₂O, to be spun as before. The final pellet was immediately frozen by immersion in liquid nitrogen and stored at -70°C.

To extract the expressed fusion protein from the yeast cells, the frozen pellet was quickly thawed by resuspension in 100 μ l Complete Cracking Buffer per 7.5 OD₆₀₀ units (see APPENDIX I, p.132). The OD₆₀₀ units were estimated by multiplying the final culture volume by the OD₆₀₀ reading obtained from the spectrophotometer. To determine the absorbance at 600 nm, 1 ml culture was used. The Complete Cracking Buffer had been pre-warmed at 60 °C and the pellet was briefly incubated in a water bath at the same temperature for no longer than 2 min to avoid the risk of proteolysis. The cell suspension was transferred to a 1.5 ml screw-cap microfuge tube which contained 80 μ l sterile glass beads (Sigma) per 7.5 OD₆₀₀ units, and subsequently incubated in a water bath at 70 °C for 10 min. 100mM PMSF (1% in Complete Cracking Buffer) was added and the sample was vortexed for 1 min. Cellular debris and unlysed cells were pelleted by centrifugation at 13,000 rpm for 5 min at 4 °C, and the supernatant (S1) was removed into a sterile 1.5 ml screw-cap microfuge tube and placed on ice. The pellets were re-suspended in 50 μ l Complete Cracking Buffer and boiled at 100 °C for 5 min. PMSF was added as previously and the suspension was vortexed vigorously for 1 min. This was followed by centrifugation at 13,000 rpm at 4 °C for 5 min and then the supernatant (S2) was combined with S1. The final supernatant was boiled for 4 min and immediately loaded onto an SDS polyacrylamide gel for protein separation by electrophoresis (SDS-PAGE).

2.3.2 Western Blotting

Proteins resolved according to size by SDS-PAGE were transferred onto nitrocellulose membrane (0.45 μ m, Schleicher & Schuell) in a buffer containing 25 mM Tris-HCl pH 8.3, 250 mM glycine and 20% methanol. The transfer was carried out in a Hoefer Mighty Small Transphor Unit (Pharmacia Biotech) refrigerated

apparatus for 2 h at 0.5 A. The nitrocellulose filter was then blocked in 5% dried skimmed milk, 0.1% Triton X-100 in PBS overnight. It was subsequently rinsed with 0.2% gelatin, 0.1% Triton X-100 in PBS and incubated with the primary antibody, diluted in the same buffer, for 1 h on a shaker. The primary antibodies, raised in rabbits, were specific for the C-terminus of periaxin for PeriC1 and PeriC2 (1369-1383 aa, provided by Prof. P.J. Brophy) and the repeat region of the protein for PeriRA3 (713-728 aa, obtained from N. Groome). Following 3 washes, for 10 min each, the filter was incubated with donkey anti-rabbit IgG HRP-labelled antibody (SAPU), in the same buffer as for the primary antibody, for 1 h. Excess secondary antibody was removed with three 10- minute washes. The peroxidase was detected using the enhanced chemiluminescence (ECL) method (Amersham).

2.4 YEAST TRANSFORMATION IN THE LiAc/ss-DNA/PEG PROTOCOL

Yeast *S. cerevisiae* cultures (2.5×10^8 cells) were grown at 30 °C, with shaking at 210 rpm, in a 50 ml culture supplemented with glucose (20% final concentration), until the cell density reached 2×10^7 cells/ml (approximately after 5 h). The culture was harvested in a sterile 50 ml Falcon tube and pelleted by centrifugation at 3,000 rcf (Megafuge 1.0 Heraeus benchtop centrifuge) for 5 min. The supernatant was discarded and the cell pellet was re-suspended in 25 ml sterile MilliQ H₂O. It was subsequently spun for 3 min at 3,000 rcf. The supernatant was removed and the cells were re-suspended in 100 mM LiAc (1 ml) and transferred to a 1.5 ml microfuge tube. The cells were precipitated at 13,000 rpm (Biofuge 13 Heraeus benchtop centrifuge) for 15 s and the LiAc was removed. They were subsequently resuspended in 100 mM LiAc, to a final volume of 400 µl and mixed by vortexing. The yeast cell suspension was

distributed to sterile 1.5 ml microfuge tubes (50 μ l/tube). The LiAc was removed following centrifugation for 20 s. The transformation mix consisted of the following components, added in the order listed below: 50% PEG (240 μ l), 1 M LiAc (36 μ l), 2 mg/ml ss-DNA (25 μ l) previously boiled for 5 min and kept on ice, 0.1-10 μ g plasmid DNA and MilliQ H₂O to a final volume of 50 μ l. The contents of each tube were mixed by vortexing and subsequently incubated in a 30 °C water bath for 30 min. This was followed by heat shocking in a 42 °C water bath for 22 min. The transformation mix was then spun at 6,000 rpm for 15 s. The supernatant was removed and the cell pellet was re-suspended in 1 ml MilliQ H₂O. A fraction of the transformation mix was delivered onto the appropriate dropout medium plates, which were subsequently incubated at 30 °C for 2-4 days to allow growth of the transformants.

2.5 REPORTER GENE AUTOACTIVATION TESTS AND TRANSFORMATION EFFICIENCY CONTROLS

Yeast strains CG1945 and Y190 were transformed, according to the LiAc/ssDNA/PEG transformation protocol, with each of the constructs and allowed to grow on media lacking the amino acid tryptophan (-T) or both tryptophan and histidine (-TH). The plates were assessed for expression of lacZ in the former case, and growth in the latter. Expression of lacZ would give a blue product upon reaction of its product, β -galactosidase, with the chromogenic substrate X-gal. This was investigated by filter lifts on the -T plates according to the Colony Filter-Lift Assay (see section 2.6). A positive control for the lacZ reaction is the interaction between pVA3-1 and pTD1-1. PVA3-1 encodes a DNA-BD fusion of murine p53 in the cloning vector pAS2-1 whereas pTD1-1 codes for SV40 large T-antigen fused to

DNA-AD in pACT II. The former plasmid contains the TRP1 gene as a nutritional marker whereas the latter expresses the LEU2 gene which encodes the amino acid leucine. Interaction between the two fusion proteins encoded by these plasmids would permit growth on -TLH medium. The negative control for this reaction was the co-transformation with plasmids pTD1-1 and pLam5'-1. The latter plasmid contains the TRP1 gene and encodes a fusion of the GAL4 DNA binding domain with human lamin which has been reported not to form complexes nor to interact with most other proteins. Yeast carrying these two plasmids would be able to grow deprived of tryptophan and leucine but would require the presence of histidine in the growth medium. Empty pODB80 vector was used as a control for autoactivation. This plasmid has the same backbone as pODB8, but lacks the HA epitope found in this vector. It was considered possible that this epitope could interfere with the activation of the lacZ gene.

2.6 COLONY FILTER-LIFT ASSAY

The detection of an interaction between proteins in the yeast two-hybrid is accomplished by the observation of growth in media that lack certain amino acids and by the expression of lacZ. In the latter case, reconstitution of a functional transcription factor, as a result of the association of the two test proteins, leads to expression of the downstream lacZ gene. This is observed by the formation of a blue product upon interaction of β -galactosidase, the product of the lacZ gene, with its substrate X-gal. The colony filter- lift assay is based on the visualisation of this reaction by the appearance of a blue product.

Following a three-day incubation at 30 °C, the plates containing yeast colonies grown in the absence of the amino acids tryptophan and/or leucine, were removed from the incubator and overlaid with a circular 70 mm sterile filter paper (Whatman # 5) that was allowed to soak on the agar for a few seconds. The filter paper was subsequently removed with forceps and soaked in liquid nitrogen for 15 s (colony face up). The frozen filter was then allowed to thaw on 3 MM paper, before it was placed in a 90 mm petri dish, on top of a second filter which had been soaked in 1ml Z buffer (60 mM Na₂HPO₄ • 2 H₂O, 40 mM NaH₂PO₄ • 2 H₂O, 10 mM KCL, 0.1 mM MgSO₄ • 7 H₂O), supplemented with 5% X-gal (20 mg/ml stock in DMF) and 0.27% β-mercaptoethanol (Sigma M3148). The petri dishes were placed in tightly sealed Ziploc plastic bags and incubated at 37 °C. They were checked periodically for the appearance of blue colouration, which would take from approximately 30 min to 8 h.

2.7 RAT SCIATIC NERVE cDNA LIBRARY SCREEN IN THE YEAST- TWO HYBRID SCREEN

PeriC1 was chosen as "bait" in order to screen a rat sciatic nerve cDNA library by employing the yeast two-hybrid method. The choice was based on the fact that it was the largest construct and encompassed regions of L-periaxin that were present in every other construct generated for the yeast two-hybrid screen.

The cDNA library was constructed by Dr C.S. Gillespie. Poly-A mRNA from P9 and P14 rat sciatic nerve was isolated and reverse transcribed using random nonamers incorporating a XhoI site at the 5' end of the transcript. Second strand synthesis and EcoRI adaptor ligation were carried out using the cDNA Synthesis kit (Stratagene # 200401) according to the manufacturer's instructions. Size fractionated

cDNA was ligated to λ ACT II between the EcoRI and XhoI restriction sites of the vector. The complexity of the directional cDNA library was estimated at 2.8×10^6 independent clones. Since the transformation efficiency was $1.36 \times 10^5/\mu\text{g}$, transformation with $30\mu\text{g}$ library DNA would result in screening the library 1.4 times. Yeast strain Y190 was transformed with $60 \mu\text{g}$ PeriC1 in pODB8 and $30 \mu\text{g}$ library DNA following the protocol described in section 2.4. The transformation mixture was plated on -TLH 30 mM 3-AT plates ($400 \mu\text{l}/\text{plate}$) and also $1 \mu\text{l}$ of a 1:10 dilution, $1 \mu\text{l}$ and $2 \mu\text{l}$ on -TL plates to estimate the efficiency of the transformation. The transformation efficiency was estimated according to the following formula; $\text{cfu} \times \text{resuspension vol. } (\mu\text{l}) / \text{Vol. Plated } (\mu\text{l}) \times \text{library DNA } (\mu\text{g})$. This was calculated at 1.07×10^5 which means that the complexity of the library was covered once. The plates were allowed to grow at $30 \text{ }^\circ\text{C}$ for 2 weeks.

2.8 TESTING FOR SPECIFIC LIBRARY-“BAIT” INTERACTIONS

The colonies grown on -TLH 30 mM 3-AT were subsequently used in further tests to assess the specificity of interaction with PeriC1. The possibility of interaction with the rest of the constructs was also assessed. The procedure to accomplish this included segregation of the AD and BD plasmids brought about by growth in Synthetic Dropout (SD) medium (2.58 ml) with 50% glucose ($120 \mu\text{l}$) and a dropout amino acid solution that lacks leucine ($300 \mu\text{l}$) for 48 h at $30 \text{ }^\circ\text{C}$, 210 rpm. Segregation was followed by isolation of yeast plasmid from the putative positive clones.

2.8.1 Isolation of plasmid from yeast

Overnight cultures in SD/Glucose/-L medium (3 ml) were centrifuged for 1 min at 13,000 rpm and the supernatant discarded. The pellet was re-suspended in 200 µl 100 mM NaCl, 10 mM Tris-HCl pH8.0, 1 mM EDTA, 0.1% SDS and glass beads (0.45 mm, SIGMA) were added just before addition of 200 µl phenol: chloroform. The samples were vortexed for 1 min and centrifuged at 13,000 rpm for 1 min. The top aqueous layer was retained and re-extracted with 200 µl phenol: chloroform as before. The top layer was collected in a 1.5 ml eppendorf tube and the DNA was purified with QIAEX kit for plasmid DNA purification (Qiagen) according to the manufacturer's instructions. The purified DNA was used to transform *E.coli* DH5α (Inoue et al., 1990).

2.8.2 Isolation of yeast plasmid from bacteria and insert analysis

Alkaline lysis of the bacteria and isolation of amplified plasmid was necessary for assessment of the presence and size of a library insert. *E.coli* colonies transformed with yeast plasmid were grown overnight at 37°C, 210 rpm in 5 ml LB Broth with 20 µl ampicillin (25 mg/ml). The culture (3 ml) was centrifuged for 1 min at 13,000 rpm and the pellets were re-suspended in 100 µl 25 mM Tris-HCl pH 8.0, 10 mM EDTA, 0.9% w/v glucose followed by addition of 200 µl 200 mM NaOH, 1% SDS. After a 5-min incubation on ice, 150 µl 11.5% v/v glacial acetic acid, 29.4% w/v potassium acetate in Milli Q water were added and the samples were incubated on ice for 5 min. Subsequently, a phenol: chloroform extraction step was performed with 450 µl phenol:chloroform, vigorous vortexing and centrifugation for 10 min at 13,000 rpm. The supernatant (350 µl) was removed and precipitated with 2 vol absolute ethanol at -70 °C for 15-20 min and spun for 20 min at 4 °C, 13,000 rpm. The pellets were

washed with 70% ethanol (500 μ l), centrifuged for 5 min and dried at room temperature. The dried pellets were re-suspended in 30 μ l TE/RNase cocktail (Ambion) (50:1).

Isolated plasmid was used in a series of digests with either EcoRI/XhoI restriction enzymes, as the library inserts had been cloned between those two sites, or BglII which flanks the whole multiple cloning site of pACT II vector. Plasmid DNA (2 μ l) was digested in a reaction with 6 μ l Milli Q water, 1 μ l enzyme buffer and 10 U restriction enzyme (or 0.5 U of each enzyme in a double digest) in a total volume of 10 μ l. Failure of segregation of the two plasmids which would lead to the indication of a false positive interaction with PeriC1, was accounted for by double digests with the restriction enzymes EcoRI and BamHI. These are the sites in which PeriC1 had been cloned into pODB8. A band of \sim 2kb, which is the size of PeriC1, would indicate the presence of the binding domain vector in the clone.

Clones found to contain a library insert and devoid of the binding domain vector were subsequently used in transformations with PeriC1 and the empty pODB80 vector in Y190. Activation of lacZ was again tested by filter lifts. Colonies that displayed a specific interaction with PeriC1 were subsequently tested for interaction with the rest of the L-periaxin constructs by filter lifts. Positively interacting clones were sequenced with the GAL4 AD forward primer (5' AGG GAT GTT TAA CAC TAC 3') by automated sequencing.

2.9 VERIFICATION OF INTERACTIONS BY BIOCHEMICAL METHODS

2.9.1 Generation, expression and purification of GST-fusion proteins of the interacting clones

2.9.1.1 Generation procedure

GST-fusions of the positively interacting library clones 11a and 26a were generated in the cloning vector pGEX-KG .

Clone 11a

Clone 11a in the activation domain plasmid pACT II (200 ng) was digested with EcoRI and XhoI (5 U each enzyme) in a total volume of 20 μ l with 2 μ l Buffer H and 12 μ l MilliQ H₂O. The reaction was carried out at 37°C for 1.5 h. The digested DNA was purified from a 1% agarose TAE gel using the QIAEX II kit (Qiagen) and ligated into vector pGEX-KG that had previously been digested with the same restriction enzymes. For the ligation reaction, which was performed at room temperature overnight, purified 11a (4 μ l) and empty vector pGEX-KG (4 μ l) were incubated with T4 DNA Ligation buffer (1 μ l) and T4 DNA Ligase (1 U) (Fermentas, MBI).

Clone 26a

To construct a GST-fusion of clone 26a, a PCR product was generated using primers 26aF3 and 26a R1 that contained an EcoRI and a SalI restriction site, respectively. Primer sequences are shown in Table 4. The PCR reaction mix (50 μ l) consisted of 2 μ l template (200 ng), 5 μ l 2 mM dNTPs, 5 μ l 5 μ M primers, 5 μ l Dynazyme Buffer x10, sterile Milli Q water and 0.5 U Dynazyme thermostable DNA polymerase. A negative (no template) control reaction was also performed. The conditions used were: denaturation at 94 °C for 40 s, annealing at 60°C for 1min and extension at 72°C for 1.5 min for 5 cycles, followed by 28 cycles of 94 °C for 40 s, 60

°C for 30 s and 72 °C for 1.5 min. The final stage comprised 1 cycle of denaturation at 94 °C for 40 s, annealing at 60 °C for 30 s and elongation at 72 °C for 3 min. The PCR product was digested with EcoRI/ SalI and ligated into pGEX-KG as described for clone 11a.

Primer	Sequence (5' to 3')	Restriction Site (underlined)
26aF2	<u>CGGGATCC</u> GAGAAGAAGCTCCTTGC TT	BamHI
26aF3	<u>GGAATTC</u> GAGAAGAAGCTCCTTGCT G	EcoRI
26aF6	<u>AGGCGCGCC</u> GCCACCATGGATT ACAAG	AscI
26aR1	ACGCGTC <u>GACTT</u> ATGTGGACTCTCTG GAAGAGG	SalI,STOP codon
26aR7	<u>AGGCGCGCC</u> TATGTGGACTCTCTGG AAGA	AscI,STOP codon
26aR8	GCGCCTGTGAGCACGAGCG	

Table 4. Oligonucleotide primers for clone 26a.

2.9.1.2 Expression of GST- fusion proteins

GST-fusion constructs were expressed in the bacterial strain *E. coli* BL21 CodonPlus RIL (DE3) (Stratagene) at 25 °C (clone 11a) and 30 °C (clone 26a). Overnight cultures of both clones (5 ml LB Broth / 20 µl ampicillin) grown at 37 °C, were diluted 1:100 and incubated with shaking at the temperature indicated above until OD₆₀₀ was 0.5. At this point, 400 µl culture was removed, spun at 13,000 rpm for 3 min and the pellet was re-suspended in 100 µl MilliQ water, 50 µl protein sample

buffer (X3) and 10 μ l 1 M DTT. It was then boiled for 4 min and stored at -20 °C as an un-induced sample. The rest of the culture was induced with 1mM IPTG (final concentration) and samples were removed and processed as before, at 30, 60 and 120 min following induction. Samples were separated on 12% SDS gel and stained with Coomassie Blue.

2.9.1.3 Purification of GST- fusion proteins

GST-fusions of clones 11a and 26a were grown in 2X 500 ml cultures each, at 25 and 30 °C respectively, to an OD₆₀₀ of 0.5- 0.6 and subsequently induced with 1mM IPTG for 2 h. The cultures were spun down at 4,000 rpm, for 10 min at 4 °C and subsequently re-suspended in 13 ml TBS/ 2 mM DTT/ Protease inhibitors (1 tablet per 50 ml TBS) (Boehringer). The re-suspended pellets were sonicated 6 x 10" and then spun for 40 min at 10,000 rpm, 4 °C. The supernatants were incubated with Glutathione Sepharose 4B (Pharmacia) on a rotating wheel at 4 °C for 30 min. The Sepharose resin was pelleted by centrifugation at 1,700 rpm for 5 min at room temperature and subsequently washed 3 times with 10 ml 1X PBS containing 2 mM DTT, 1 mM benzamidine and 0.5 mM PMSF. (The final wash was carried out without PMSF). The matrix was loaded into a column (Biorad) 10 cm X 1 cm and the fusion proteins were eluted with 5 ml 10 mM Glutathione (Sigma) in 50 mM Tris-HCl pH 8.0. The protein yield was estimated both by reading the A₂₈₀, and by SDS-PAGE on a 12% SDS gel stained with Coomassie Blue. The intensity of the bands to BSA samples of known concentration was compared.

2.9.2 Pull down assay from sciatic nerve homogenate

Four sciatic nerves from P13 rats were homogenised in 160 μ l lysis buffer containing 25 mM Tris HCl pH 7.5, 150 mM NaCl, 0.5% CHAPS, 5 mM NaF, 100

$\mu\text{g/ml}$ leupeptin (Sigma), $100 \mu\text{g/ml}$ antipain (Sigma), $7 \mu\text{g/ml}$ chymostatin (Sigma), 1 mM benzamidine, 1 mM TLCK (Sigma), 10 mM EDTA, 10 mM EGTA 1 mM PMSF. The homogenate was placed on ice for 5 min and subsequently spun at $13,000 \text{ rpm}$ for 10 min at $4 \text{ }^\circ\text{C}$. The supernatant was split into two tubes, each containing $100 \mu\text{l}$ Sepharose beads. The volume was taken up to $700 \mu\text{l}$ with lysis buffer and the lysate was pre-cleared on a wheel at $4 \text{ }^\circ\text{C}$ for 45 min. 10% of the sciatic nerve lysate was boiled in sample buffer and stored at $-20 \text{ }^\circ\text{C}$ as "input" lysate. GST-fusion protein ($6 \mu\text{g}$), or GST -alone (negative control) were conjugated to $40 \mu\text{l}$ Sepharose beads at $4 \text{ }^\circ\text{C}$ for 45 min. The beads were washed 3 times with 1 ml lysis buffer to remove unbound protein. Pre-cleared sciatic lysate ($280 \mu\text{l}$) was then added to the conjugates, which were incubated for a further 45 min at $4 \text{ }^\circ\text{C}$ in a rotating wheel. The samples were subsequently spun for 1 min at $3,000 \text{ rpm}$, $4 \text{ }^\circ\text{C}$ and the supernatants were discarded. The pellets were washed 5 times with 1 ml buffer, re-suspended in $60 \mu\text{l}$ H_2O / Sample Buffer/DTT and boiled for 4 min. The proteins were resolved by electrophoresis on an 8% SDS gel and a Western Blot was performed to assess the presence of L-periaxin bound to the fusion proteins.

2.9.3 Preparation of *in vitro* transcribed/ translated L-periaxin

2.9.3.1 (a) *In vitro* transcription of L-periaxin

In vitro transcription of full length L-periaxin in the vector pSV-SPORT was carried out using $1 \mu\text{g}$ DNA, $5 \mu\text{l}$ transcription buffer, $2 \mu\text{l}$ DTT, $0.5 \mu\text{l}$ Rnasin (Promega kit), $2 \mu\text{l}$ RNA CAP and $1 \mu\text{l}$ T7 polymerase to a final volume of $20 \mu\text{l}$ with MilliQ water. The reaction was performed for 1 h at $37 \text{ }^\circ\text{C}$. $1 \mu\text{l}$ of the product was run out on a 1% agarose TAE gel to check the quality of the synthesised RNA and $1 \mu\text{l}$ RQ1 Dnase (Rnase free) was added to the reaction mix to eliminate any unused DNA

template by incubating at 37 °C for 15 min. DEPC treated H₂O (100 µl) was added to the mix, followed by 1 vol of phenol/chloroform. The mix was vortexed and spun for 3 min at 13,000 rpm at room temperature. The top layer was removed into a clean tube, and an equal volume of chloroform was added. The contents of the tube were mixed using a benchtop vortex and subsequently spun for 3 min at 13,000 rpm, at room temperature. The top layer was again retained and the RNA was precipitated with 0.5 vol. 7.5 M ammonium acetate and 2.5 vol. 100% ethanol at -70 °C overnight. The mix was subsequently spun for 30 min at 13,000 rpm, 4 °C and the RNA was re-suspended in 15 µl DEPC H₂O. The concentration was estimated by reading the A₂₆₀.

2.9.3.1 (b) *In vitro* translation of L-periaxin

In vitro translation was carried out using the Rabbit Reticulocyte Lysate system (Promega, L4960) according to the manufacturer's instructions. 1 µg RNA was incubated with 35 µl rabbit reticulocyte lysate, 1 µl amino acid mix (-methionine), 4 µl ³⁵S-methionine (ICN), 1 µl Rnasin Inhibitor (Promega) in a total volume of 50 µl with DEPC H₂O, at 30 °C for 1.5 h. 1 µl of the translation product was removed to estimate the efficiency of radioactivity incorporation and the rest was frozen in liquid N₂ and stored at - 70 °C.

The retained 1 µl was placed onto a circle of 3MM paper (Whatman) and was allowed to dry for 30 min. The 3MM paper filter was incubated in 300 ml 10% TCA for 15 min on ice and then in 300 ml 5% TCA for 5 min on ice. It was subsequently boiled in 300 ml 5% TCA for 15 min and then washed twice for 5 min with 300 ml ice cold 5% TCA. Finally, the filter was washed in 300 ml 100% ethanol for 3 min and allowed to dry for 30 min before being decolourised with 5 µl 15% H₂O₂. The filter

was placed in a scintillation vial with 5 ml Optiphase Hisafe (Wallac Scintillation Products) and the ^{35}S incorporation was estimated in a scintillator (Beckman LS 6500).

2.9.3.2 Pull down assay using in vitro transcription/ translation product of L-periaxin

GST-fusions of 11a and 26a as well as GST-alone in the vector pGEX-KG (6 μg) were coupled to 33 μl Glutathione Sepharose 4B in the presence of 300 μl binding buffer (25 mM Tris HCl pH 7.5, 150 mM NaCl, 1 mM EDTA, 0.05% NP 40, 1 mM DTT, 10 $\mu\text{g}/\text{ml}$ leupeptin, 2 $\mu\text{g}/\text{ml}$ pepstatin, 0.7 $\mu\text{g}/\text{ml}$ chymostatin, 10 $\mu\text{g}/\text{ml}$ antipain, 1 mM benzamidine, 0.5 mM TLCK, 1 mM PMSF). The Sepharose beads had previously been washed twice with 100 μl binding buffer to remove residual ethanol. The binding of the fusion proteins to the beads was carried out at room temperature for 40 min on a rotating wheel. The beads were subsequently washed 3 times with 1 ml buffer to remove unbound material and 1×10^6 cpm of translated L-periaxin was added to each tube with 350 μl binding buffer and allowed to mix on a wheel for 1.5 h at 4 $^{\circ}\text{C}$. The beads were washed 5 times with 1 ml binding buffer and re-suspended in 25 μl $\text{H}_2\text{O}/\text{protein sample buffer}/\text{DTT}$. The mix was boiled for 3 min and the proteins were resolved on an 8% SDS gel by SDS-PAGE. The gel was stained with Coomassie Blue for 30 min and destained with 10% acetic acid/ 20% methanol to assess protein loading. It was then processed for fluorography using Amplify (Amersham Pharmacia Biotech) with mild shaking for 30 min and dried on 3 MM paper (RAPIDRY). Autoradiography was performed overnight.

2.10 NORTHERN BLOTTING OF 26a

2.10.1 Construction of hybridisation probe for northern blot

A hybridisation probe comprising the C-terminal 750 bp of clone 26a (376-1100 bp) was generated in the cloning vector pGEM 11 (Promega) that contains the sequences of promoters SP6 and T7. Clone 26a in the vector pACT II (cloned between EcoRI and XhoI) was digested with 5 U XhoI in a total volume of 10 µl, with 1 µl REact 2 buffer. The clone contained an internal XhoI site at position 376 bp. A fragment of 750 bp generated by the digest was ligated into pGEM 11 that had previously been digested with XhoI. The ligation reaction (4 µl vector, 4 µl insert, 1 µl Ligation buffer, 4 µl T₄ DNA ligase) was performed at 14 °C overnight. The orientation of the insert was assessed by restriction enzyme analysis.

2.10.2 Radioactive labeling of hybridisation probe

The probe (30 ng) was labeled using RANDOM PRIME DNA LABELLING kit (Gibco BRL). The DNA was boiled in distilled water (23 µl total volume) for 3 min and subsequently placed on ice for 1 min. Following a brief spin, nucleotide mix (6 µl) and random primers mix (15 µl) were added. The probe was subsequently incubated with 1.85 M Beq ³²P (ICN) and 3 U Klenow fragment enzyme at 25 °C for 1 h. The reaction was terminated with 5 µl STOP buffer and 100 µl 10mg/ml sheared salmon sperm DNA. The labelled probes were stored at -70 °C.

2.10.3 Preparation of RNA samples

Trigeminal nerve and brain total RNA from a P15 rat (5 µg) was dried in 0.5 ml eppendorf tubes and re-suspended in 10 µl denaturation buffer (50% formamide, 20% formaldehyde, 10% DEPC H₂O, 10% 10X MOPS, 10% 0.5 mg/ml ethidium bromide). The samples were incubated for 10 min at 70 °C, placed on ice for 1 min

and spun briefly. Sterile sample buffer was added (1 μ l) and the samples were separated on a 1.35% agarose/formaldehyde gel by electrophoresis at 70 V, 200 mA for approximately 2 h. The RNA was transferred onto a nylon transfer membrane (Schleicher & Schuell) for 2 h under a pressure of 50 mbar. The filter was dried overnight at 80 °C.

2.10.4 Hybridisation process

The membrane was soaked briefly in distilled water and placed in a 50 ml Falcon tube with 6 ml Quickhyb solution (Qiagen) and allowed to warm up at 65 °C for 30 min. The probe was boiled at 98 °C for 10 min and allowed to hybridise to the filter at 65 °C for 1.5 h. Following hybridisation, the filter was washed twice with Low Stringency buffer (2X SSC, 0.1% SDS) for 10 min each time, at room temperature. It was subsequently washed twice with Low Stringency buffer (0.2 X SSC, 0.1% SDS) for 30 min each time. The filter was dried at room temperature and wrapped in Saran film. Autoradiography was performed over a period of 48 h.

2.11 ISOLATION OF FULL LENGTH 26a (rFbx16) cDNA

The missing 5' end sequence of the full length 26a cDNA was obtained by 5' RACE (Rapid Amplification of cDNA Ends). Sciatic nerve RNA from P3, 9 and 16 rats (5 μ g) was used in a 5' RACE reaction with the clone-specific reverse primer 26aR8 and the 5' RACE primer provided in the GeneRacer kit (Invitrogen, Cat. No. 45-0079). The reaction was performed according to the manufacturer's instructions, by Dr CS Gillespie.

2.12 GENERATION OF C-TERMINAL ANTIBODIES AGAINST CLONE 26a IN RABBITS

2.12.1 Preparation of KLH-coupled peptides for injection

In order to raise antibodies specific to the C-terminus of clone 26a, the following peptides were synthesised by Research Genetics and supplied as dehydrated PBS salts: 26aC1: CLPRGLKRAYRGGLEEV and 26aC2: CSLNLRGTRVTPSTVSSV. Both peptides were provided as amidated at their C-termini and coupled to Keyhole Limpet Haemocyanin (KLH) via their N-terminal Cysteine residues. Conjugation to KLH enhances antigenicity. The supplied dehydrated salts were re-suspended in MilliQ H₂O to a final concentration of 1 mg/ml and dissolved at room temperature. Aliquots (2 ml) were prepared in 50 ml Falcon tubes and stored at -40 °C. Prior to injection, each 2 ml aliquot was mixed with 3 ml Complete Freund's Adjuvant (Sigma) and mixed by vigorous shaking at 4 °C overnight. The mix was spun briefly and 1.5 ml aliquots, 3 for each peptide, were prepared in 3 ml syringes (Becton Dickinson). Each aliquot was administered to a female New Zealand White rabbit. A boost injection was performed 3 weeks later. This time, the peptides were mixed with 3 ml Incomplete Freund's Adjuvant (Sigma). The rabbits were bled 2 weeks later to test for antibody production. All injections were carried out by Professor P.J. Brophy at the CTVM Facilities, Easter Bush, Edinburgh.

2.12.2 Assessment of rabbit anti-serum by Western Blotting

Test bleeds (3 ml) were collected in 5 ml Bijoux tubes and were allowed to clot at 4 °C overnight. The serum was removed into 1.5 ml microfuge tubes and spun at 13,000 rpm, 4 °C for 2 min to remove clotted blood. It was then aliquoted and stored at -40 °C. To assess the specificity of the anti-serum, a Western blot was performed using 10 ng

purified GST-26a protein and GST-alone (negative control) with 26aC1 and 26aC2 at 1:2,000 dilution. The secondary antibody used was anti-rabbit IgG-HRP at a dilution of 1:2,000 (Diagnostics Scotland). The ECL method (Amersham) was applied as described earlier. A Western blot was also performed to test the affinity purified anti-serum using 10 and 25 ng of GST-26a. The 26a antibodies were used at a dilution of 1:1,000. The dilution of the secondary α -rabbit antibody was 1:2,000.

2.12.3 Affinity purification of anti-serum

The anti-serum obtained from 4 rabbits (2 for each peptide), was affinity purified using an α -aminohexyl Sepharose 4B column, conjugated to non-KLH-coupled peptide. α -aminohexyl Sepharose 4B (1ml) was pipetted into a 15 ml Falcon tube, spun briefly to remove excess ethanol and washed 4 times with 3 ml 1X PBS. It was re-suspended in 2 ml 1 X PBS and 5 mg of MBS were added. The tube was placed on a rotating wheel at room temperature for 2 h and was subsequently spun, and washed 4 times with 3 ml 1 X PBS. The final spin (5 min) served to pack the Sepharose gel. The buffer was removed and the gel was incubated with non-KLH coupled peptide on a windmill at room temperature overnight. Prior to incubation with α -aminohexyl Sepharose 4B, 10 mg of each peptide were dissolved in 800 μ l 10 mM HCl in a 1.5 ml microfuge tube. The pH was adjusted to 6.0 with 100 mM NaOH.

The peptide/ Sepharose conjugate was washed 4 times with 1 X PBS. Anti-serum (5 ml) was added to the column and allowed to mix on a windmill at 4 °C overnight. Following an overnight incubation, the slurry was loaded onto a 10 cm X 1 cm column (Biorad) and was allowed to settle. The flow-through was collected in 20 ml Universal tubes and kept on ice in case the anti-serum hadn't bound to the matrix. The column was washed with 5 ml 20 mM sodium citrate until A_{280} was \sim 0. 50 mM citric acid pH

2.5 (6 ml) was added, and 0.5 ml fractions were collected into 1.5 ml microfuge tubes, already containing 0.35 ml 1 M HEPES pH 7.5. The yield was determined by reading the A_{280} of the collected fractions. When the absorbance at 280 nm reached approximately 0, the column was washed 4 times with 20 mM sodium citrate pH 7.7 and 4 times with 1 X PBS. It was stored in 1 X PBS/ 0.01% sodium azide at 4 °C.

2.13 UBIQUITINATION EXPERIMENTS

Isolation of the full sequence of clone 26a, revealed that it was part of the rat homologue of a previously identified F-box containing protein, namely Fbl6/Fbx16 (rFbx16). F-box proteins are known to be components of ubiquitin ligases, responsible for the recruitment of ubiquitination substrates. This was indicative of a potential role of rFbx16 in the ubiquitin-mediated proteolysis of L-periaxin. To investigate this possibility, a series of experiments to assess ubiquitination of L-periaxin as well as the involvement of the proteasome in its turnover, were conducted as described below.

2.13.1 Immunoprecipitation of ubiquitinated L-periaxin and β -catenin from P21 mouse sciatic nerve

The sciatic nerves from four P21 wild type mice were treated with either the proteasomal inhibitor epoxomicin (5 μ M) or its solvent DMSO (1%) as described in section 2.14.2 and boiled in 2% SDS (120 μ l/4 nerves) for 10 min. The tubes were subsequently spun for 10 min at room temperature. The supernatants were removed to sterile microfuge tubes, where 4 vol of Solution A (50 mM Tris HCl pH 7.5, 150 mM NaCl, 1 mM EDTA, 1 mM EGTA, 2.5% Triton X-100, 10 μ g/ml leupeptin, 10 μ g/ml antipain, 1 mM benzamidine, 0.5 mM TLCK, 1 mM PMSF) were added. The supernatant was divided into two tubes. Half was pre-cleared with 25 μ l 50% slurry of Protein A/ 500 μ l buffer (for periaxin) and the other half with 25 μ l Protein G/ 500 μ l

buffer (for β -catenin), at room temperature for 30 min. The tubes were spun for 1 min at 4 °C. The supernatants were retained and incubated with either 3 μ l rabbit polyclonal α -repeat periaxin antibody, or 5 μ l mouse monoclonal anti- β -catenin antibody (Santa Cruz) at room temperature for 2 h on a windmill. Protein A (or Protein G) slurry (30 μ l) was subsequently added to each tube and they were placed back on the windmill for 1 h. The mix was spun for 2 min at 4 °C and the supernatant was discarded. The pellets were washed 5 times with 1 ml Solution A, re-suspended in 25 μ l H₂O/protein sample buffer/DTT and boiled for 10 min. The proteins were resolved by SDS-PAGE on a 6% SDS gel (periaxin) and 12% SDS gel (β -catenin). Western blots were performed to assess the presence of ubiquitinated forms of L-periaxin and β -catenin in sciatic nerve, using a mouse monoclonal anti-ubiquitin antibody (Santa Cruz) at 1:500 dilution. To ensure that both L-periaxin and β -catenin had been immunoprecipitated from sciatic nerve, the blots were also probed with anti-repeat periaxin (1:20,000) and anti- β -catenin (1:1,000) antibodies.

2.13.2 Inhibition of the proteasomal pathway with epoxomicin to block L-periaxin degradation

Sciatic nerves from eight P21 wild type mice were removed and placed in 35 mm petri dishes containing 1 ml 1 X PBS. The nerves were stripped of the epineurium and placed in a 24-well tissue culture plate (Greiner), as follows: 8 nerves were incubated in 200 μ l RPMI-1640 medium (Sigma), supplemented with 2 mM L-Glutamine and 5 μ M epoxomicin (Calbiochem), the rest were incubated with 1 % DMSO (vehicle control) in 200 μ l RPMI-1640/ 2 mM L-Glutamine. The nerves were allowed to metabolise at 37 °C, 5% CO₂ for 90 min. Four epoxomicin- treated sciatics and four DMSO-treated ones were taken and boiled in 2% SDS, to be used in an

immunoprecipitation experiment exactly as described in section 2.9.1. The purpose was to investigate whether there would be an increase in the levels of immunoprecipitated periaxin by inhibiting the function of the proteasome. One sciatic nerve from each group (ie. Epoxomicin- treated, DMSO- treated) was also taken and boiled in 25 μ l H₂O/ protein sample buffer/DTT for 4 min and stored at -20 °C. To the rest of the samples, the translation inhibitor cycloheximide (CHX) (Sigma) was added to a final concentration of 50 μ g/ml and the nerves were placed back in the incubator at 37 °C, 5% CO₂. One nerve from each group was removed and boiled as before at 45, 90 and 180 min following addition of CHX. The proteins were resolved on an 8% SDS gel by SDS PAGE and a Western blot was performed using the rabbit anti-repeat periaxin antibody (1:20,000).

2.14 TISSUE DISTRIBUTION OF 26a

The level of expression of 26a in different tissues was assessed by Western Blot using homogenates from brain, spinal cord, sciatic nerve, liver, lung, kidney, heart and skeletal muscle from P21 mice.

The tissues were homogenised in 160- 320 μ l lysis buffer (150 mM NaCl, 50 mM Tris-HCl pH 7.5, 10 μ g/ml leupeptin, 0.7 μ g/ml chymostatin, 10 μ g/ml antipain, 200 mM benzamidine, 100 mM TLCK, 1 mM EDTA, 1 mM EGTA, 1 mM PMSF, 1% SDS) using a drill. The homogenate was boiled for 10 min and spun for 5 min at 13,000 rpm. The supernatant was removed to a clean tube and the protein concentration was estimated using the Micro BCA Protein Assay Reagent Kit (Pierce) according to the instructions provided by the manufacturer. A fraction of total protein (30 μ g) was separated on a 12% SDS polyacrylamide gel by SDS-PAGE and the

presence of Fbx16 was detected by Western Blotting using the 26aC1 antibody at 1:1,000 dilution.

2.15 TRANSGENESIS

The effect of L-periaxin stabilisation in the process of myelination in the sciatic nerve was investigated by inhibiting the turnover of the protein. To accomplish this, transgenic mice would be generated which over-expressed a deletion mutant of rFbx16, (rFbx16 Δ F) that lacked the F-box motif (dominant negative). The mutant version of rFbx16 would be able to bind L-periaxin via its C-terminal LRR region, but fail to target it to the SCF complex for ubiquitination and subsequent degradation. The original library clone found to interact with L-periaxin, 26a, comprised the LRR region but did not contain the F-box, so it was suitable to use in the transgenic construct.

2.15.1 Generation of rFbx16 Δ F transgenic construct

To generate rFbx16 Δ F, a fusion of FLAG-tagged clone 26a in the vector pBluescript SK II under the control of the mouse P0 promoter (construct mPo TOT asp, provided by Dr. L. Wrabetz), was created. 26a was initially cloned into the FLAG vector pCMV-2B (Stratagene). A PCR product was formed with primers 26aF2 and 26aR1 (see Table 4) that contained a BamHI and a Sall restriction site respectively, using 26a in pACT II as template (1:500). The reaction was performed under the conditions described in section 2.7.1. The PCR product (~ 1.1 kb) was purified as before and ligated into pCMV-2B between the BamHI and Sal I sites of its MCS.

FLAG-26a was subsequently cloned into mP0 TOT asp in the AscI site of the vector (Figure 20). A PCR product was generated using 26a in pCMV-2B as template (1:500) with primers 26aF6 and 26aR7 that contained an AscI restriction site (Table 4). The conditions used were: denaturation at 94 °C for 1 min, annealing at 58 °C for 1min and extension at 72 °C for 30 s, for 5 cycles, followed by 28 cycles of 94 °C for 40 s, 58 °C for 1 min and 72°C for 30 s. The final stage comprised 1 cycle of denaturation at 94 °C for 40 s, annealing at 58 °C for 1 min and elongation at 72 °C for 5 min. The product was purified and digested with 15 U AscI in a reaction mix of 35 µl, containing 3.5 µl NE Buffer 4 (New England Biolabs). Vector mP0 TOT asp (200 ng) was also digested with 10 U AscI in a total volume of 10 µl, with 1 µl NE Buffer 4. The reactions were carried out at 37 °C for 2 h. FLAG-26a was ligated into mP0 TOT asp overnight at room temperature.

FLAG-26a in mP0 TOT vector was used to transform *E.coli* DH5α cells, and the transgenic DNA was purified using the CLONTECH MIDI PREP kit according to the manufacturer's instructions. In order to remove the vector sequence, the DNA (46 µg) was digested with 30 U PacI in a total volume of 150 µl with 15 µl NE Buffer 1, supplemented with 1.5 µl BSA (10 mg/ml) at 37 °C, overnight. This was subsequently digested with 60 U NotI, to a final volume of 200 µl, with 20 µl REact 3 buffer. The digested DNA was separated on 0.8% low melting point agarose gel in TAE. The band corresponding to the transgene was excised and incubated with 0.04 vol 25 X agarase buffer (Boehringer) at 65 °C for 15 min. It was subsequently cooled down to 45 °C for 10 min before addition of 3.6 U of agarase (Boehringer). The reaction was allowed to proceed for 2 h at 45 °C.

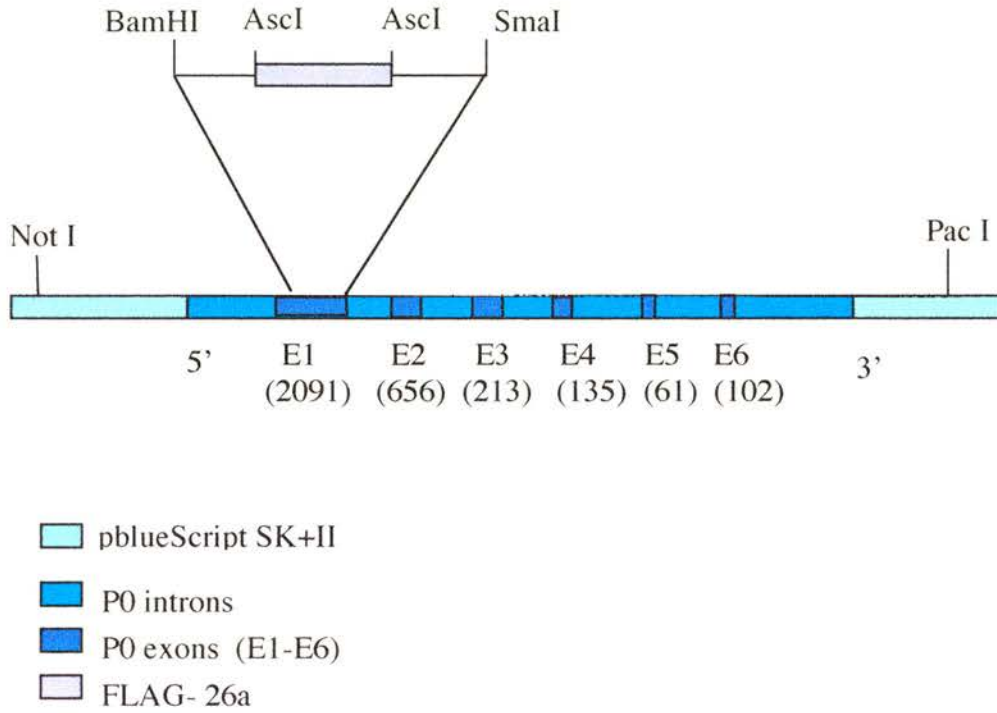


FIGURE 20. Structure of rFbxl6 Δ F construct for transgenesis. A fusion of rFbxl6 that lacks the F-box motif (original 26a clone), with a FLAG tag at its N-terminus, was introduced to Exon 1 of the mouse P0 gene in the cloning vector pblueScript SK+II. (Exon sizes in kb are shown in brackets).

2.15.2 Purification of transgenic DNA for nuclear transfer

The transgene was purified using an Elutip D-column Set (Schleicher & Schuell) according to the manufacturer's instructions. Following agarase treatment, the DNA was diluted in 10 ml low salt buffer (0.2 M NaCl, 20 mM Tris HCl pH 7.5, 1 mM EDTA pH 7.4) and put through the Elutip.

Elution was performed with high salt buffer (1 M NaCl, 20 mM Tris HCl pH 7.5, 1 mM EDTA pH 7.4) and the DNA was collected in a pre-cleaned microfuge tube. It was precipitated with 2 vol 100% ethanol at -70°C for 30 min and spun for 40 min at 4°C . The pellet was washed with 500 μl 70% ethanol, spun for 5 min at room temperature and allowed to dry. It was subsequently re-suspended in 50 μl millipore filtered injection buffer (10 mM Tris HCl pH 7.5, 0.1 mM EDTA pH 8.0). The concentration was estimated by running 1 μl and 1:1 dilution on a 1% agarose TAE gel, against 2 and 4 μl High DNA Mass Ladder. An aliquot of the DNA ($\sim 1.75\ \mu\text{g}$) was dialysed against 1 l injection buffer at 4°C for 48 h, with 3 changes of buffer over that period of time. The DNA sample to be dialysed was placed on the interior of the cap of a microfuge tube that had been cut so that the rim of the tube was still intact. A small square piece of prepared dialysis tubing (SIGMA) was placed over the cap and the rim was fitted over the tubing to keep it in place. (The dialysis tubing was prepared by boiling in water/ EDTA/sodium bicarbonate for 10 min and was rinsed in injection buffer just prior to use). The DNA sample was flicked onto the tubing and the cap was floated on the injection buffer. The DNA concentration was estimated after dialysis, as described previously. The sample was diluted with injection buffer to 2.5 $\mu\text{g}/\text{ml}$ and stored in 20 μl aliquots at -70°C .

2.16 IMMUNOSTAINING OF SCIATIC NERVE SECTIONS

Sciatic nerve transverse cryosections (7 μm in thickness) from P21 mouse were used to investigate the pattern of immunostaining of 26aC2 antibody. The tissue was fixed with 4% paraformaldehyde (PFA) on TESPA-treated microscope slides for 5 min. Excess PFA was removed with 1 X PBS and the tissue was subsequently incubated in methanol at $-70\text{ }^{\circ}\text{C}$ for 10 min. To prevent non-specific binding, the tissue was treated with blocking buffer (5% fish gelatin, 0.1% Triton X-100, 1X PBS) for 1 h, prior to incubation with the primary antibodies 26aC1 (1:200) and periC2 (1:5,000) in the same buffer, overnight. The primary layer was removed with 5 washes with 0.1% Triton in PBS. The secondary antibodies, goat anti-rabbit FITC (1:200) (SAPU) and donkey anti sheep TRITC (1:100) (Northeast), were applied for 1.5 h. Unbound antibodies were removed with 1 X PBS (4-5 washes for 5 min each time). The slides were sealed with coverslips (22X22 mm) (BDH) and the sections were viewed under the electron microscope (Olympus BX60).

APPENDIX I

20X SSC (3 M NaCl, 0.3 M Na Citrate)

10X MOPS (0.2 M MOPS, 50 mM Na Acetate, 10 mM EDTA)

TBS (For 50 ml use 0.4 g NaCl, 0.01 g KCl, 0.15 g Trizma base, pH 7.4)

0.2M sodium phosphate buffer pH7.4 (0.5 M Na₂HPO₄, 0.5 M NaH₂PO₄)

Cracking Buffer stock solution (8 M Urea, 5% w/v SDS, 40 mM Tris-HCl pH6.8, 0.1 mM EDTA, 0.4 mg/ml Bromophenol blue, MilliQ H₂O)

Complete Cracking Buffer (88.5% v/v Cracking buffer stock, 0.88% v/v β-mercaptoethanol, 45 mM PMSF, 0.1 mg/ml Pepstatin A, 0.03 mM leupeptin, 145 mM benzamidine, 0.37 mg/ml aprotinin)

Plasmid resuspension buffer (25 mM Tris-HCl pH 8.0, 10 mM EDTA, 0.9% w/v glucose)

Plasmid lysis buffer (200 mM NaOH, 1% SDS). 11.5% v/v glacial acetic acid, 29.4% w/v potassium acetate in Milli Q

Plasmid neutralisation buffer (11.5% v/v glacial acetic acid, 29.4% w/v potassium acetate in Milli Q)

Solution A (50 mM Tris HCl pH 7.5, 150 mM NaCl, 1 mM EDTA, 1 mM EGTA, 2.5% Triton X-100, 10 µg/ml leupeptin, 10 µg/ml antipain, 1 mM benzamidine, 0.5 mM TLCK, 1 mM PMSF)

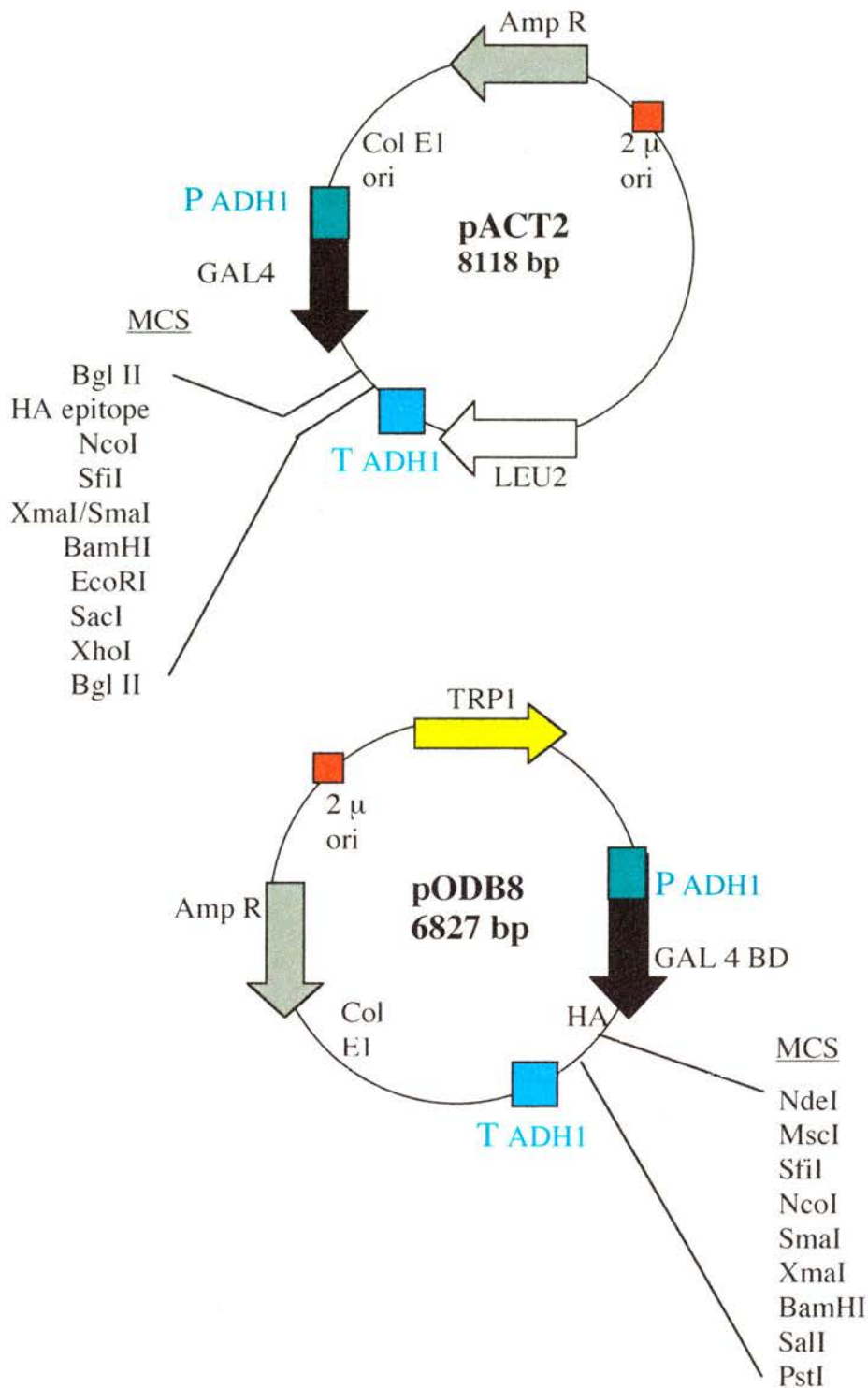
Lysis Buffer (25 mM Tris HCl pH 7.5, 150 mM NaCl, 0.5% CHAPS, 5 mM NaF, 100 µg/ml leupeptin, 100 µg/ml antipain, 7 µg/ml chymostatin, 1 mM benzamidine, 1 mM TLCK, 10 mM EDTA, 10 mM EGTA, 1 mM PMSF).

Glutathione Sepharose 4B binding buffer (25 mM Tris HCl pH 7.5, 150 mM NaCl, 1 mM EDTA, 0.05% NP 40, 1 mM DTT, 10 µg/ml leupeptin, 2 µg/ml pepstatin, 0.7 µg/ml chymostatin, 10 µg/ml antipain, 1 mM benzamidine, 0.5 mM TLCK, 1 mM PMSF).

Z buffer (60 mM Na₂HPO₄ • 2 H₂O, 40 mM NaH₂PO₄ • 2 H₂O, 10 mM KCL, 0.1 mM MgSO₄ • 7 H₂O),

YPAD (2% w/v Difco peptone, 1% w/v yeast extract, 2% v/v glucose, 0.003% adenine hemisulphate)

SD (0.67% w/v yeast nitrogen base without amino acids, 10% v/v sterile 10 X amino acid dropout solution, 2% v/v glucose)



pACT2 and pODB8 hybrid cloning vectors. pACT2 generates a hybrid that contains amino acids 768-881 of the GAL AD and pODB8 generates a hybrid which contains amino acids 1-147 of the GAL4 DNA-BD. Both vectors comprise a hemagglutinin (HA) peptide at the 3' end of the GAL4 sequence. The hybrid proteins are expressed from the constitutive ADHI promoter (P). The transcription is terminated at the ADHI transcription termination (T) signal. pACT2 contains the nutritional marker LEU2, whereas pODB8 carries the TRP1 marker for nutritional selection. Restriction sites of the multiple cloning sites (MCS) are shown.

Results

3. RESULTS

3.1 PERIAXIN CONSTRUCTS PERIC1, PERIC2 AND PERIRA3 WERE EXPRESSED IN YEAST, AS REVEALED BY WESTERN BLOTS

Total protein extracts from yeast strains Y190 and CG1945 transformed with PeriC1, PeriC2 and PeriRA3 in the cloning vector pODB8, and empty pODB80 vector were resolved by SDS-PAGE (12% gel). Following electrophoresis, the Western Blotting technique was used to assess the expression of the three constructs. Periaxin anti- C-terminus rabbit antibody (1:20,000) (PJ Brophy) followed by donkey anti-rabbit IgG HRP-labelled antibody (1:2,000) (Diagnostic Scotland) were used to reveal the expression of PeriC1 (85 kDa) and PeriC2 (60 kDa). The use of periaxin anti-repeat rabbit antibody (1:15,000) (PJ Brophy) with the same secondary antibody as for the other two constructs, allowed the detection of PeriRA3 (57 kDa) (Figure 21). The Western Blots revealed the expression of all three constructs in both strains indicating that they were not toxic to yeast and therefore would be suitable to use for detection of interacting partners.

3.2 REPORTER GENES LACZ AND HIS3 WERE NOT AUTOACTIVATED BY PERIAXIN CONSTRUCTS

In order to be able to use the periaxin constructs as “baits” in a yeast-two hybrid screen, the possibility of autoactivation of the two reporter genes (*lacZ* and *HIS3*), thus giving a false positive interaction, was investigated. Yeast strains Y190 and CG1945 are described as “leaky” for the expression of *HIS3* gene (Clontech Manual PT 3024-1) which reflects the fact that basal levels of *HIS3* expression in those two strains are sufficient to sustain growth on synthetic dropout medium which lacks

histidine. To overcome this problem, 3-amino, 1-2-4 triazole (3-AT) was used, at an optimum concentration, in -TH and -TLH media to suppress background growth. 3-AT is an inhibitor of HIS3-encoded imidazole glycerol phosphate (IGP) dehydratase and thus blocks histidine synthesis. IGP-dehydratase then converts imidazole glycerol phosphate to imidazole acetol phosphate in the biosynthetic pathway of histidine from PRPP (5-phosphoribosyl- α -pyrophosphate) (Stryer, 1975). The concentration of 3-AT sufficient to suppress background growth in CG1945 was 2 mM and in Y190 was 30 mM. In both cases a range of 3-AT concentrations was tried; 0-7 mM for CG1945 and 25-45 mM for Y190.

The results are summarised in Table 5 and indicate no autoactivation of either reporter gene.

Sample	Medium/ Growth		Medium/ lacZ	
pODB80	-TH	no	-T	white
PeriC1/pODB8	-TH	no	-T	white
PeriC2/pODB8	-TH	no	-T	white
PeriRA3/pODB8	-TH	no	-T	white
PVA3-+pTD1-1	-TLH	yes	-TLH	blue
PTD11+pLam5-1	-TLH	no	-TL	white

Table 5. Assessment of autoactivation of the reporter genes lacZ and HIS3 of PeriC1, PeriC2 and PeriRA3 periaxin constructs in the binding domain (BD) vector pODB8, in yeast strains CG1945 and Y190.

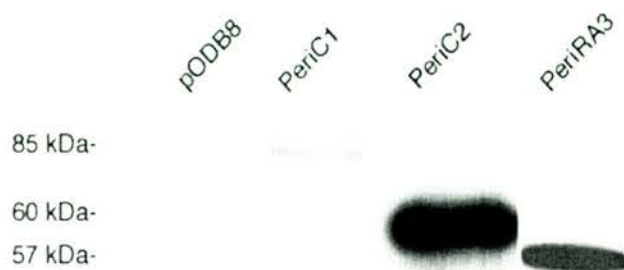


FIGURE 21. Expression of PeriC1, PeriC2 and PeriRA3 constructs in yeast strain Y190. PeriC1 (85 kDa) appears to be expressed at much lower levels than PeriC2 (60 kDa) and PeriRA3 (57 kDa).

3.2.1 Transformation efficiency tests

PeriC1 was used to screen a sciatic nerve cDNA library, prepared using RNA from 9-day and 14-day old rats, which was cloned into pACT2 activation domain vector between the EcoRI and XhoI sites. pACT2 contains the LEU2 gene for nutritional selection. The efficiency of transformation of the periaxin “bait” PeriC1 with the library “prey” plasmid in both yeast strains was assessed by co-transforming PeriC1 with 1 and 2 µg library DNA. The amount of “bait” was in all cases double that of the library used. 1 and 5 µl of the transformation mixtures were plated on –TL plates and the number of colonies formed were counted. The results obtained are shown in Table 6.

Although the efficiency in CG1945 was higher when 1 µg library DNA were used and the values obtained for 2 µg library were not significantly different for the two yeast strains, it was decided that Y190 would be used for the library screen because it is more sensitive in quantitative β-gal assays (Clontech Manual PT 3024-1).

YEAST STRAIN: CG1945

PeriC1 (μg)	Rat Sciatic Nerve Library cDNA (μg)	Transformation Efficiency (cfu/μg library DNA)
2	1	1.42×10^5
4	2	1.24×10^5

YEAST STRAIN: Y190

PeriC1 (μg)	Rat Sciatic Nerve Library cDNA (μg)	Transformation Efficiency (cfu/μg library DNA)
2	1	4.2×10^4
4	2	1.36×10^5

Table 6. Transformation efficiency of PeriC1 and rat sciatic nerve library cDNA co-transformed in yeast strains CG1945 and Y190. Co-transformation efficiency was not significantly different between the two strains tested. Although CG1945 showed higher efficiency, Y190 was selected for the library screen due to its higher sensitivity in β -gal assays.

3.3 ISOLATION AND HANDLING OF PUTATIVE PERIC1 POSITIVE INTERACTING LIBRARY CLONES

3.3.1 Assessment of interaction between the positive library clones and PeriC1, PeriC2 & PeriRA3

During a 2-week incubation period at 30 °C, 167 colonies (~2 mm diameter) were recovered and re-grown on –TLH 30 mM 3-AT medium. The colonies, allowed to grow for 3 days, were tested by X-gal filter lift to assess for activation of the lacZ gene. Of the 167 colonies picked originally, 118 gave a positive blue colour as a result of hydrolysis of X gal by β -galactosidase, the enzyme encoded by lacZ. Plasmid DNA rescued from these colonies, which was found to contain a library insert and lack the binding domain vector, was subsequently used with PeriC1 to co-transform yeast strain Y190. Co-transformations with empty pODB80 vector served as negative controls. Activation of lacZ was again tested by filter lifts, which revealed that 11 colonies out of 118 specifically interacted with PeriC1. Interaction of these library clones with PeriC2 and PeriRA3 was also assessed. The results are shown in Table 7. It is apparent that the clones interacted with variable strength with different periaxin constructs. All clones were sequenced with the Gal4 AD forward primer. The sequences obtained, revealed that clones 8a & 19d, 11a & 18b, as well as clones 26a & 13a, were replicates.

Clone	Size (kb)	Specific Interactions with		
		PeriC1	PeriC2	PeriRA3
11a 18b	1.1	+++	++	-
26a 13a	1.0	+++	+	++
11c	0.4	++	+	+
4c	1.1	+	+	-
8a 19d	1.8	+++	-	++
22j	2.0	+++	++	-
14f	1.2	+	+	-
19e	0.4	++	+++	++

Table 7. Specific interactions of clones isolated from a rat sciatic cDNA library screen with periaxin constructs PeriC1, PeriC2 and PeriRA3 using the yeast two-hybrid system. (Key: +++: strong; ++: medium; +: weak and -: no interaction). The strength of the interactions was assessed by the relative time required for blue colonies to appear on the filter and the strength of the blue colouration compared with the interaction between pVA3-1 and pTD1-1 (positive control).

3.3.2 Clones 11a (18b) and 26a (13a) were chosen for further study

Sequencing of all the library clones which interacted with PeriC1 and/ or PeriC2 & PeriRA3 allowed the prediction of their amino acid sequence using the Mac Vector™ 7.0 package. The prediction was feasible because the sciatic nerve library fragments were cloned into pACT in - frame with the Gal4 AD. This translation reading frame was predetermined. Clones 8a (19d) and 4c translated to only a few amino acids (4 and 5, respectively) and were subsequently abandoned. The NCBI database was searched for proteins that bore similarities to the clones isolated from the yeast two-hybrid library screen. The BLAST analysis package revealed that clone 11a (18b) was novel. It displayed 50% identity with the *Drosophila melanogaster* gene product CG13293, a protein of unknown function, whose sequence was obtained during the *D. melanogaster* genome sequence project by Celera Genomics (NCBI accession no. AAF50701).

Clone 26a (13a), was identified as the rat homologue of the *Mus musculus* F-box protein containing leucine-rich repeats (Fbl6/Fbx16), to which it was 94.3% identical (NCBI accession no. NM_013909). F-box proteins have been identified as components of SCF ubiquitin ligase complexes that are involved in the turnover of regulatory proteins.

Clones 11c and 14f were eliminated as false positives. 11c encoded the rat homologue of Bip, which is an ER chaperonin (Flynn et al., 1991). L-periaxin is synthesised on free polysomes and would not, under physiological conditions, encounter luminal ER proteins. 14f was 97% identical with murine fibulin-2, which is a protein localised to the extracellular matrix (Grassel et al., 1999). L-periaxin is not a

transmembrane protein and therefore would not associate with fibulin-2 in the cellular environment.

The remaining two clones did not seem to represent strong candidates for binding partners of L-periaxin. Clone 22j translated to 34 aa. Its N-terminal 23 residues displayed 78% identity with human myeloid/ lymphoid or mixed lineage leukaemia (NCBI accession no. gi 5174571). The nucleotide sequence of clone 19e showed 100% identity (over a 20 bp region) with human DNA sequence from clone RPI-47A22 from chromosome 20q12 (NCBI accession no. AL117374). The predicted amino acid sequence of 19e (27 aa residues) did not display any significant similarities with sequences in the NCBI database.

The interactions of L-periaxin with clones 11a and 26a were the subject of further investigation, in order to prove their validity and deduce their significance. The choice of the two clones was based on the fact that 11a was novel and could subsequently prove of interest, whereas 26a, being a member of the F-box family of proteins, could mediate the regulation of periaxin by the Ubiquitin system. Nucleotide sequences of clones 11a and 26a are shown in APPENDIX II (p.169-170).

3.3.3 GST-fusions of clones 11a and 26a interacted with L-periaxin in sciatic nerve pull down assays

To prove the validity of the observed interactions of clones 11a and 26a with L-periaxin in the yeast two-hybrid screen, biochemical methods were employed. A pull down experiment using sciatic nerve homogenate and GST-fusions of 11a and 26a was performed. The aim was to detect L-periaxin in sciatic nerve, bound to the GST-fusion protein, which had previously been attached to Sepharose beads. The detection of L-periaxin would be carried out by Western Blotting, using a periaxin specific antibody. GST-fusions of clones 11a and 26a were generated in the vector pGEX-KG as

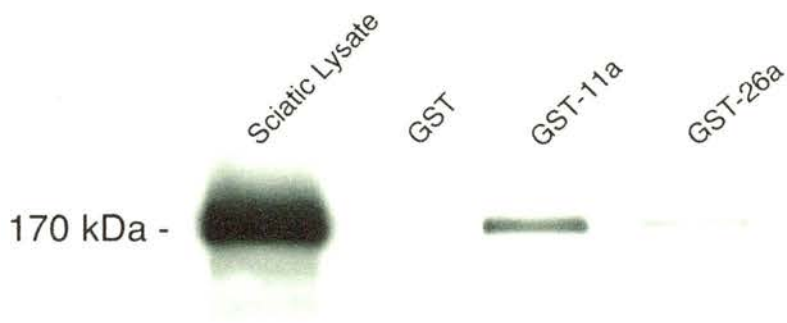


FIGURE 22. L-periaxin interacts with GST-fusions of clones 11a and 26a in sciatic nerve pull down assays. L-periaxin was detected after binding to the GST-fusion proteins of clones 11a and 26a, but not to GST alone, by Western Blotting using the Periaxin anti-repeat antibody (1:20,000).

described in section 2.9.1. As can be seen in Figure 22, the GST-tagged clones were able to interact with L-periaxin from sciatic nerve homogenate. This interaction was specific, since GST-alone failed to bind to L-periaxin. It also appeared that the association of 11a with L- periaxin was stronger than the 26a-Periaxin interaction.

3.3.4 GST-11a and GST-26a interacted with an *in vitro* transcription/translation product of L-periaxin

To obtain further evidence in support of a true interaction between the library clones 11a & 26a and L-periaxin, an *in vitro* transcription/translation of L-periaxin was produced, to be used in pull down assays. The purpose was to assess binding of the *in vitro* transcription/translation product to GST-fusions of the two clones. The pull down assay, carried out as described in section 2.9.3.2 revealed that both clones interacted with L-periaxin *in vitro* (Figure 23, A & B), as detected by autoradiography.

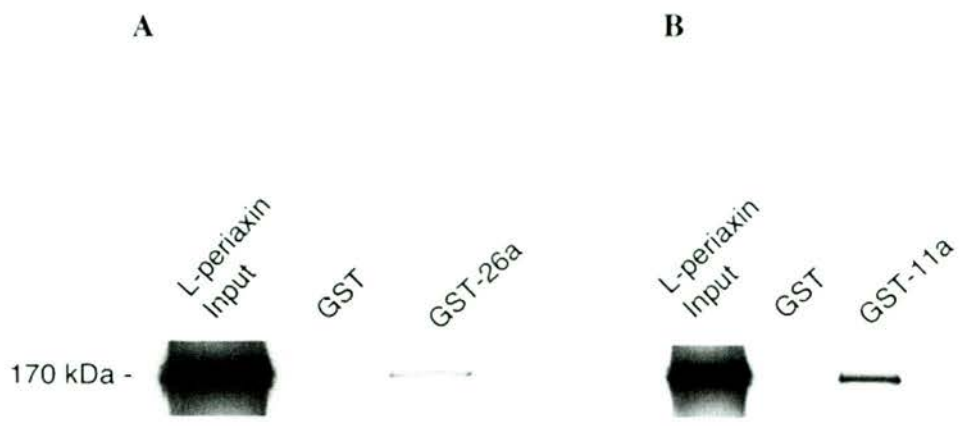


FIGURE 23. GST-fusions of clones 26a (A) and 11a (B) interact specifically with L-periaxin generated by *in vitro* transcription/translation. Radioactively labelled (³⁵S-Met) L-periaxin generated by *in vitro* transcription/translation binds to GST-fusions of clones 11a and 26a, as detected by autoradiography. The protein did not associate with GST alone.

3.3.5 Clone 11a interacts with a region of 170 aa of L-periaxin including the entire acidic domain, whereas clone 26a requires a minimum of 85 residues, which comprises part of the acidic region of L-periaxin

Clones 11a and 26a were isolated from a rat sciatic nerve cDNA library screen due to their association with a construct of L-periaxin, which comprised the C-terminal 623 amino acid residues of the protein (PeriC1). The possibility of an interaction with constructs PeriC2 and PeriRA3 was also assessed (Table 7) before moving on to the smaller constructs, in an attempt to deduce the minimal region of L-periaxin that participates in these interactions. Yeast two-hybrid assays were performed with both clones and all of the periaxin constructs (Figure 24).

It is apparent from Figure 24 that neither the extreme C-terminus, nor the end of the repeat region of L-periaxin is required for interaction with either of the two clones. Clone 11a did not associate with PeriRA3, PeriR5, or the C-terminal constructs PeriC8 and PeriC9. Its interaction with PeriC2 and PeriA6, with equal strength indicates the necessity of the acidic region for association with L-periaxin. The fact that the whole of the acidic region is needed is indicated by failure to interact with PeriA7, a truncation of the acidic domain.

Clone 26a displayed relatively strong association with construct PeriA7, whereas association with its larger version (PeriA6) was weaker (possibly due to protein folding issues). This was indicative of the requirement of 85 aa of L-periaxin, including part of the acidic domain, for interaction with 26a.



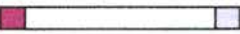
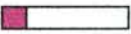

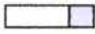
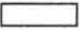

			β -gal	
			11a	26a
PeriC1	(762-1383)		+++	+++
PeriC2	(996-1383)		++	+
PeriRA3	(709-1080)		-	++
PeriR5	(709-996)		-	-
PeriA6	(996-1165)		++	+
PeriA7	(996-1080)		-	++
PeriC8	(1168-1383)		-	-
PeriC9	(1330-1383)		-	-

FIGURE 24. Yeast two-hybrid assay to investigate potential interactions of clones 11a and 26a with all L-periaxin constructs. Clone 11a requires the whole of the acidic domain of L-periaxin (996-1165) for interaction, whereas clone 26a associates with 85 aa that include the start of the acidic region (996-1080). (Amino acid residues shown in brackets, β -gal assay: +++ : strong, ++: moderate, -: no interaction).

3.4 FOCUSING ON CLONE 26a

The interactions of both 11a and 26a with L-periaxin were confirmed biochemically by the application of pull down assays. The region involved in the observed interaction was narrowed down to 996-1165 aa of L-periaxin for clone 11a, and 996-1080 aa of the protein, for clone 26a.

Clone 26a was identified as 94.3% identical with the C-terminal region of a mouse F-box-containing protein, namely Fbx16. F-box-containing proteins are components of SCF ubiquitin ligase complexes and so the association of such a polypeptide with L-periaxin would imply its targeting to the ubiquitin pathway for protein degradation. It was, therefore, decided to pursue further the investigation of the role of clone 26a as a binding partner of L-periaxin. The determination of the size of the mRNA molecule coding for the full -length 26a protein was determined by Northern Blotting. Isolation of the full-length protein, in order to assess the presence of an F-box motif, was carried out by Dr CS Gillespie in 5' RACE reactions. In order to study the functional significance of the interaction between clone 26a and L-periaxin, the possibility of ubiquitination of the latter protein was investigated. The involvement of the proteasome in its degradation was also assessed. Finally, the generation of a transgenic mouse, which overexpressed clone 26a (ie an F-box deletion mutant of rFbx16), was attempted in an effort to study the impact of L-periaxin accumulation on sciatic nerve morphology and the process of PNS myelination. Clone 11a was not pursued further by me.

3.4.1 The size of the mRNA of the full length 26a protein was determined by Northern Blotting

A hybridisation probe, comprising the C-terminal 750 bp of clone 26a, was used in Northern Blotting with brain and trigeminal nerve total mRNA from P15 rat. The probe was radioactively labelled and hybridised as described in sections 2.10.2-2.10.4. Autoradiography was carried out over a period of 48 h. A message of approximately 1.7 kb was present in both brain and trigeminal nerve (Figure 25).

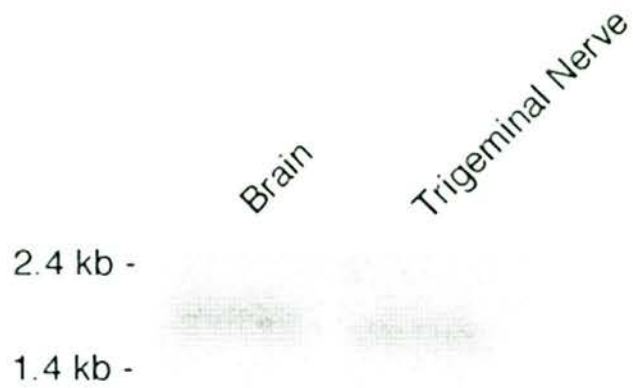


FIGURE 25. mRNA of clone 26a was detected in both brain and trigeminal nerve of P15 rat, by Northern Blotting. The size of the message of the full-length 26a protein was estimated at approximately 1.7 kb. Its presence in brain indicates that it is not a PNS- specific protein.

3.4.2 Full length 26a protein is the rat homologue of the mouse F-box-containing protein Fbl6/Fbx16

Isolation of the full length 26a protein, proved that it was indeed the rat homologue of mouse Fbx16, to which it displayed 95% identity (Figure 26). The full length cDNA was 1692 bp, of which 197 bp, represented 5' end UTR sequence (Figure 27). This was in agreement with the size determined by Northern Blot. The predicted size of the protein was 487 amino acids, with an expected MW of 53.5 kDa. In Western blots of sciatic nerve, using the C-terminal 26aC1 antibody at a 1:1,000 dilution, the protein was detected to run near the 60 kDa MW marker.

rFbx16 contained an F-box, proximal to its N-terminus at positions 59-101 aa and an LRR region at its C-terminus, which was involved in the interaction with L-periaxin (Figure 26). The relation between the originally isolated clone 26a and the full-length protein rFbx16 is shown in Figure 28.

FIGURE 26. Amino acid sequence alignment (Clustal W) of the mouse (m) and rat (r) F-box-containing protein Fbxl6. Identical residues are shown in purple and non-identical ones in yellow. The two proteins display 95% identity.

		10	20	30	40	
mFbx16		M L L V L P D L E P P R A R A H R R A R R R A P R S L A R G P T A V A K P R T K P R P				
rFbx16		M L L V L P D L E P T R A R A H R R A P R R A P R S L A R G P T A V A K P R A K P R P				
		50	60	70	80	
mFbx16		E P S L D Q G L D S G W G D R I P L E V L V H I F G L L V A A H G P M P F L G R A A R				
rFbx16		E P S L D Q G L D S G W G D R I P L E V L V H I F G L L V A A H G P M P F L G R A A R				
		90	100	110	120	
mFbx16		V C R H W H E A T S H P S L W H T V T L S P S L V G R A G K G N L K G E K K L L A C L				
rFbx16		V C R H W H E A T S H P S L W H T V T L S P A L V G R A A K G N L K G E K K L L A C L				
		130	140	150	160	170
mFbx16		E W L V P N R F S Q L Q S L T L I H W K S Q V H S V L E L V S K F C P R L T F L K L S				
rFbx16		E W L I P N R F S Q L Q R L T L I H W K S Q V H S V L E L V S K F C P R L T F L K L S				
		180	190	200	210	
mFbx16		D C H T V T A E T L V M L A R A C C Q L H S L D L H H S M V E S T A V V S F L E E A G				
rFbx16		D C H G V T A E T L V M L A K A C C Q L H S L D L H H S M V E S T A V V S F L E E A G				
		220	230	240	250	
mFbx16		S R M R K L W L T Y S S Q T T A I L G A L L D N C C P Q L Q V L Q V S T G M N C N N T				
rFbx16		S R M R R L W L T Y S S Q T T A I L G A L L G N C C P Q L Q V L E V S A G M S C N N T				
		260	270	280	290	300
mFbx16		P L Q L P V E A L Q K G C P Q L Q V L R L L N L I W L P K P C G R G V P Q G P G F P S				
rFbx16		P L Q L P V E A L Q R G C P Q L Q V L R L L N L I W L P K P C G R G A P Q G P G F P S				
		310	320	330	340	
mFbx16		L E E L C L A G S T C N F V S N E V L G R L L H R S P K L R M L D L R G C A R V T P S				
rFbx16		L E E L C L A G S T C S F V S N E V L G R L L H C S P K L R L L D L R G C A R I T P T				
		350	360	370	380	
mFbx16		G L C H L P C Q E L E Q L Y L G L Y G I S D G L T L A K D G S P L L T R K W Y H T L R				
rFbx16		G L C H L P C Q E L E Q L Y L G L Y G M S D G L A L A K D G S P L L T Q K W Y H T L R				
		390	400	410	420	430
mFbx16		E L D F S G Q G F S E K D L E Q A L A V F S G T P G G L H P A L C S L N L R G T R V T				
rFbx16		E L D F S G Q G F S E K D L E Q A L A V F S G T T E G L P P A L C S L N L R G T R V T				
		440	450	460	470	
mFbx16		P S T V S S V I S S C P G L L Y L N L E S C R C L P R G L K R V Y R G L E E V Q W C L				
rFbx16		P S T V S S V I S S C P G L L Y L N L E S C R C L P R G L K R A Y R G L E E V Q W C L				
		480	490			
mFbx16		E Q L L T S P P S A K E P T				
rFbx16		E Q L L T S P P S S R E S T				

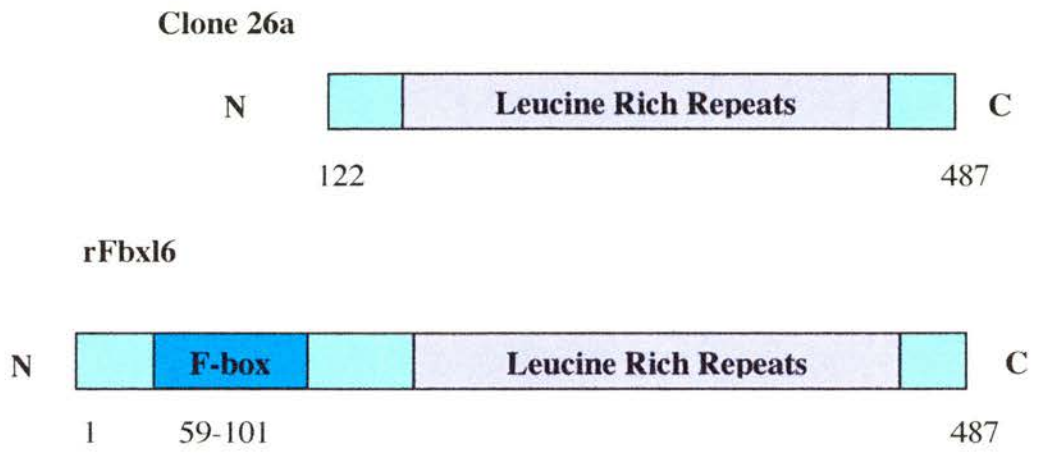


FIGURE 28. Domain structure of clone 26a and rFbx16. Clone 26a represents the C-terminal region of rFbx16. It comprises a LRR domain but lacks the F-box motif.

3.4.3 Alternative models of the 3D structure of Fbx16 based on crystallographic data from other F-box-containing proteins.

F-box- containing proteins with a region that is rich in leucine repeats at their carboxy termini adopt a shape that resembles a horseshoe (see Figure 14). This arrangement facilitates the interaction between the F-box protein and its substrate by creating a catalytic groove within which the association between the substrate and the F-box protein takes place. LRRs are structural components of this arrangement and therefore the determination of the number of these repeats is necessary for the deduction of the precise overall structure of the molecule. Multiple alignments of the LRR region of rFbx16 using the Clustal W method (Mac Vector) followed by manual re-adjustment, revealed that it belongs to the Cysteine-containing subfamily (see Table 2). Figure 29 illustrates a predicted distribution of the LRRs in the rFbx16 molecule. The consensus sequence CPXLXXLXX, where C, P and L represent the amino acids cysteine, proline and leucine respectively, whereas X is any amino acid, suggests the presence of twelve complete (1-12) and one incomplete (13) repeat in rFbx16. The complete repeats range in size from 24 to 32 residues.

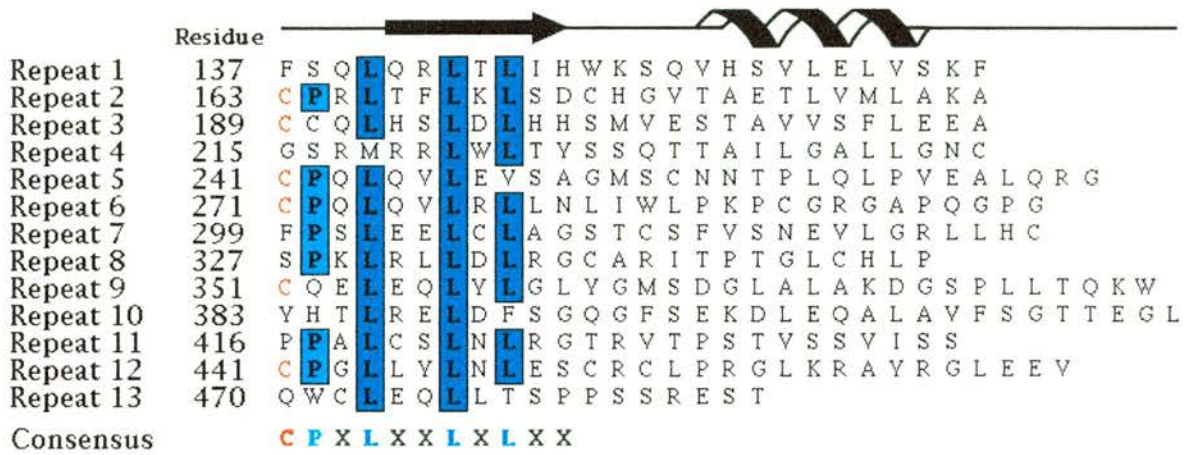


FIGURE 29. Clustal W alignment of the LRR region of rFbx16. The C-terminus of rFbx16 contains a LRR region, which was identified as a member of the Cysteine-containing subfamily. The consensus sequence CPXLXXLXLXX reveals the presence of a conserved P residue in the repeat region. Each repeat comprises a highly conserved region, where the L residues are localised, which gives rise to a β -sheet and a low homology region that generates an α -helix. (C: cysteine, P: proline, L: leucine, X: any amino acid). (Adapted from Court, 2001).

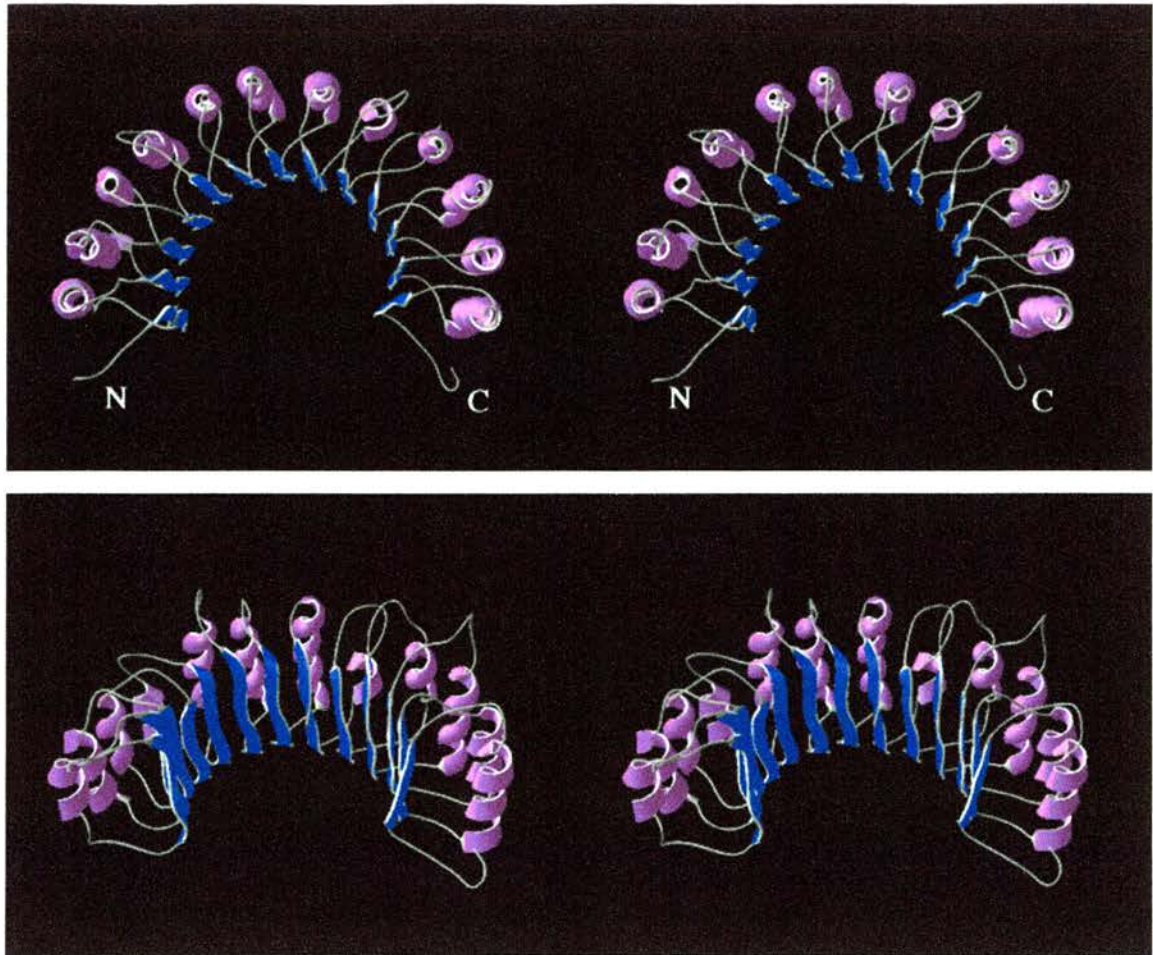


FIGURE 30. Proposed 3D structural model 1 (M1) of the LRR region of rFbx16. The LRR domain of rFbx16 is arranged in 13 repeats which comprise β -sheets (blue) that line the inner circumference and α -helices (purple) that flank the outer circumference of a concave surface. The overall structure resembles a horseshoe. The sheets and helices form surfaces, which are parallel to a common axis, perpendicular to which they are viewed in the upper panel. The lower panel shows a view rotated by approximately 45° about the horizontal axis with respect to the upper panel (N- and C-: amino- and carboxy- terminus, respectively) (After Court, 2001).

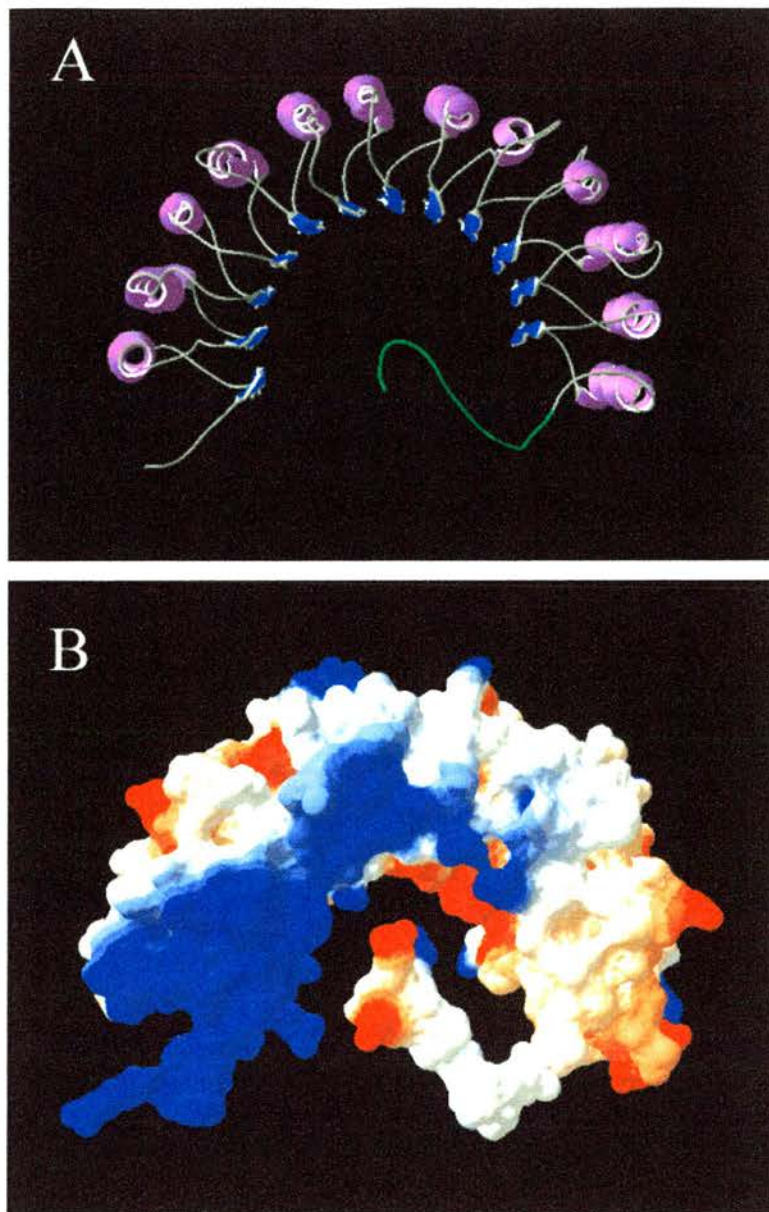


FIGURE 31. Proposed 3D structural model 2 (M2) of the LRR region of rFbx16. (A) An alternative model (M2) suggests the substitution of the incomplete 13th repeat of rFbx16 by a 12-amino acid C-terminal tail (shown in green). (B) The electrostatic potential of this arrangement revealed the possibility of an interaction between the positively charged N-terminal region (blue) and the negative residues of the tail (red) (Used by permission from Court, 2001).

A structural model of rFbx16, which comprised 13 repeats, was created by Mr F. Court. It was based on crystallographic data available for RI (see Figure 14) using the pdb viewer software. According to this model (M1)(Figure 30), each of the 13 putative repeats of rFbx16 comprises a β -sheet, which lines the inner circumference of a concave surface, and an α -helix flanking the outer circumference. However, in this model there is an extra β -sheet without a corresponding α -helix (there are only 12 α -helices but 13 β -sheets). The putative 13th repeat did not conform to the consensus sequence shown in Figure 29 and was previously described as incomplete. Failure to conform to the consensus sequence and lack of an accompanying α -helix, in conjunction with its shorter size, compared to the rest of the repeats, implied that the 13th repeat may not in fact constitute a part of the LRR structure. Crystallographic data obtained for Skp2, an F-box protein of the LRR superfamily, revealed the presence of a 25-residue C-terminal tail. This tail was found to reside within the concave face of the LRR structure and associate with the β -sheet lining in an electrostatic manner. It was proposed that this feature might participate in or regulate substrate binding. The likelihood of it being a substrate itself was also raised, considering that the levels of Skp2 oscillate during the cell cycle (Schulman et al., 2000). The possibility of attributing such a function to the C-terminal region of rFbx16 was investigated. An alternative model (M2) emerged, following constructive discussions with Mr F. Court. According to M2, deletion of the putative 13th repeat would give rise to a 12-residue C-terminal tail (shown in Figure 31 A). Calculation of the electrostatic potential of the resulting overall structure revealed a highly positively charged region at the N-terminus of the LRR domain which was available for association with the negatively charged residues of the tail (Figure 31 B). It is not yet known whether interaction of

the negatively charged tail with the positively charged region of the LRR structure actually occurs but the evidence suggests that it is theoretically possible. The positively charged surface of the LRR is most probably employed in the interaction with the negative charges of phosphate groups attached to substrates of the SCF complex (eg. β -catenin, $\text{I}\kappa\text{B}\alpha$). Both models are based on crystallographic data available for other LRR-containing proteins and neither can be verified until the crystallographic structure of Fbx16 is obtained.

3.4.4 rFbx16 mediates ubiquitination of L-periaxin in the sciatic nerve

The role of rFbx16 in targeting L-periaxin for ubiquitination via an SCF complex was assessed by investigating the possibility of formation of an L-periaxin-Ub conjugate in sciatic nerves. The sciatic nerves of four P21 mice that had been incubated with either the proteasomal inhibitor epoxomicin (5 μM) or its solvent DMSO (vehicle control), were boiled in 2% SDS. The purpose of this treatment was to inhibit degradation of ubiquitinated protein, in case the proteasome was involved in its turnover, and hence observe elevated levels of L-periaxin conjugated to Ub. The supernatant, which contained denatured proteins, was used in immunoprecipitations (IP) with either L-periaxin or β -catenin. β -catenin is a known substrate of the SCF complex (Kitagawa et al., 1999) and was used as a positive control for detection of ubiquitination. The IP was performed using the rabbit polyclonal anti-repeat antibody for L-periaxin, and the mouse monoclonal anti- β -catenin antibody to precipitate β -catenin. The detection of ubiquitinated proteins was attempted by Western Blots, using a mouse monoclonal anti-ubiquitin antibody (Santa Cruz) at 1:500 dilution.

As can be seen in Figure 32, L-periaxin was immunoprecipitated from sciatic nerve homogenate (a), and it was also recognised by the anti-ubiquitin antibody (b),

which suggests the presence of Ub residues attached to the protein's lysine side chains. L-periaxin was not detectable in the non-immune fraction of the IP, with either the anti-ubiquitin or the anti-Periaxin antibodies. This suggests that the bands seen in the DMSO- and Epoxomicin-treated lanes represent immunoprecipitated periaxin, and in (b) conjugated to ubiquitin. It is noteworthy that the epoxomicin-treated samples appear to contain more protein than the DMSO-treated ones, which indicates a build-up of ubiquitinated protein when the degradation pathway is inhibited. In the Periaxin immunoblot (IB), the equivalent of one sciatic nerve was loaded per lane, which makes the protein levels comparable, whereas in the ubiquitin IB the equivalent of three sciatic nerves were used in each lane. The mobility of the protein on SDS PAGE did not appear to be significantly altered by the presence of ubiquitin. This suggests that either a single Ub residue is conjugated to L-periaxin, or that residues of the Ub tag were removed by the action of ubiquitin hydrolases which were not inhibited in the experiment.

β -catenin was immunoprecipitated from sciatic nerve homogenate as shown in (c) and detected as a ubiquitin-conjugate in (d). Assessment of β -catenin ubiquitination was a positive control for the L-periaxin ubiquitination assay, since β -catenin has been well documented as a substrate of the F-box-containing protein FWD1/ β -TrCP/Slimb, which targets it for ubiquitination by the SCF complex. However, the process of ubiquitination of β -catenin has only been demonstrated in transfected cell lines before (Kitagawa et al., 1999) (Munemitsu et al., 1995) (Orford et al., 1997). This is the first demonstration of the occurrence of the process in whole sciatic nerve cultures.

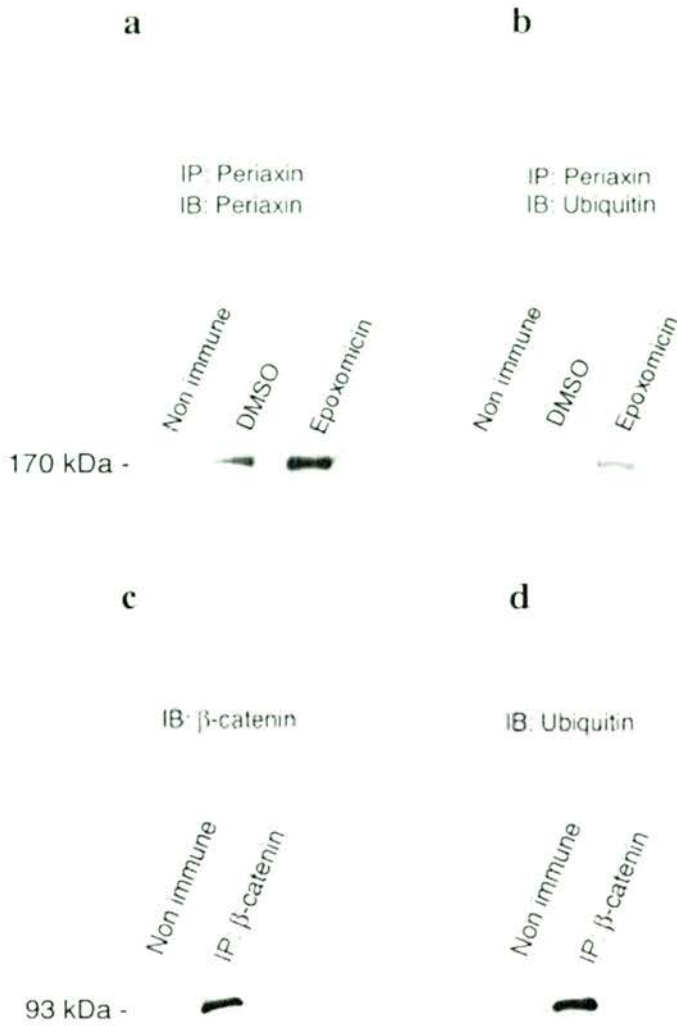


FIGURE 32. L-periaxin and β -catenin are ubiquitinated in sciatic nerve. L-periaxin was immunoprecipitated from sciatic nerve treated with 1% DMSO or 5 μ M epoxomicin (a) and was also detected as a ubiquitin conjugate (b). Treatment with epoxomicin appears to result in accumulation of the protein. β -catenin was also immunoprecipitated from sciatic nerve homogenate (c) and shown to be ubiquitinated (d).

3.4.5 The proteasome is involved in the turnover of L-periaxin in the sciatic nerve

Immunoprecipitation of L-periaxin from sciatic nerve homogenate which had been treated with the proteasomal inhibitor epoxomicin, and subsequent immunoblotting with the anti-ubiquitin antibody, revealed that L-periaxin formed a conjugate with ubiquitin. The apparently increased levels of the protein upon treatment of the sciatic nerve with the proteasomal inhibitor epoxomicin, compared to incubation of the nerve in the solvent DMSO, (Figure 32 a) suggested the involvement of the proteasomal pathway in regulation of the levels of L-periaxin. To investigate this possibility, the sciatic nerves of four P21 mice were treated with either 1% DMSO or 5 μ M epoxomicin, as described in section 2.13.2, and were subsequently assessed for changes in the levels of L-periaxin by Western Blot.

As can be seen in Figure 33, inhibition of the proteasome with epoxomicin results in accumulation of undegraded L-periaxin. Use of the translation inhibitor CHX throughout the course of the experiment serves to block protein synthesis and thus maintains a fixed pool of protein in which changes in the level of L-periaxin could be detected. In the absence of epoxomicin, the DMSO solvent has no effect on the proteasome, which functions to degrade L-periaxin; hence the observed decline in the protein levels by Western Blotting. To ensure that equal amounts of total protein were loaded on each well, the protein content of each sciatic nerve was established by using the Micro BCA Protein Assay Reagent Kit (Pierce) according to instructions provided by the manufacturer.

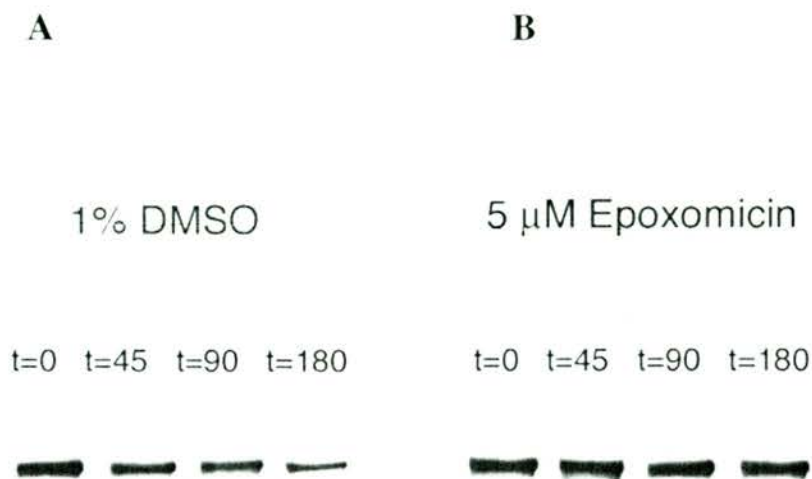


FIGURE 33. L-periaxin is stabilised in sciatic nerve upon inhibition of the proteasome by epoxomicin. (A) The levels of L-periaxin in sciatic nerves appear to decline with time when the proteasome is not inhibited (DMSO/CHX-treated nerves). (B) Upon treatment with the proteasomal inhibitor epoxomicin, L-periaxin is stabilised following addition of the translation inhibitor CHX for 180 min (t: time in min).

The experiment was carried out three times in order to ensure reproducibility. The mean density of the bands obtained by Western Blotting was estimated by using the NIH Image 1.61 software. The data obtained from all three experiments were averaged and are displayed in Figure 34. The average figures were expressed as percentage decline of protein levels, assuming that at $t=0$, the levels of L-periaxin represent 100% of the protein present in sciatic nerve. Taken in conjunction, Figures 33 and 34 suggest that the proteasome plays a major role in the regulation of the levels of L-periaxin in sciatic nerve. Upon proteasomal inhibition, L-periaxin is stabilised.

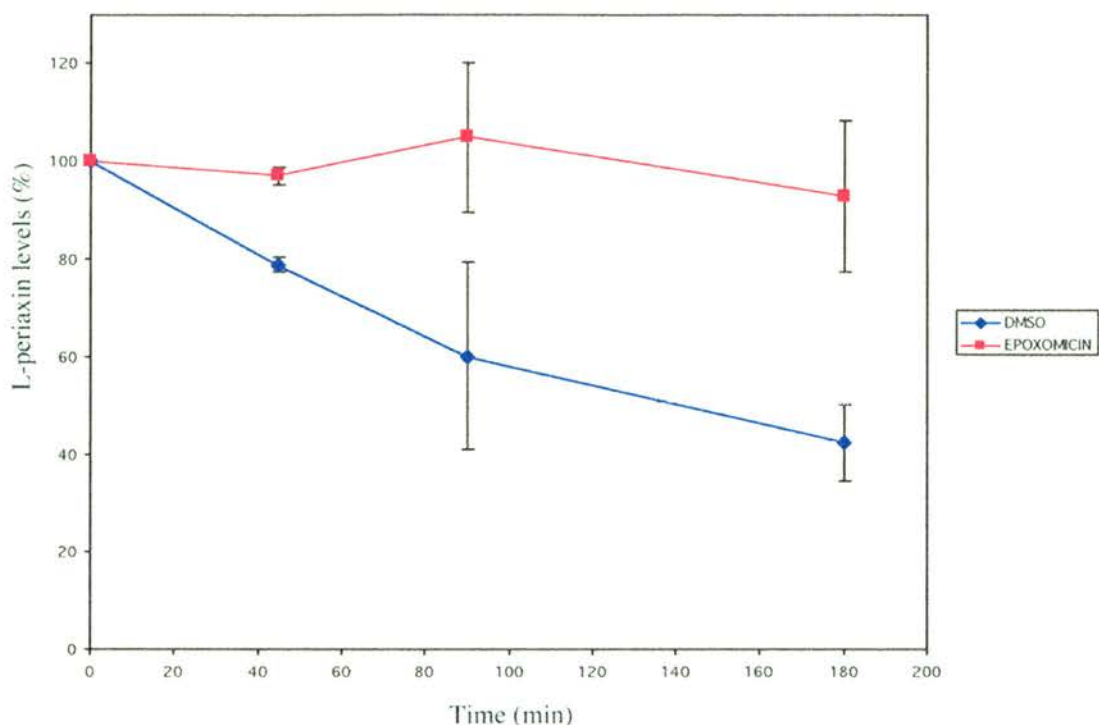


FIGURE 34. Effect of inhibition of the proteasome on the levels of L-periaxin in sciatic nerve. The proteasomal inhibitor epoxomicin (5 μ M) applied to whole sciatic nerves in culture, appears to maintain the levels of endogenous L-periaxin near to 100% following a period of 3 h treatment with CHX, which prevents further protein synthesis (red squares). The application of the solvent DMSO (1%) does not interfere with proteasomal function and the protein levels decline to approximately 50% by 120 min after application of CHX (blue triangles).

3.4.6 Fbx16 is expressed in a variety of tissues

The expression pattern of Fbx16 was assessed by Western Blotting using a variety of tissues obtained from P21 mice, with the 26aC1 antibody. Total protein (30 µg) from each homogenised tissue sample was resolved by SDS –PAGE on a 12% SDS polyacrylamide gel and assessed for the presence of Fbx16 by probing with the 26aC1 antibody. As can be seen in Figure 35, the protein is expressed in comparable levels in all tissues examined, namely brain, spinal cord, sciatic nerve, skeletal muscle, heart, lung, kidney and liver. It has also been detected in trigeminal nerve, ovary and testis samples (data not shown). It seems, therefore, that Fbx16 is not PNS-specific but that it is also expressed in tissues where L-periaxin is absent. This suggests the existence of other substrates of Fbx16 besides L-periaxin.

3.4.7 Investigation of the significance of L-periaxin ubiquitination by transgenesis

Due to lack of time, it has not been possible to perform the analysis of the transgenic animals yet and the results of this study will not be included in this thesis.

3.4.8 The C-terminal antibodies 26aC1 and 26aC2 did not immunostain sciatic nerve sections

Immunostaining of P11, P14 and P21 mouse sciatic nerve sections was attempted with the C-terminal antibodies 26aC1 and 26aC2 in order to determine the localisation of Fbx16. The staining observed with both antibodies was not specific and firm conclusions could not be drawn. In order to obtain a better view of the distribution of the protein, an antibody against its N-terminus will be generated.

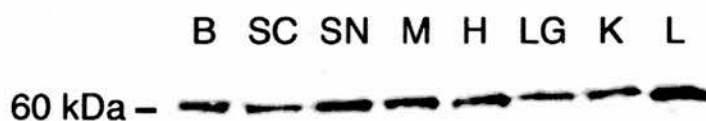


FIGURE 35. Fbx16 is expressed in a variety of tissues. Fbx16 was detected by Western Blot in homogenates (30 μ g total protein) of brain (B), spinal cord (SC), sciatic nerve (SN), skeletal muscle (M), heart (H), lung (LG) and liver (L) from P21 mice. The blot was probed with 26aC1 antibody (1: 1,000).

APPENDIX II

10 20 30 40 50 60
 CCC GAG CGA GCC CTG CGG CCG CCG GAG CAT CTC CCG CGG CGG AGC AGG AGC CGG ATG GTC
 70 80 90 100 110 120
 AGA GGA GCC CGG CAG TCC CAG CAG CCG CGG AGT CGC CTG GCC CCC AGA CTG TCT GGC ACA
 130 140 150 160 170 180
 GTG GAG AAA CCA CCT CGA AAA CGG AAA AGC AGG ACT GAA TTT ACT CTT AAA GAA ACC ATG
 190 200 210 220 230 240
 TCC TCT GGA GGT GCT GAA GAT GAT ATC CCA CAG GGA GAG AGG AAG ACA GTT ACA GAT TTC
 250 260 270 280 290 300
 TGT TAT CTT TTG GAT AAA TCC AAG CAA CTG TTT AAT GGC TTA AGA GAT TTG CCT CAG TAT
 310 320 330 340 350 360
 GGA CAG AAG CAG TGG CAG TCC TAC TTC GGA AGA ACT TTT GAT GTT TAC ACC AAA CTC TGG
 370 380 390 400 410 420
 AAA TTC CAG CAG CAG CAT CGA CAA GTC TTG GAT AAT CGG TAT GGC TTG AAG CGG TGG CAA
 430 440 450 460 470 480
 ATA GGG GAA ATC GCT TCC AAG ATC GGG CAG CTG TAT TAC CAC TAT TAT TTA CGA ACT TCT
 490 500 510 520 530 540
 GAA ACC AGT TAT TTG AAT GAG GCT TTC TCC TTC TAC TCT GCA ATC AGA CAG AGG TCA TAC
 550 560 570 580 590 600
 TAC TCT CAA GTC AAC AAA GAG GAC AGG CCT GAG TTG GTT GTT AAG AAA CTC CGA TAC TAT
 610 620 630 640 650 660
 GCA AGA TTT ATA GTA GTT TGT CTT CTT CTT AAT AAA ATG GAC GTT GTG AAA GAC CTG GTA
 670 680 690 700 710 720
 AAG GAA TTG TCT GAT GAA ATT GAA GAT TAT ACT CAT CGC TTT AAT ACT GAA GAT CAA GTT
 730 740 750 760 770 780
 GAG TGG AAC CTG GTG CTC CAA GAG GTA GCA GCA TTC ATT GAG GCA GAC CCT GTA ATG GTG
 790 800 810 820 830 840
 TTA AAT GAT GAT AAT ACC ATT GTT ATC ACA TCC AAT CGC CTT GCT GAG ACA GGA GCC CCC
 850 860 870 880 890 900
 TTG CTG GAG CAA GGC ATG ATA GTG GGA CAG TTG TCT CTG GCT GAT GCA CTC ATT ATT GGT
 910 920 930 940 950 960
 AAT TGT AAC AAT CAG GTC AAA TTC AGC GAA TTA ACT GTT GAC ATG TTC CGG ATG TTA CAA
 970 980 990 1000 1010 1020
 GCC TTG GAA AGG GAG CCA ATG AAT TTA GCT TCC CAG ATG AAT AAG CCG GGA ATA CAG GAG
 1030 1040 1050 1060
 CCA GCT GAC AAG CCT ACC AGA CGA GAA AAC GAA CTA GTC TCG AG

Nuceotide sequence of clone 11a

10 20 30 40 50 60
 GAG AAG AAG CTC CTT GCT TGC CTG GAG TGG CTC ATA CCC AAT CGG TTC TCA CAG CTC CAG
 70 80 90 100 110 120
 AGG TTG ACC CTC ATC CAC TGG AAG TCT CAA GTA CAC TCC GTG TTG GAG CTG GTT AGC AAG
 130 140 150 160 170 180
 TTC TGT CCA CGG CTC ACC TTC CTG AAG CTT TCA GAT TGC CAC GGT GTG ACA GCT GAA ACG
 190 200 210 220 230 240
 CTG GTC ATG TTA GCA AAA GCC TGC TGT CAG CTC CAC AGC CTA GAT CTA CAC CAT TCC ATG
 250 260 270 280 290 300
 GTC GAG TCC ACA GCT GTG GTG AGC TTC TTG GAG GAG GCG GGG TCC CGG ATG CGG AGG CTG
 310 320 330 340 350 360
 TGG CTG ACC TAC AGT TCC CAG ACC ACA GCC ATC TTG GGT GCA CTG CTG GGC AAC TGC TGC
 370 380 390 400 410 420
 CCC CAG CTC CAA GTC CTC GAG GTC AGC GCT GGC ATG AGC TGC AAC AAC ACA CCC TTG CAG
 430 440 450 460 470 480
 CTG CCT GTG GAA GCC CTA CAG AGA GGC TGC CCC CAG CTG CAG GTG CTA CGG CTG CTG AAT
 490 500 510 520 530 540
 CTG ATT TGG CTT CCC AAG CCT TGT GGC CGA GGA GCG CCC CAG GGA CCA GGA TTC CCC AGT
 550 560 570 580 590 600
 CTG GAG GAG CTC TGC TTG GCT GGC TCC ACC TGC AGC TTT GTG AGC AAT GAG GTT CTG GGC
 610 620 630 640 650 660
 CGC TTG CTC CAC TGC TCC CCC AAA CTG CGC CTG CTG GAT CTT CGA GGC TGT GCT AGA ATC
 670 680 690 700 710 720
 ACT CCT ACT GGG CTG TGT CAT TTG CCG TGT CAA GAG TTG GAG CAG CTC TAC CTG GGC CTG
 730 740 750 760 770 780
 TAT GGC ATG TCT GAT GGG TTG GCT CTA GCC AAG GAT GGC AGC CCC CTG TTG ACC CAG AAG
 790 800 810 820 830 840
 TGG TAT CAC ACC CTG AGG GAG CTG GAC TTC AGT GGC CAA GGC TTC AGC GAG AAA GAC TTG
 850 860 870 880 890 900
 GAA CAG GCC CTG GCT GTT TTC TCA GGC ACC ACT GAG GGC TTA CCC CCA GCC TTG TGC TCC
 910 920 930 940 950 960
 CTC AAC CTA AGG GGT ACC CGA GTT ACA CCA AGC ACA GTC AGT TCT GTG ATT AGC AGT TGC
 970 980 990 1000 1010 1020
 CCG GGG CTG CTG TAT CTC AAT CTG GAG TCC TGT CGT TGT CTC CCA CGA GGT CTG AAG CGT
 1030 1040 1050 1060 1070 1080
 GCC TAC AGG GGC CTG GAG GAA GTC CAG TGG TGT CTA GAG CAG CTA CTT ACG AGC CCG CCC
 1090 1100 1110 1120 1130
 TCT TCC AGA GAG TCC ACA TAA CTC AAG ACG GCT CCC CGC TTT GCC CTG CCC TG

Nucleotide sequence of clone 26a

Discussion

4. DISCUSSION

This work has focused on the identification of binding partners of L-periaxin, in an effort to investigate its role in the myelin-forming Schwann cell and its involvement in the process of PNS myelination. The C-terminal domain of the protein was used to screen a rat sciatic nerve cDNA library by the yeast two-hybrid method. The validity of the observed interactions was assessed biochemically. The study of the significance of the association of L-periaxin with one particular library protein was also attempted by transgenesis.

4.1 L-periaxin and the F-box hypothesis

Yeast two-hybrid screening of a rat sciatic nerve cDNA library revealed that the C-terminus of L-periaxin formed an association with the rat homologue of a previously identified protein in mouse, termed Fbx16/Fbl6 (Cenciarelli et al., 1999) (Winston et al., 1999a). Truncated versions of the C-terminus of L-periaxin pointed to a region which comprised 85 aa residues of its acidic domain, as being sufficient for the observed interaction.

The clone isolated from the cDNA library represented the C-terminal region of rat Fbx16 (rFbx16), which comprised a leucine rich repeat (LRR) motif. LRRs have been identified as structural motifs which are implicated in the formation of protein-protein interactions (Kobe and Deisenhofer, 1995b). The arrangement of the α -helices and β -sheets, the constituents of each individual repeat, results in the formation of a characteristic horseshoe-like molecule, which facilitates the association between the LRR-containing protein and its substrate (Figure 14, section 1.6.5.2 (d)) (Kobe and Deisenhofer, 1995a).

Following verification of the yeast two-hybrid interaction by *in vitro* pull down assays, the full-length rFbx16 cDNA was isolated by 5' RACE. The predicted amino acid sequence indicated the presence of an F-box motif at the N-terminus of the protein. F-box motifs are features of proteins involved in the recruitment of substrates for the ubiquitin pathway of protein degradation (Craig and Tyers, 1999). F-box-containing proteins comprise a C-terminal motif (e.g. WD40 or LRR) which serves the association with their substrates, whereas the N-terminal F-box component is necessary to dock the substrate-bearing F-box protein to the core ubiquitin ligase enzyme (Bai et al., 1996). The complete complex, termed SCF (Skp1/Cullin/F-box), is responsible for the ubiquitination of the target protein. rFbx16 appeared to interact with L-periaxin through its LRR region, as anticipated, leaving the F-box motif free to associate with the core SCF complex. The interaction of L-periaxin with rFbx16 implicated the ubiquitin pathway in the regulation of the levels of L-periaxin in the sciatic nerve. The proposed role of L-periaxin in the stabilisation of the myelin sheath in the PNS, based on evidence from Prx null mice (Gillespie et al., 2000), as well as its translocation to the nucleus (Sherman and Brophy, 2000), would require tight temporal and spatial regulation of the levels of the protein. The ubiquitin pathway could serve to ensure that an efficient control mechanism operates.

4.1.1 rFbx16 is expressed in a variety of tissues and may associate with multiple substrates

Fbx16 was detected by Western Blot in a variety of tissues including brain, spinal cord, sciatic nerve, trigeminal nerve, skeletal muscle, heart, lung, kidney, liver, ovary and testis. Given the fact that L-periaxin is a PNS-specific protein, the observed pattern of expression of Fbx16 implied that it could be implicated in the recruitment of other protein(s) for ubiquitination. Work undertaken by Mr F. Court in Prof. PJ

Brophy's lab, suggests that rFbx16 may mediate the ubiquitination of transcription factors, RNA-binding proteins and cytoplasmic polypeptides (Court, 2001). Although the validity of the described interactions awaits confirmation, it is likely that rFbx16 plays a role in the control of more than one cellular process by regulation at the transcriptional, translational or protein level.

4.1.2 Predicting the 3D structure of the LRR region of Fbx16: two possible models emerge

The crystallographic data available for the LRR-containing proteins Ribonuclease inhibitor (RI) and Skp2 were used as guides in order to predict the number and arrangement of the repeats in the LRR region of Fbx16. Alignment of the repeats was performed using the Clustal W method (Mac Vector) followed by manual re-adjustment, according to the general consensus sequence LXXLXLXX of the LRR superfamily. This revealed a more specific consensus sequence: CPXLXXLXLXX (where C: cysteine, L: leucine, P: proline, and X: any amino acid), which groups rFbx16 in the Cysteine-containing subfamily of LRR-containing proteins. The alignment shown in Figure 29 predicts the existence of 13 repeats. The first L residue in the consensus sequence is not part of the β -sheet but marks the end of the preceding α -helix (F. Court, personal communication). The second conserved L of the consensus sequence is found in all repeats, whereas the third conserved L is missing from repeats 5, 10 and 13. In repeats 5 and 10, the L residue is substituted by V (valine) and F (phenylalanine) respectively, which are also hydrophobic amino acids. However, in the 13th repeat, L is substituted by the unrelated hydrophilic amino acid T (threonine). The fact that it does not completely conform to the deduced consensus sequence, in conjunction with the absence of an α -helix to accompany the 13th β -sheet, implies that there may not be a 13th repeat in the LRR region of Fbx16. In

accordance with this view, Winston and co-workers have predicted the existence of 12 repeats in human Fbx16 (Winston et al., 1999a).

Looking for an alternative arrangement of the LRR region of rFbx16, Mr. F. Court and I turned our attention to the F-box-LRR-containing protein Skp2, whose crystallographic structure was also available (Schulman et al., 2000). A C-terminal tail of 25 aa residues was identified in Skp2 to reside within the concave surface of the LRR region. Its association with the β -sheet interface was of an electrostatic nature.

In the case of rFbx16, a 12-residue-C-terminal tail results by abolishing the 13th repeat. As shown in Figure 31 B, the tail comprises negatively charged residues, which could interact with the positively charged region of the N-terminus of the LRR, thus assuming a conformation similar to that of Skp2. The putative roles of this tail include participation in or regulation of substrate binding, as well as autoregulation by recruiting the LRR-containing protein to the ubiquitination pathway (Galan and Peter, 1999) (Schulman et al., 2000). Until the crystallographic structure of rFbx16 has been deduced, it is not possible to prove the validity of either model.

4.2 Conjugation of ubiquitin residues to L-periaxin

rFbx16 associates with L-periaxin through its LRR motif and targets the protein for ubiquitination and subsequent degradation by the proteasome. Covalent attachment of ubiquitin on the target protein takes place on lysine side chains of the substrate. There are no consensus sequences for ubiquitin- accepting lysines but it has been demonstrated that both p27 and I κ B α are ubiquitinated at specific lysines which are found proximal to their respective F-box protein binding sites (Shirane et al., 1999) (Spencer et al., 1999). The selection of lysine residues for ubiquitin conjugation is

determined by spatial and stereochemical constraints imposed by the interaction between the F-box protein-substrate complex and the SCF catalytic core (Schulman et al., 2000). The ubiquitin- accepting lysine(s) of L-periaxin have not been identified (see Future Work), however, it is possible that like p27 and I κ B α , these may be found close to the rFbx16 binding region of the protein. The region of I κ B α which interacts with the F-box protein β -TrCP (21-41 aa), comprises the two ubiquitinated lysines at positions 21 and 22, as well as the two serines (S32 and 36) whose phosphorylation is essential for β -TrCP binding (Spencer et al., 1999). The rFbx16 binding site in L-periaxin (996- 1080 aa) comprises seven lysine residues, which could be considered as candidates for conjugation with ubiquitin. Two lysine residues found just upstream of the binding site (K993 and K995) may also be involved. Mutation of these residues to arginines and assessment of ubiquitination of L-periaxin could provide the means to deduce the ubiquitination site of the protein. The region of L-periaxin, which is employed in the interaction with rFbx16, is also rich in putative phosphorylation sites. It is not known whether phosphorylation of the protein is necessary for association with rFbx16. The seven serines and five threonines found within the 85 aa binding site of L-periaxin could potentially serve as mediators of the interaction with rFbx16 via phosphorylation. This possibility remains to be investigated.

4.3 Investigation of the L-periaxin- rFbx16 interaction by transgenesis

rFbx16 was identified as the F-box -containing protein involved in targeting L-periaxin to the ubiquitin/proteasome pathway for degradation. Inhibition of the pathway would be expected to result in accumulation of L-periaxin in peripheral nerve. One way to impede the normal function of the ubiquitin/proteasome -mediated

turnover mechanism would be to express a dominant-negative version of rFbx16 in an attempt to abolish L-periaxin ubiquitination. A transgenic construct of rFbx16 which lacked the F-box motif (rFbx16 Δ F) was generated under the control of the mouse P0 promoter to ensure PNS-specific expression. rFbx16 Δ F would compete with endogenous rFbx16 for binding to L-periaxin but, unlike its wild-type counterpart, it would be unable to associate with the core SCF complex and thus fail to ubiquitinate L-periaxin. Investigation of the effects of accumulation of the rFbx16-bound L-periaxin was the purpose of this study. The possibility that failure to ubiquitinate and thus degrade L-periaxin might be the cause of peripheral neuropathy that resembles the CMT4F type, (observed in patients with a mutation that abolishes the C-terminal region of the protein including the Fbx16 binding site), is very intriguing (Anna Williams, personal communication). Excessive levels of L-periaxin might have an impact in the stability of the myelin sheath or induce nuclear translocation and uncontrolled gene expression, assuming that L-periaxin has a functional role in the nucleus. Due to a lack of time, the outcome of the transgenic experiment will not be included in this thesis.

4.4 L-periaxin, β -catenin and the ubiquitin/proteasome pathway: more than just a matter of elimination

Immunoprecipitation of L-periaxin from mouse sciatic nerve homogenates and subsequent Western blotting with an anti-ubiquitin antibody revealed that L-periaxin was subjected to modification by the conjugation of ubiquitin residue(s). This modification did not alter the relative mobility of the protein on SDS- polyacrylamide gels significantly, which implied that the conjugate comprised a few or even a single ubiquitin molecule. Despite reports that a minimum of four ubiquitin residues are required for recognition by the proteasome and that mono-ubiquitination serves

mainly subcellular targeting, the major ubiquitinated form of neuronal nitric oxide synthase (nNOS), a protein degraded by the proteasome, is also believed to comprise only one or a few ubiquitin molecules (Bender et al., 2000). It is also possible that L-periaxin associates with a number of ubiquitin residues (≥ 4), which were removed during the course of the immunoprecipitation experiment via the action of uninhibited ubiquitin hydrolases.

To obtain an insight on the potential significance of the involvement of the ubiquitin/proteasome pathway in the regulation of L-periaxin, we turned our attention to β -catenin, a well-documented substrate of the pathway (Maniatis, 1999) (Winston et al., 1999b).

4.4.1 β -catenin: a protein implicated in alternative F-box -mediated pathways of destruction

β -catenin has been shown to interact with the F-box-containing protein FWD1/ β TrCP/Slimb, which mediates its ubiquitination via the SCF^{FWD1/ β TrCP/Slimb} complex. The protein is subsequently degraded by the proteasome (Kitagawa et al., 1999; Latres et al., 1999). Recently, a novel pathway for the regulation of the abundance of β -catenin has been described, which links β -catenin degradation to p53 responses (Matsuzawa and Reed, 2001). Matsuzawa and co-workers have elucidated a network of interactions between Siah-1, which is a RING-finger protein whose expression is induced by p53, SIP (a novel Siah-interacting protein) and the F-box protein Ebi, which binds unphosphorylated β -catenin (unlike the F-box protein β -TrCP). According to this pathway, DNA damage-induced p53 expression leads to an increase in the levels of the RING-finger protein Siah-1, which associates with SIP. SIP binds to Skp-1 in a complex with Ebi instead of β -TrCP together with β -catenin. The common component of the Wnt and Siah-1 pathways is APC, which appears to

be irreplaceable in the process of β -catenin degradation. β -catenin is an example of a protein which is not only regulated by two different F-box proteins, namely β -TrCP and Ebi, but also shares one of its F-box binding partners (β -TrCP) with two other ubiquitination substrates, I κ B α and Vpu (Winston et al., 1999b) (Margottin et al., 1998). It is therefore apparent that a single F-box protein may mediate the ubiquitination of more than one substrate and each substrate may associate with more than one F-box protein in alternative ubiquitin/proteasome –mediated destruction pathways. The process of ubiquitination of β -catenin has so far only been demonstrated in cell lines transfected with β -catenin (Kitagawa et al., 1999) (Munemitsu et al., 1995) (Orford et al., 1997). In this work, the occurrence of β -catenin ubiquitination in the sciatic nerve has also been shown.

β -catenin associates with the cytoplasmic tail of E-cadherin, a protein that mediates cell adhesion, and links it to the actin cytoskeleton by interacting with α -catenin (Gottardi et al., 2001). This cell adhesion complex clusters β -catenin to the cortical cytoskeleton and has been found to be responsible for the stabilisation of both proteins (Huber et al., 2001). The C-terminal tail of E-cadherin contains motifs which target the protein to the ubiquitin/proteasome pathway. These motifs overlap the previously identified β -catenin-binding site and are therefore masked in the E-cadherin/ β -catenin complex. Cellular adhesiveness also appears to be dependent on interaction with β -catenin, as the cytoplasmic region of cadherin seems to be unstructured in the absence of β -catenin (Huber et al., 2001).

Free cytoplasmic β -catenin is either degraded by the ubiquitin/proteasome pathway or accumulates upon extracellular signalling (e.g. Wnt) and translocates to the nucleus where it acts as a transcription factor. Meigs and co-workers have

recently suggested that, through mechanisms that are not yet fully understood, β -catenin may be released from the cadherin complex and translocate to the nucleus in order to exert its transcriptional regulatory effects (Meigs et al., 2001). They have presented evidence that members of the G12 subfamily of heterotrimeric G proteins bind to the cytoplasmic region of cadherins, resulting in the release of β -catenin from the complex. Displacement of β -catenin from cadherins via an activation-dependent interaction involving G12 proteins leads to manifestation of β -catenin mediated transcriptional responses in transfected HEK293 cells. Relocalisation of β -catenin in HEK293 cells from the adherens junction to the nucleus was observed upon expression of activated G12 proteins (Meigs et al., 2001).

4.4.2 A hypothetical model for the ubiquitin-mediated regulation of L-periaxin, based on evidence for β -catenin

Significant similarities in the cellular distribution of L-periaxin and β -catenin in conjunction with the involvement of the ubiquitin/proteasome pathway in the regulation of the abundance of both proteins, have pointed to the possibility of similarity in the cellular roles of the two proteins. As can be seen in Figure 36, both proteins may be seen clustered to the cortical cytoskeleton through associations with multi-protein complexes. L-periaxin participates in the recently identified DRP2-dystroglycan complex (Sherman et al., 2001), whereas β -catenin links E-cadherin to α -catenin, which in turn tethers the complex to the actin cytoskeleton in adherens junctions (Aberle et al., 1994). β -catenin is released from E-cadherin via the action of G12 proteins and translocates to the nucleus where it acts as a transcriptional activator for the expression of genes under the control of TCF/LEF transcription factors (Huber et al., 1996). L-periaxin has also been found to localise to the nuclei of both embryonic and post-natal Schwann cells. L-periaxin, permanently expressed in

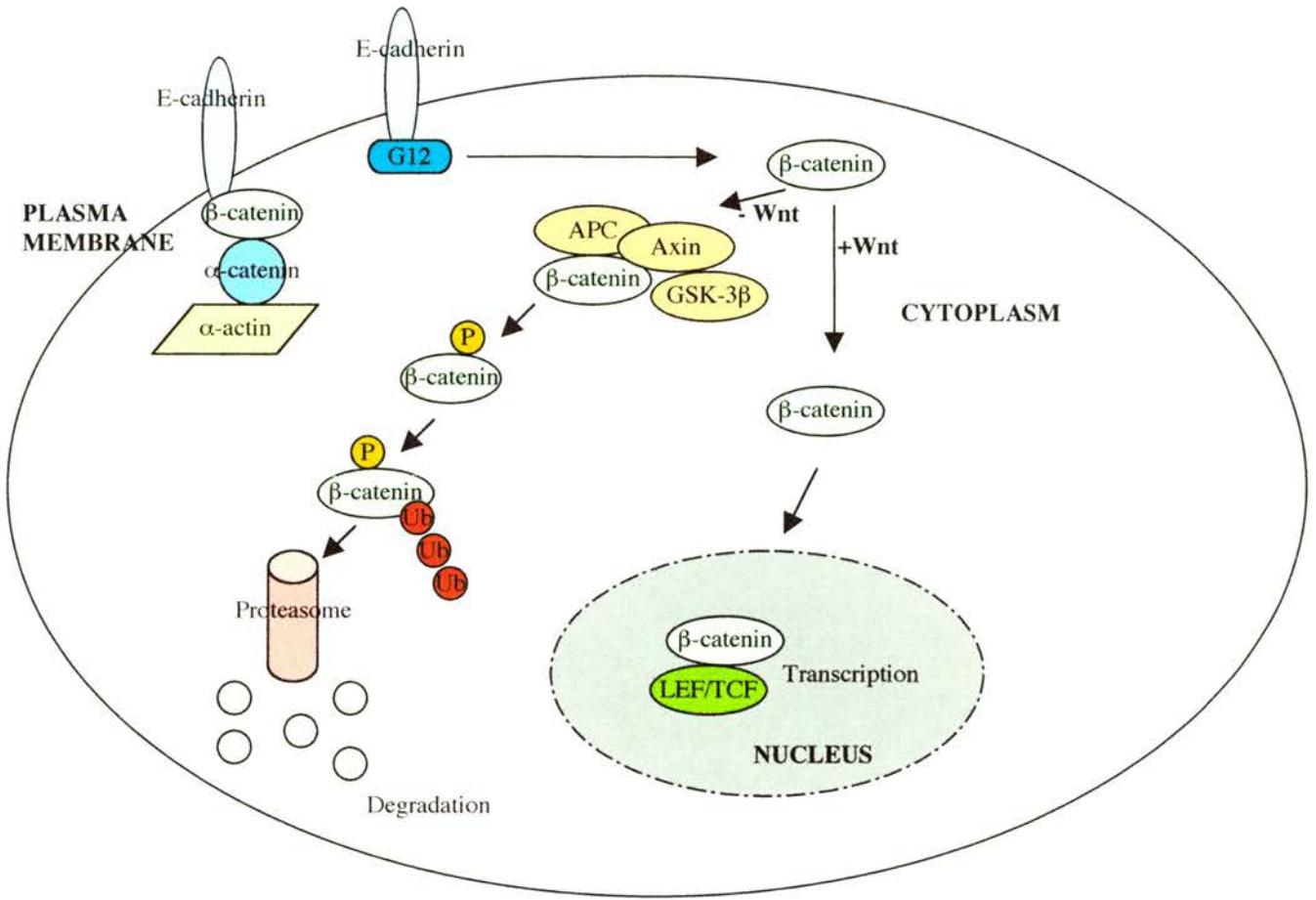
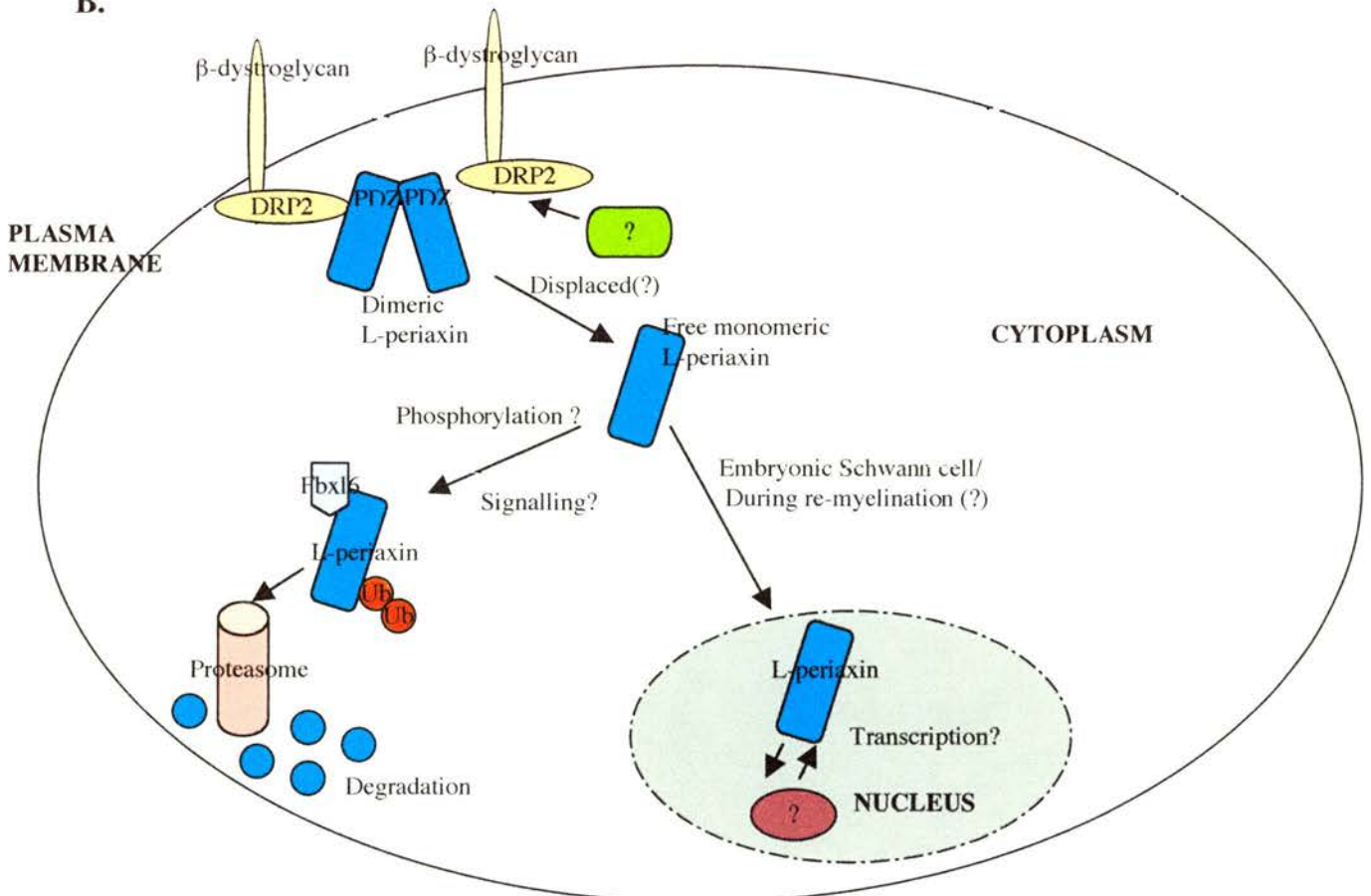
the Schwann cell line 33B (derived from P5 rats), displayed a cell density- dependent pattern of nucleocytoplasmic distribution. In sub-confluent monolayers of 33B cells L-periaxin was predominantly localised to the nucleus. This nuclear accumulation was lost in denser cultures and re-established upon wounding of the monolayer with a pipette tip (Sherman and Brophy, 2000). Its presence in the nucleus suggests that L-periaxin may act as a transcription factor, possibly for the regulation of genes that encode proteins involved in myelination. This view is based on the observation that L-periaxin is present in the nucleus of Schwann cells prior to the expression of the myelin proteins P0, MBP and MAG (Scherer et al., 1995) (Sherman and Brophy, 2000). In accordance with the proposed mechanism of translocation of β -catenin from the cortical cytoskeleton to the nucleus (Meigs et al., 2001), it is possible that binding of an as yet unidentified molecule to the C-terminal tail of DRP2, may result in release of L-periaxin from the complex and subsequent relocation to the nucleus. Displacement of L-periaxin from the DRP2 complex could also occur through an association of the L- and S- periaxin isoforms via their PDZ domains.

Shift in the localisation of L-periaxin from the Schwann cell membranes apposing the axon (adaxonal) to those apposing the basal lamina (abaxonal) has also been reported to occur as the myelin sheath begins to mature (Scherer et al., 1995), in a mechanism that has not yet been elucidated.

Finally, the abundance of both proteins is regulated by the ubiquitin/proteasome pathway of protein degradation. β -catenin appears to be recruited for ubiquitination by the F-box protein β -TrCP in a phosphorylation-dependent manner and the heterodimer subsequently associates with the core SCF complex (Latres et al., 1999). Alternatively, unphosphorylated β -catenin is bound by the F-box protein Ebi and is

recruited to a distinct E3 ligase complex (Matsuzawa and Reed, 2001). Although this work has shown that L-periaxin associates with the F-box protein Fbx16, which mediates its ubiquitination, it is not yet known whether this interaction requires the phosphorylation of the protein. It is also not clear whether it involves the participation of the SCF or an alternative E3 complex (see Future Work). Most recently Fbx16, (along with 16 other F-box-containing proteins), was tested by Koepp and co-workers as a potential mediator of the ubiquitination of Cyclin E (Koepp et al., 2001). Their data demonstrated that although Fbx16 was not responsible for recruitment of Cyclin E to the pathway, it was able to associate with the core SCF complex. Recruitment of L-periaxin to the ubiquitin/proteasome pathway is a means for its precisely timed and efficiently controlled regulation, implying an important role for this protein in the process of myelination. This suggestion is borne out by the severe phenotype of the periaxin-deficient mouse and the human disease CMT4F.

FIGURE 36. (A) Cellular functions and regulation of β -catenin. β -catenin links the cytoplasmic region of E-cadherin to α -catenin and the actin cytoskeleton in adherens junctions. Displacement of β -catenin from the complex by G12 gives rise to a pool of free cytoplasmic protein. Upon Wnt signalling, cytoplasmic β -catenin translocates to the nucleus where it acts as a transcription factor. In the absence of Wnt, the protein is targeted for destruction in the ubiquitin/proteasome pathway. **(B) Hypothetical model of the function and regulation of L-periaxin.** L-periaxin is able to dimerise through its PDZ domain and participate in a DRP2-dystroglycan complex which clusters it to the cortical cytoskeleton. Release from the complex in a mechanism similar to that which applies for β -catenin, would yield a pool of free monomeric L-periaxin. This would be subject to one of the following fates: 1. nuclear translocation and possible function as a transcription factor 2. targeting, via association with Fbx16, to the ubiquitin/ proteasome pathway for degradation.

A.**B.**

5. FUTURE WORK

The work presented in this thesis has implicated the ubiquitin/proteasome pathway in the turnover of L-periaxin. The identification of the F-box-LRR protein Fbx16 as the mediator of L-periaxin targeting to the pathway, signals the beginning of a new series of experiments, that could be designed to investigate the specific function(s) of the protein.

Identification of the ubiquitin-accepting lysine(s) of L-periaxin and investigation of the phosphorylation requirements of the interaction with rFbx16 are two issues which could be pursued. Evidence from other substrates of the SCF complex suggests that the ubiquitin-bearing lysines may reside within or near the F-box protein-binding site of the substrate. Mutation of the seven lysines found within the rFbx16 binding site of L-periaxin to arginines, either in turn or in clusters, may lead to the identification of the residue(s) involved in conjugation of ubiquitin to the protein.

The association of an F-box –containing protein with its substrate(s) may require the phosphorylation of specific serines or threonines of the target protein, as has been observed for β -catenin and I κ B α . To investigate whether this phosphorylation requirement applies to the interaction of L-periaxin with rFbx16, putative phosphorylation sites found within the region of L-periaxin employed in rFbx16 binding could be mutated. In the case of phosphorylation being a requisite for L-periaxin targeting to the SCF complex for ubiquitination, various approaches could be taken to exploit this fact.

Abolishing phosphorylation of L-periaxin by mutating the phosphate-accepting residue(s) of the protein could serve as a mechanism to prevent ubiquitin-mediated degradation. Conversely, to mimic constitutive phosphorylation of L-periaxin by

mutation of the serine(s)/threonine(s) involved in its interaction with rFbx16, might cause an increase in the turnover rate of L-periaxin. The effects of inhibiting or enhancing the degradation of L-periaxin by manipulating its phosphorylation state could be addressed in either a cell culture system or a transgenic animal model. It would be anticipated that such experiments would specifically target the function of L-periaxin, while excluding other proteins, which may also be substrates of the same SCF complex. This may not be the case in dominant negative and over-expression experiments involving rFbx16 (see later), where the function of additional proteins could also be disrupted.

Generation of a transgenic mouse that expresses the F-box deletion mutant of rFbx16 (rFbx16 Δ F) could provide valuable information on the effects of L-periaxin accumulation in the Schwann cell. The morphology of the Schwann cell and the structure of the myelin sheath could be assessed as a function of L-periaxin stabilisation. The shift in L-periaxin localisation from the adaxonal to the abaxonal Schwann cell membranes could be investigated, as well as any apparent changes in the structure of the DRP2-L-periaxin complex. The question of the significance of nuclear localisation of L-periaxin may also be addressed in the transgenic mouse model. The possibility that L-periaxin stabilisation could induce nuclear translocation with potential effects in gene expression, is also a matter to be considered. Candidates upon which L-periaxin might exert transcriptional control are likely to include genes encoding myelin-associated proteins. The regulation of P0, MBP and MAG in the rFbx16 Δ F transgenic mouse could also be investigated.

The effect of rFbx16 over-expression on the abundance and sub-cellular distribution of L-periaxin could be assessed in transfected Schwann cell lines

permanently expressing L-periaxin. An increase in the turnover rate of L-periaxin, caused by over-expression of rFbx16, might deplete the levels of cytoplasmic L-periaxin. As a result, inhibition of the nuclear translocation of the protein would be expected. It would also be interesting to establish whether clustering to the cortical DRP2-dystroglycan complex rescues L-periaxin from uncontrolled degradation due to excessive levels of rFbx16.

Identification of the rest of the components of the SCF^{Fbx16} complex by means of immunoprecipitation from a cell culture system may also be attempted. This could be achieved by the use of an antibody against rFbx16 to “pull-down” the SCF complex in which it participates. Characterisation of the putative additional substrates of rFbx16 could provide an insight to the cellular processes in which it plays a regulatory role. Determination of the sub-cellular distribution of rFbx16 by immunostaining, would be useful in establishing co-localisation with its substrates. An antibody against the N-terminus of the protein is currently being raised in rabbits for possible use in the above experiments. It would also be interesting to deduce the manner of regulation of the abundance of endogenous rFbx16. Determine whether the ubiquitin/proteasome pathway is implicated in the turnover of this protein and if so, whether its targeting for destruction is self-mediated or accomplished by another F-box-containing protein.

The ubiquitin/proteasome pathway is involved in the control of a number of complex cellular signalling cascades, which is accomplished via multi-component mechanisms. To gain an insight into the regulation of various cellular functions, it would be useful to identify substrates of the pathway and elucidate the precise mechanisms employed for their turnover. Deduction of potential associations between

the target proteins could serve as a means to resolve the signalling pathways in which they may participate.

References

6. REFERENCES

- Aberle, H., Butz, S., Stappert, J., Weissig, H., Kemler, R., and Hoschuetzky, H. (1994). Assembly of the cadherin-catenin complex in vitro with recombinant proteins, *J Cell Sci* *107*, 3655-63.
- Alkalay, I., Yaron, A., Hatzubai, A., Jung, S., Avraham, A., Gerlitz, O., Pashut-Lavon, I., and Ben-Neriah, Y. (1995). In vivo stimulation of I kappa B phosphorylation is not sufficient to activate NF-kappa B, *Mol Cell Biol* *15*, 1294-301.
- Arenzana-Seisdedos, F., Thompson, J., Rodriguez, M. S., Bachelier, F., Thomas, D., and Hay, R. T. (1995). Inducible nuclear expression of newly synthesized I kappa B alpha negatively regulates DNA-binding and transcriptional activities of NF-kappa B, *Mol Cell Biol* *15*, 2689-96.
- Arnold, J., Dawson, S., Fergusson, J., Lowe, J., Landon, M., and Mayer, R. J. (1998). Ubiquitin and its role in neurodegeneration, *Prog Brain Res* *117*, 23-34.
- Baeuerle, P. A., and Baltimore, D. (1996). NF-kappa B: ten years after, *Cell* *87*, 13-20.
- Bai, C., Sen, P., Hofmann, K., Ma, L., Goebel, M., Harper, J. W., and Elledge, S. J. (1996). SKP1 connects cell cycle regulators to the ubiquitin proteolysis machinery through a novel motif, the F-box., *Cell* *86*, 263-274.
- Baichwal, R., and De Vries, G. H. (1991). A myelin-related mitogen from cultured Schwann cells. In *Myelin: Biology and Chemistry.*, R. Martenson, ed. (Boca Raton, FL, CRC Press).
- Baumeister, W., Walz, J., Zuhl, F., and Seemuller, E. (1998). The proteasome: paradigm of a self-compartmentalizing protease, *Cell* *92*, 367-80.
- Bebington, C., Doherty, F. J., and Fleming, S. D. (2001). The possible biological and reproductive functions of ubiquitin, *Hum Reprod Update* *7*, 102-11.
- Bender, A. T., Demandy, D. R., and Osawa, Y. (2000). Ubiquitination of neuronal nitric-oxide synthase in vitro and in vivo, *J Biol Chem* *275*, 17407-11.
- Benjamins, J. A., and Smith, M. E. (1977). Metabolism of myelin. In *Myelin*, P. Morell, ed. (New York, Plenum).
- Bernier, L., Horvath, E., and Braun, P. (1989). GTP-binding proteins in CNS myelin., *Trans Am Soc Neurochem* *20*, 254.
- Bharucha, V. A., Peden, K. W., and Tennekoon, G. I. (1994). SV40 large T antigen with c-Jun down-regulates myelin P0 gene expression: a mechanism for papovaviral T antigen-mediated demyelination, *Neuron* *12*, 627-37.

- Boerkoel, C. F., Takashima, H., Stankiewicz, P., Garcia, C. A., Leber, S. M., Rhee-Morris, L., and Lupski, J. R. (2001). Periaxin mutations cause recessive Dejerine-Sottas neuropathy, *Am J Hum Genet* 68, 325-33.
- Bogyo, M., McMaster, J. S., Gaczynska, M., Tortorella, D., Goldberg, A. L., and Ploegh, H. (1997). Covalent modification of the active site threonine of proteasomal beta subunits and the Escherichia coli homolog HslV by a new class of inhibitors, *Proc Natl Acad Sci U S A* 94, 6629-34.
- Bonifacino, J. S., and Weissman, A. M. (1998). Ubiquitin and the control of protein fate in the secretory and endocytic pathways, *Annu Rev Cell Dev Biol* 14, 19-57.
- Boulias, C., and Moscarello, M. A. (1989). Guanine nucleotides stimulate hydrolysis of phosphatidyl inositol bis phosphate in human myelin membranes., *Biochem Biophys Res Commun* 162, 282-287.
- Braun, P. E. (1977). Molecular architecture of myelin. In *Myelin*, P. Morell, ed. (New York, Plenum), pp. 91-115.
- Braun, P. E., Horvath, E., Yong, V. W., and Bernier, L. (1990). Identification of GTP-binding proteins in myelin and oligodendrocyte membranes., *J Neurosci Res* 30, 540-544.
- Bunge, M. B., Bunge, R. P., Kleitman, N., and Dean, A. C. (1989(a)). Role of peripheral nerve matrix in Schwann cell function and in neurite regeneration., *Dev Neurosci* 11, 348-360.
- Bunge, M. B., Williams, A. K., and Wood, P. M. (1982). Neuron-Schwann cell interaction in basal lamina formation., *Dev Biol* 92, 449-460.
- Bunge, R. P., Bunge, M. B., and Bates, M. (1989(b)). Movements of the Schwann cell nucleus implicate progress of the inner (axon-related) Schwann cell process during myelination., *J Cell Biol* 109, 273-284.
- Bunge, R. P., Bunge, M. B., and Eldridge, C. F. (1986). Linkage between axonal ensheathment and basal lamina production by Schwann cells, *Annu Rev Neurosci* 9, 305-328.
- Bunge, R. P., and Fernandez-Valle, C. (1995). Basic biology of the Schwann Cell. In *Neuroglia*, H. a. R. Kettenmann, B.R., ed. (New York, Oxford University Press).
- Campagnoni, C. W., Garbay, B., Micevych, P., Pribyl, T., Kampf, K., Handley, V. W., and Campagnoni, A. T. (1992). DM-20 mRNA splice product of the myelin proteolipid protein gene is expressed in the murine heart., *J NeurosciRes* 33, 148-155.
- Carrano, A. C., and Pagano, M. (2001). Role of the F-box protein Skp2 in adhesion-dependent cell cycle progression, *J Cell Biol* 153, 1381-90.

- Cenciarelli, C., Chiaur, D. S., Guardavaccaro, D., Parks, W., Vidal, M., and Pagano, M. (1999). Identification of a family of human F-box proteins, *Curr Biol* 9, 1177-9.
- Cenciarelli, C., Hou, D., Hsu, K. C., Rellahan, B. L., and Wiest, D. L. (1992). Activation-induced ubiquitination of the T cell antigen receptor., *Science* 257, 795-797.
- Chance, P. F., Alderson, M. K., Leppig, K. A., Lensch, M. W., Matsunami, N., Smith, B., Swanson, P. D., Odelberg, S. J., Disteché, C. M., and Bird, T. D. (1993). DNA deletion associated with hereditary neuropathy with liability to pressure palsies, *Cell* 72, 143-151.
- Chen, A., Wu, K., Fuchs, S. Y., Tan, P., Gomez, C., and Pan, Z. Q. (2000). The conserved RING-H2 finger of ROC1 is required for ubiquitin ligation, *J Biol Chem* 275, 15432-9.
- Chen, Z., Hagler, J., Palombella, V. J., Melandri, F., Scherer, D., Ballard, D., and Maniatis, T. (1995). Signal-induced site-specific phosphorylation targets I kappa B alpha to the ubiquitin-proteasome pathway, *Genes Dev* 9, 1586-97.
- Ciechanover, A. (1998). The ubiquitin-proteasome pathway: on protein death and cell life, *Embo J* 17, 7151-60.
- Clark, M. B., and Bunge, M. B. (1989). Cultured Schwann cells assemble normal-appearing basal lamina only when they ensheath axons., *Dev Biol* 133, 393-404.
- Court, F. (2001) Searching for substrates targeted to the ubiquitin-dependent degradation pathway, MSc by Research, University of Edinburgh, Edinburgh.
- Coux, O., and Goldberg, A. L. (1998). Enzymes catalyzing ubiquitination and proteolytic processing of the p105 precursor of nuclear factor kappaB1, *J Biol Chem* 273, 8820-8.
- Coux, O., Tanaka, K., and Goldberg, A. L. (1996). Structure and functions of the 20S and 26S proteasomes, *Annu Rev Biochem* 65, 801-47.
- Craig, K. L., and Tyers, M. (1999). The F-box: a new motif for ubiquitin dependent proteolysis in cell cycle regulation and signal transduction, *Prog Biophys Mol Biol* 72, 299-328.
- Cummings, C. J., Reinstein, E., Sun, Y., Antalffy, B., Jiang, Y., Ciechanover, A., Orr, H. T., Beaudet, A. L., and Zoghbi, H. Y. (1999). Mutation of the E6-AP ubiquitin ligase reduces nuclear inclusion frequency while accelerating polyglutamine-induced pathology in SCA1 mice, *Neuron* 24, 879-92.

- D'Urso, D., Brophy, P. J., Staugaitus, S. M., Gillespie, C. S., Frey, A. B., Stempak, J. G., and Colman, D. R. (1990). Protein zero of peripheral nerve myelin: biosynthesis, membrane insertion and evidence for homotypic interaction, *Neuron* 2, 449-460.
- Deshaies, R. J. (1999). SCF and Cullin/Ring H2-based ubiquitin ligases, *Annu Rev Cell Dev Biol* 15, 435-67.
- Devor, M. (1989). Pathophysiology of injured nerve. In *Textbook of pain*, P. D. Wall, and R. Melzack, eds. (London, Churchill- Livingston), pp. 63-81.
- Dick, L. R., Cruikshank, A. A., Grenier, L., Melandri, F. D., Nunes, S. L., and Stein, R. L. (1996). Mechanistic studies on the inactivation of the proteasome by lactacystin: a central role for clasto-lactacystin beta-lactone, *J Biol Chem* 271, 7273-6.
- Diehl, J. A., Zindy, F., and Sherr, C. J. (1997). Inhibition of cyclin D1 phosphorylation on threonine-286 prevents its rapid degradation via the ubiquitin-proteasome pathway, *Genes Dev* 11, 957-72.
- Dytrych, L. M. (1997) Structure and Expression of the Murine Periaxin Gene, University of Edinburgh, Edinburgh.
- Enekel, C., Lehmann, A., and Kloetzel, P. M. (1998). Subcellular distribution of proteasomes implicates a major location of protein degradation in the nuclear envelope-ER network in yeast, *Embo J* 17, 6144-54.
- Etlinger, J. D., and Goldberg, A. L. (1977). A soluble ATP-dependent proteolytic system responsible for the degradation of abnormal proteins in reticulocytes, *Proc Natl Acad Sci U S A* 74, 54-8.
- Fannon, A. M., Sherman, D. L., Ilyina-Gragerova, G., Brophy, P. J., Friedrich, V. L. J., and Colman, D. R. (1995). Novel E-cadherin-mediated adhesion in peripheral nerve: Schwann cell architecture is stabilized by autotypic adherens junctions, *J Cell Biol* 129, 189-202.
- Fenteany, G., Standaert, R. F., Reichard, G. A., Corey, E. J., and Schreiber, S. L. (1994). A beta-lactone related to lactacystin induces neurite outgrowth in a neuroblastoma cell line and inhibits cell cycle progression in an osteosarcoma cell line, *Proc Natl Acad Sci U S A* 91, 3358-62.
- Fields, S., and Song, O. (1989). A novel genetic system to detect protein-protein interactions, *Nature* 340, 245-6.
- Filbin, T. M., Walsh, F. S., and Trapp, B. D. (1990). Role of myelin Po as a homophilic adhesion molecule., *Nature* 344.
- Finley, D., Bartel, B., and Varshavsky, A. (1989). The tails of ubiquitin precursors are ribosomal proteins whose fusion to ubiquitin facilitates ribosome biogenesis, *Nature* 338, 394-401.

- Flynn, G. C., Pohl, J., Flocco, M. T., and Rothman, J. E. (1991). Peptide-binding specificity of the molecular chaperone BiP, *Nature* 353, 726-30.
- Fraher, J. P. (1976). The growth and myelination of central and peripheral segments of ventral motoneuron axons. A quantitative ultrastructural study., *Brain Res* 105, 193-211.
- Freemont, P. S. (2000). RING for destruction?, *Curr Biol* 10, R84-7.
- Friede, R. L., and Miyagishi, T. (1972). Adjustment of the myelin sheath to changes in axon caliber, *Anat Rec* 172, 1-14.
- Fruttiger, M., Montag, D., Schachner, M., and Martini, R. (1995). Crucial role for the myelin associated glycoprotein in the maintenance of axon-myelin assembly., *Eur J Neurosci* 7, 511-515.
- Galan, J. M., and Peter, M. (1999). Ubiquitin-dependent degradation of multiple F-box proteins by an autocatalytic mechanism, *Proc Natl Acad Sci U S A* 96, 9124-9.
- Geier, E., Pfeifer, G., Wilm, M., Lucchiari-Hartz, M., Baumeister, W., Eichmann, K., and Niedermann, G. (1999). A giant protease with potential to substitute for some functions of the proteasome, *Science* 283, 978-81.
- Gietz, R. D., Triggs-Raine, B., Robbins, A., Graham, K. C., and Woods, R. A. (1997). Identification of proteins that interact with a protein of interest: applications of the yeast two-hybrid system, *Mol Cell Biochem* 172, 67-79.
- Gillespie, C. S., Sherman, D. L., Blair, G. E., and Brophy, P. J. (1994). Periaxin, a novel protein of myelinating Schwann cells with a possible role in axonal ensheathment, *Neuron* 12, 497-508.
- Gillespie, C. S., Sherman, D. L., Fleetwood-Walker, S. M., Cottrell, D. F., Tait, S., Garry, E. M., Wallace, V. C., Ure, J., Griffiths, I. R., Smith, A., and Brophy, P. J. (2000). Peripheral demyelination and neuropathic pain behavior in periaxin-deficient mice, *Neuron* 26, 523-31.
- Golly, F., Larocca, J. N., and Ledeen, R. W. (1990). Phosphoinositide breakdown in isolated myelin is stimulated by GTP analogues and calcium., *J Neurosci Res* 27, 342-348.
- Gottardi, C. J., Wong, E., and Gumbiner, B. M. (2001). E-cadherin suppresses cellular transformation by inhibiting beta-catenin signaling in an adhesion-independent manner, *J Cell Biol* 153, 1049-60.
- Gould, R. M., Byrd, A. L., and Barbarese, E. (1995). The number of Schmidt-Lanterman incisures is more than doubled in shiverer PNS myelin sheaths, *J Neurocytol* 24, 85-98.

- Grassel, S., Sicot, F. X., Gotta, S., and Chu, M. L. (1999). Mouse fibulin-2 gene. Complete exon-intron organization and promoter characterization, *Eur J Biochem* 263, 471-7.
- Grunwald, G. B. (1993). The structural and functional analysis of cadherin calcium-dependent cell adhesion molecules, *Curr Opin Cell Biol* 5, 797-805.
- Guilbot, A., Williams, A., Ravise, N., Verny, C., Brice, A., Sherman, D. L., Brophy, P. J., LeGuern, E., Delague, V., Bareil, C., *et al.* (2001). A mutation in periaxin is responsible for CMT4F, an autosomal recessive form of Charcot-Marie-Tooth disease, *Hum Mol Genet* 10, 415-21.
- Gumbiner, B. M. (1995). Signal transduction of beta-catenin, *Curr Opin Cell Biol* 7, 634-40.
- Hall, S. M., and Williams, P. L. (1970). Studies of the "incisures" of Schmidt and Lanterman, *J Cell Sci* 6, 767-791.
- Hammerschmidt, M., Brook, A., and McMahon, A. P. (1997). The world according to hedgehog, *Trends Genet* 13, 14-21.
- Harbers, K., Muller, U., Grams, A., Li, E., Jaenisch, R., and Franz, T. (1996). Provirus integration into a gene encoding a ubiquitin-conjugating enzyme results in a placental defect and embryonic lethality, *Proc Natl Acad Sci U S A* 93, 12412-7.
- Hatakeyama, S., Yada, M., Matsumoto, M., Ishida, N., and Nakayama, K. I. (2001). U-Box proteins as a new family of ubiquitin-protein ligases, *J Biol Chem* 276, 2111-2116.
- Hayasaka, K., Himoro, M., Sawaishi, Y., Nanao, K., Takahashi, T., Takada, G., Nicholson, G. A., Ouvrier, R. A., and Tachi, N. (1993). De novo mutation of the myelin P0 gene in Dejerine-Sottas disease (hereditary motor and sensory neuropathy type III), *Nat Genet* 5, 266-8.
- Hendil, K. B., Khan, S., and Tanaka, K. (1998). Simultaneous binding of PA28 and PA700 activators to 20S proteasomes, *Biochemical Journal* 332, 749-754.
- Hershko, A. (1996). Lessons from the discovery of the ubiquitin system, *Trends Biochem Sci* 21, 445-9.
- Hershko, A., and Ciechanover, A. (1998). The ubiquitin system, *Annu Rev Biochem* 67, 425-79.
- Hershko, A., Ciechanover, A., Heller, H., Haas, A. L., and Rose, I. A. (1980). Proposed role of ATP in protein breakdown: conjugation of protein with multiple chains of the polypeptide of ATP-dependent proteolysis, *Proc Natl Acad Sci U S A* 77, 1783-6.

- Hershko, A., Ciechanover, A., and Varshavsky, A. (2000). The ubiquitin system, *Nat Med* 6, 1073-1081.
- Hicke, L. (1999). Gettin' down with ubiquitin: turning off cell-surface receptors, transporters and channels, *Trends Cell Biol* 9, 107-12.
- Hicke, L., and Riezman, H. (1996). Ubiquitination of a yeast plasma membrane receptor signals its ligand- stimulated endocytosis, *Cell* 84, 277-87.
- Hirsch, C., and Ploegh, H. L. (2000). Intracellular targeting of the proteasome, *Trends in Cell Biology* 10, 268-272.
- Hochstrasser, M. (1996). Ubiquitin-dependent protein degradation, *Annu Rev Genet* 30, 405-39.
- Hoppe, T., Matuschewski, K., Rape, M., Schlenker, S., Ulrich, H. D., and Jentsch, S. (2000). Activation of a membrane-bound transcription factor by regulated ubiquitin/proteasome-dependent processing, *Cell* 102, 577-86.
- Hsiung, Y. G., Chang, H. C., Pellequer, J. L., La Valle, R., Lanker, S., and Wittenberg, C. (2001). F-box protein Grr1 interacts with phosphorylated targets via the cationic surface of its leucine-rich repeat, *Mol Cell Biol* 21, 2506-20.
- Huber, O., Korn, R., McLaughlin, J., Ohsugi, M., Herrmann, B. G., and Kemler, R. (1996). Nuclear localization of beta-catenin by interaction with transcription factor LEF-1, *Mech Dev* 59, 3-10.
- Huber, A. H., Stewart, D. B., Laurents, D. V., Nelson, W. J., and Weis, W. I. (2001). The cadherin cytoplasmic domain is unstructured in the absence of beta- catenin. A possible mechanism for regulating cadherin turnover, *J Biol Chem* 276, 12301-9.
- Huibregtse, J. M., Scheffner, M., Beaudenon, S., and Howley, P. M. (1995). A family of proteins structurally and functionally related to the E6-AP ubiquitin-protein ligase, *Proc Natl Acad Sci U S A* 92, 5249.
- Jackson, P. K., Eldridge, A. G., Freed, E., Furstenthal, L., Hsu, J. Y., Kaiser, B. K., and Reimann, J. D. (2000). The lore of the RINGs: substrate recognition and catalysis by ubiquitin ligases, *Trends Cell Biol* 10, 429-439.
- Jeffers, M., Taylor, G. A., Weidner, K. M., Omura, S., and Vande Woude, G. F. (1997). Degradation of the Met tyrosine kinase receptor by the ubiquitin-proteasome pathway., *Molecular Cell Biology* 17, 799-808.
- Jessen, K. R., and Mirsky, R. (1991). Schwann cell precursors and their development., *Glia* 4, 185-194.

- Jessen, K. R., and Mirsky, R. (1992). Schwann cells: early lineage, regulation of proliferation and control of myelin formation, *Current Opinion in Neurobiology* 2, 575-581.
- Jessen, K. R., and Mirsky, R. (1999). Schwann cells and their precursors emerge as major regulators of nerve development, *Trends Neurosci* 22, 402-10.
- Jiang, J., and Struhl, G. (1998). Regulation of the Hedgehog and Wntless signalling pathways by the F-box/WD40-repeat protein Slimb, *Nature* 391, 493-6.
- Joazeiro, C. A., and Weissman, A. M. (2000). RING finger proteins: mediators of ubiquitin ligase activity, *Cell* 102, 549-52.
- Johnson, E. S., Ma, P. C., Ota, I. M., and Varshavsky, A. (1995). A proteolytic pathway that recognizes ubiquitin as a degradation signal, *J Biol Chem* 270, 17442-56.
- Johnston, J. A., Ward, C. L., and Kopito, R. R. (1998). Aggresomes: A cellular response to misfolded proteins, *Journal of Cell Biology* 143, 1883-1898.
- Kajava, A. V. (1998). Structural diversity of leucine-rich repeat proteins, *J Mol Biol* 277, 519-27.
- Kalchman, M. A., Graham, R. K., Xia, G., Koide, H. B., Hodgson, J. G., Graham, K. C., Goldberg, Y. P., Gietz, R. D., Pickart, C. M., and Hayden, M. R. (1996). Huntingtin is ubiquitinated and interacts with a specific ubiquitin-conjugating enzyme, *J Biol Chem* 271, 19385-94.
- Kamizono, S., Hanada, T., Yasukawa, H., Minoguchi, S., Kato, R., Minoguchi, M., Hattori, K., Hatakeyama, S., Yada, M., Morita, S., *et al.* (2001). The SOCS box of SOCS-1 accelerates ubiquitin-dependent proteolysis of TEL-JAK2, *J Biol Chem* 276, 12530-8.
- Kamura, T., Koepp, D. M., Conrad, M. N., Skowrya, D., Moreland, R. J., Iliopoulos, O., Lane, W. S., Kaelin, W. G., Jr., Elledge, S. J., Conaway, R. C., *et al.* (1999). Rbx1, a component of the VHL tumor suppressor complex and SCF ubiquitin ligase, *Science* 284, 657-61.
- Kamura, T., Sato, S., Haque, D., Liu, L., Kaelin, W. G., Jr., Conaway, R. C., and Conaway, J. W. (1998). The Elongin BC complex interacts with the conserved SOCS-box motif present in members of the SOCS, ras, WD-40 repeat, and ankyrin repeat families, *Genes Dev* 12, 3872-81.
- Kandel, E. R., and Schwartz, J. H. (1985). *Principles of Neural Science*, 2nd edn (New York, Elsevier).

- Katzmann, D. J., Babst, M., and Emr, S. D. (2001). Ubiquitin-dependent sorting into the multivesicular body pathway requires the function of a conserved endosomal protein sorting complex, ESCRT-1, *Cell* 106, 145-155.
- Kitagawa, M., Hatakeyama, S., Shirane, M., Matsumoto, M., Ishida, N., Hattori, K., Nakamichi, I., Kikuchi, A., and Nakayama, K. (1999). An F-box protein, FWD1, mediates ubiquitin-dependent proteolysis of beta-catenin, *Embo J* 18, 2401-10.
- Kobe, B., and Deisenhofer, J. (1994). The leucine-rich repeat: a versatile binding motif., *TIBS* 19, 415-421.
- Kobe, B., and Deisenhofer, J. (1995a). Proteins with leucine-rich repeats, *Curr Opin Struct Biol* 5, 409-16.
- Kobe, B., and Deisenhofer, J. (1995b). A structural basis of the interactions between leucine-rich repeats and protein ligands, *Nature* 374, 183-6.
- Koepp, D. M., Schaefer, L. K., Ye, X., Keyomarsi, K., Chu, C., Harper, J. W., and Elledge, S. J. (2001). Phosphorylation-dependent ubiquitination of cyclin E by the SCFFbw7 ubiquitin ligase, *Science* 294, 173-7.
- Kolling, R., and Losko, S. (1997). The linker region of the ABC-transporter Ste6 mediates ubiquitination and fast turnover of the protein, *EMBO journal* 16, 2251-2261.
- Kopito, R. (2000). Aggresomes, inclusion bodies and protein aggregation, *Trends in Cell Biology* 10, 524-530.
- Kornitzer, D., Raboy, B., Kulka, R. G., and Fink, G. R. (1994). Regulated degradation of the transcription factor Gcn4, *Embo J* 13, 6021-30.
- Krantz, D. D., Zidovetzki, R., Kagan, B. L., and Zipurski, S. L. (1991). Amphipathic beta structure of a leucine-rich repeat peptide., *J Biol Chem* 266, 16801-16807.
- Laney, J. D., and Hochstrasser, M. (1999). Substrate targeting in the ubiquitin system, *Cell* 97, 427-30.
- Latres, E., Chiaur, D. S., and Pagano, M. (1999). The human F box protein beta-Trcp associates with the Cull1/Skp1 complex and regulates the stability of beta-catenin, *Oncogene* 18, 849-54.
- Lee, D. H., and Goldberg, A. L. (1996). Selective inhibitors of the proteasome-dependent and vacuolar pathways of protein degradation in *Saccharomyces cerevisiae*, *J Biol Chem* 271, 27280-4.

- Lee, D. H., and Goldberg, A. L. (1998). Proteasome inhibitors: valuable new tools for cell biologists, *Trends Cell Biol* 8, 397-403.
- Lees, M. B., and Brostoff, S. W. (1984). Proteins of myelin. In *Myelin*, P. Morell, ed. (New York, Plenum Publishing), pp. 197-224.
- Li, C., Tropak, M. B., Clapoff, S., Abramow-Newerly, W., Trapp, B., Peterson, A., and Roder, J. (1994). Myelination in the absence of myelin-associated glycoprotein, *Nature* 369, 747-750.
- Li, F. N., and Johnston, M. (1997). Grr1 of *Saccharomyces cerevisiae* is connected to the ubiquitin proteolysis machinery through Skp1: coupling glucose sensing to gene expression and the cell cycle, *Embo J* 16, 5629-38.
- Lisztwan, J., Marti, A., Sutterluty, H., Gstaiger, M., Wirbelauer, C., and Krek, W. (1998). Association of human CUL-1 and ubiquitin-conjugating enzyme CDC34 with the F-box protein p45(SKP2): evidence for evolutionary conservation in the subunit composition of the CDC34-SCF pathway, *Embo J* 17, 368-83.
- Lowe, J., Stock, D., Jap, B., Zwickl, P., Baumeister, W., and Huber, R. (1995). Crystal structure of the 20S proteasome from the archaeon *T. acidophilum* at 3.4 Å resolution, *Science* 268, 533-9.
- Lupas, A., Flanagan, J. M., Tamura, T., and Baumeister, W. (1997). Self-compartmentalizing proteases, *Trends Biochem Sci* 22, 399-404.
- Lupski, J. R. (1999). Charcot-Marie-Tooth polyneuropathy: duplication, gene dosage and genetic heterogeneity, *Pediatr Res* 45, 159-165.
- Lupski, J. R., Montes de Oca-Luna, R., Slaugenhaupt, S., Pentau, L., Guzzetta, V., Trask, B. J., Saucedo-Cardenas, O., Barker, D. F., Killian, J. M., Garcia, C. A., *et al.* (1991). DNA duplication associated with Charcot-Marie-Tooth disease type 1A, *Cell* 66, 219-232.
- Maef, R., and Suter, U. (1999). Impaired intracellular trafficking is a common disease mechanism of PMP22 point mutation in peripheral neuropathies, *Neurobiol Dis* 6, 1-14.
- Magee, A. I., and Buxton, R. S. (1991). Transmembrane molecular assemblies regulated by the greater cadherin family, *Curr Opin Cell Biol* 3, 854-861.
- Maniatis, T. (1999). A ubiquitin ligase complex essential for the NF-kappaB, Wnt/Wingless, and Hedgehog signaling pathways, *Genes Dev* 13, 505-10.
- Margottin, F., Bour, S. P., Durand, H., Selig, L., Benichou, S., Richard, V., Thomas, D., Strebel, K., and Benarous, R. (1998). A novel human WD protein, h-beta TrCp, that interacts with HIV-1 Vpu connects CD4 to the ER degradation pathway through an F-box motif, *Mol Cell* 1, 565-74.

- Martini, R., and Schachner, M. (1986). Immunoelectron microscopic localization of neural crest adhesion molecules (L1, N-CAM and MAG) and their shared carbohydrate epitope and myelin basic protein in developing sciatic nerve., *J Cell Biol* *103*, 2439-2448.
- Mathias, N., Johnson, S., Byers, B., and Goebel, M. (1999). The abundance of cell cycle regulatory protein Cdc4p is controlled by interactions between its F box and Skp1p, *Mol Cell Biol* *19*, 1759-67.
- Matsuzawa, S. I., and Reed, J. C. (2001). Siah-1, SIP, and Ebi collaborate in a novel pathway for beta-catenin degradation linked to p53 responses, *Mol Cell* *7*, 915-26.
- McGrath, J. P., Jentsch, S., and Varshavsky, A. (1991). UBA 1: an essential yeast gene encoding ubiquitin-activating enzyme, *Embo J* *10*, 227-36.
- Meier, C., Parmantier, E., Brennan, A., Mirsky, R., and Jessen, K. R. (1999). Developing Schwann cells acquire the ability to survive without axons by establishing an autocrine circuit involving insulin-like growth factor, neurotrophin-3, and platelet-derived growth factor-BB, *J Neurosci* *19*, 3847-59.
- Meigs, T. E., Fields, T. A., McKee, D. D., and Casey, P. J. (2001). Interaction of Galpha 12 and Galpha 13 with the cytoplasmic domain of cadherin provides a mechanism for beta -catenin release, *Proc Natl Acad Sci U S A* *98*, 519-24.
- Meng, L., Mohan, R., Kwok, B. H., Elofsson, M., Sin, N., and Crews, C. M. (1999). Epoxomicin, a potent and selective proteasome inhibitor, exhibits in vivo antiinflammatory activity, *Proc Natl Acad Sci U S A* *96*, 10403-8.
- Michel, J. J., and Xiong, Y. (1998). Human CUL-1, but not other cullin family members, selectively interacts with SKP1 to form a complex with SKP2 and cyclin A, *Cell Growth Differ* *9*, 435-49.
- Mirsky, R., and Jessen, K. R. (1996). Schwann cell development, differentiation and myelination, *Curr Opin Neurobiol* *6*, 89-96.
- Mirsky, R., Jessen, K. R., Schachner, M., and Goridis, C. (1986). Distribution of the adhesion molecules N-CAM and L1 on the peripheral neurons and glia in adult rats., *J Neurocytol* *15*, 799-815.
- Molineaux, S. M., Engh, H., de Ferra, F., Hudson, L., and Lazzarini, R. A. (1986). Recombination within the myelin basic protein gene created the dysmyelinating shiverer mouse mutation, *Proc Natl Acad Sci U S A* *83*, 7542-6.
- Montag, D., Giese, K. P., Bartsch, U., Martini, R., Lang, Y., Bluthmann, H., Karthigasan, J., Kirschner, D. A., Wintergerst, E. S., Nave, K. A., *et al.* (1994). Mice deficient for the myelin-associated glycoprotein show subtle abnormalities in myelin, *Neuron* *13*.

- Montagnoli, A., Fiore, F., Eytan, E., Carrano, A. C., Draetta, G. F., Hershko, A., and Pagano, M. (1999). Ubiquitination of p27 is regulated by Cdk-dependent phosphorylation and trimeric complex formation, *Genes Dev* 13, 1181-9.
- Montague, P., Kirkham, D., McCallion, A. S., Davies, R. W., Kennedy, P. G., Klugmann, M., Nave, K., and Griffiths, I. R. (1999). Reduced levels of a specific myelin-associated oligodendrocytic basic protein isoform in shiverer myelin, *Dev Neurosci* 21, 36-42.
- Moore, M. W., Klein, R. D., Farinas, I., Sauer, H., Armanini, M., Phillips, H., Reichardt, L. F., Ryan, A. M., Carver-Moore, K., and Rosenthal, A. (1996). Renal and neuronal abnormalities in mice lacking GDNF, *Nature* 382, 76-9.
- Mori, S., Tanaka, K., Omura, S., and Saito, Y. (1995). Degradation process of ligand-stimulated platelet-derived growth factor beta-receptor involves ubiquitin-proteasome proteolytic pathway, *J Biol Chem* 270, 29447-52.
- Munemitsu, S., Albert, I., Souza, B., Rubinfeld, B., and Polakis, P. (1995). Regulation of intracellular beta-catenin levels by the adenomatous polyposis coli (APC) tumor-suppressor protein, *Proc Natl Acad Sci U S A* 92, 3046-50.
- Muralidhar, M. G., and Thomas, J. B. (1993). The *Drosophila* bendless gene encodes a neural protein related to ubiquitin-conjugating enzymes, *Neuron* 11, 253-66.
- Musti, A. M., Treier, M., and Bohmann, D. (1997). Reduced ubiquitin-dependent degradation of c-Jun after phosphorylation by MAP kinases, *Science* 275, 400-2.
- Narayanan, V., Barbosa, E., Reed, R., and Tennekoon, G. (1988). Characterization of a cloned cDNA encoding rabbit myelin P2 protein, *J Biol Chem* 263, 8332.
- Ng, R. W., Arooz, T., Yam, C. H., Chan, I. W., Lau, A. W., and Poon, R. Y. (1998). Characterization of the cullin and F-box protein partner Skp1, *FEBS Lett* 438, 183-9.
- Notterpek, L., Ryan, M. C., Tobler, A. R., and Shooter, E. M. (1999). PMP22 Accumulation in Aggresomes: Implications for CMT1A Pathology, *Neurobiology of Disease* 6, 450-460.
- Ohta, T., Michel, J. J., Schottelius, A. J., and Xiong, Y. (1999). ROC1, a homolog of APC11, represents a family of cullin partners with an associated ubiquitin ligase activity, *Mol Cell* 3, 535-41.
- Orford, K., Crockett, C., Jensen, J. P., Weissman, A. M., and Byers, S. W. (1997). Serine phosphorylation-regulated ubiquitination and degradation of beta-catenin, *J Biol Chem* 272, 24735-8.
- Orian, A., Whiteside, S., Israel, A., Stancovski, I., Schwartz, A. L., and Ciechanover, A. (1995). Ubiquitin-mediated processing of NF-kappa B transcriptional activator

precursor p105. Reconstitution of a cell-free system and identification of the ubiquitin-carrier protein, E2, and a novel ubiquitin-protein ligase, E3, involved in conjugation, *J Biol Chem* 270, 21707-14.

Owens, G. C., and Bunge, R. P. (1989). Evidence for an early role for myelin-associated glycoprotein in the process of myelination, *Glia* 2, 119-128.

Palombella, V. J., Rando, O. J., Goldberg, A. L., and Maniatis, T. (1994). The ubiquitin-proteasome pathway is required for processing the NF- κ B precursor protein and the activation of NF- κ B, *Cell* 78, 773-85.

Pareek, S., Suter, U., Snipes, G. J., Welcher, A. A., Shooter, E. M., and Murphy, R. A. (1993). Detection and processing of peripheral myelin protein PMP22 in cultured Schwann cells, *J Biol Chem* 268, 10372-10379.

Parmantier, E., Lynn, B., Lawson, D., Turmaine, M., Namini, S. S., Chakrabarti, L., McMahon, A. P., Jessen, K. R., and Mirsky, R. (1999). Schwann cell-derived Desert hedgehog controls the development of peripheral nerve sheaths, *Neuron* 23, 713-24.

Patton, E. E., Willems, A. R., and Tyers, M. (1998). Combinatorial control in ubiquitin-dependent proteolysis: don't skip the F-box hypothesis, *TIG* 14, 236-243.

Pennisi, E. (1998). How a growth control path takes a wrong turn to cancer, *Science* 281, 1438-9, 1441.

Peters, A., Palay, S. L., and Webster, H. D. (1970). The fine structure of the nervous system (Oxford, Oxford University Press).

Ranvier, M. L. (1878). *Lecons Sur L'Histologie du Systeme Nerveux* (Paris, F.Savy).

Rechsteiner, M., and Rogers, S. W. (1996). PEST sequences and regulation by proteolysis, *Trends Biochem Sci* 21, 267-71.

Riethmacher, D., Sonnenberg-Riethmacher, E., Brinkmann, V., Yamaai, T., Lewin, G. R., and Birchmeier, C. (1997). Severe neuropathies in mice with targeted mutations in the ErbB3 receptor, *Nature* 389, 725-30.

Roa, B. B., Dyck, P. J., Marks, H. G., Chance, P. F., and Lupski, J. R. (1993). Dejerine-Sottas syndrome associated with point mutation in the peripheral myelin protein 22 (PMP22) gene, *Nature Genet* 5, 269-273.

Sadot, E., Simcha, I., Iwai, K., Ciechanover, A., Geiger, B., and Ben-Ze'ev, A. (2000). Differential interaction of plakoglobin and beta-catenin with the ubiquitin-proteasome system, *Oncogene* 19, 1992-2001.

Salzer, J. L., Bunge, R. P., and Glaser, L. (1980(b)). Studies on Schwann cell proliferation. III. Evidence for the surface localization of the neurite mitogen., *J Cell Biol* 84, 739.

- Scherer, S. S., Xu, Y. T., Bannerman, P. G., Sherman, D. L., and Brophy, P. J. (1995). Periaxin expression in myelinating Schwann cells: modulation by axon- glial interactions and polarized localization during development, *Development* *121*, 4265-73.
- Schwob, E., Bohm, T., Mendenhall, M., and Nasmyth, K. (1994). The B-type cyclin kinase inhibitor p40SIC1 controls the G1/S transition in *Saccharomyces cerevisiae*., *Cell* *79*, 233-244.
- Seol, J. H., Feldman, R. M., Zachariae, W., Shevchenko, A., Correll, C. C., Lyapina, S., Chi, Y., Galova, M., Claypool, J., Sandmeyer, S., *et al.* (1999). Cdc53/cullin and the essential Hrt1 RING-H2 subunit of SCF define a ubiquitin ligase module that activates the E2 enzyme Cdc34, *Genes Dev* *13*, 1614-26.
- Schulman, B. A., Carrano, A. C., Jeffrey, P. D., Bowen, Z., Kinnucan, E. R., Finnin, M. S., Elledge, S. J., Harper, J. W., Pagano, M., and Pavletich, N. P. (2000). Insights into SCF ubiquitin ligases from the structure of the Skp1-Skp2 complex, *Nature* *408*, 381-6.
- Shepherd, G. (1983). *Neurobiology* (Oxford, Oxford Uni Press).
- Sherman, D. L. (1998) Regulation and developmental expression of periaxin in the PNS, University of Edinburgh, Edinburgh.
- Sherman, D. L., and Brophy, P. J. (2000). A tripartite nuclear localization signal in the PDZ-domain protein L- periaxin, *J Biol Chem* *275*, 4537-40.
- Sherman, D. L., Fabrizi, C., Gillespie, C. S., and Brophy, P. J. (2001). Specific disruption of a schwann cell dystrophin-related protein complex in a demyelinating neuropathy, *Neuron* *30*, 677-87.
- Sherman, M. Y., and Goldberg, A. L. (2001). Cellular defenses against unfolded proteins: a cell biologist thinks about neurodegenerative diseases, *Neuron* *29*, 15-32.
- Shirane, M., Harumiya, Y., Ishida, N., Hirai, A., Miyamoto, C., Hatakeyama, S., Nakayama, K., and Kitagawa, M. (1999). Down-regulation of p27(Kip1) by two mechanisms, ubiquitin-mediated degradation and proteolytic processing, *J Biol Chem* *274*, 13886-93.
- Skowyra, D., Craig, K. L., Tyers, M., Elledge, S. J., and Harper, J. W. (1997). F-box proteins are receptors that recruit phosphorylated substrates to the SCF ubiquitin-ligase complex, *Cell* *91*, 209-19.

Skowyra, D., Koepp, D. M., Kamura, T., Conrad, M. N., Conaway, R. C., Conaway, J. W., Elledge, S. J., and Harper, J. W. (1999). Reconstitution of G1 cyclin ubiquitination with complexes containing SCFGrr1 and Rbx1, *Science* 284, 662-5.

Snell, R. S. (1997). *Clinical Neuroanatomy for Medical Students*, Fourth Edition edn (Philadelphia, Lippincott-Raven).

Spence, J., Gali, R. R., Dittmar, G., Sherman, F., Karin, M., and Finley, D. (2000). Cell cycle-regulated modification of the ribosome by a variant multiubiquitin chain, *Cell* 102, 67-76.

Spencer, E., Jiang, J., and Chen, Z. J. (1999). Signal-induced ubiquitination of IkappaBalpha by the F-box protein Slimb/beta-TrCP, *Genes Dev* 13, 284-94.

Spreyer, P., Kuhn, G., Hanemann, C. O., Gillen, C., Schaal, H., Kuhn, R., Lemke, G., and Muller, H. W. (1991). Axon-related expression of a Schwann cell transcript that is homologous to a 'growth arrest-specific' gene, *Mol Brain Res* 8, 209-212.

Staub, O., Dho, S., Henry, P., Correa, J., Ishikawa, T., McGlade, J., and Rotin, D. (1996). WW domains of Nedd4 bind to the proline-rich PY motifs in the epithelial Na⁺ channel deleted in Liddle's syndrome, *Embo J* 15, 2371-80.

Sternberger, N. H., Quarles, R. H., Itoyama, Y., and Webster, H. d. F. (1979). Myelin-associated glycoprotein demonstrated immunocytochemically in myelin and myelin-forming cells of developing rats, *Proc Natl Acad Sci USA* 76, 1510-1514.

Stryer, L. (1975). *Biochemistry* (San Francisco, W. H. Freeman).

Suzuki, H., Chiba, T., Suzuki, T., Fujita, T., Ikenoue, T., Omata, M., Furuichi, K., Shikama, H., and Tanaka, K. (2000). Homodimer of two F-box proteins betaTrCP1 or betaTrCP2 binds to IkappaBalpha for signal-dependent ubiquitination, *J Biol Chem* 275, 2877-84.

ter Haar, E., Harrison, S. C., and Kirchhausen, T. (2000). Peptide-in-groove interactions link target proteins to the beta-propeller of clathrin, *Proc Natl Acad Sci U S A* 97, 1096-100.

Thomas, P. K. (1955). Growth changes in the myelin sheath of peripheral nerve fibres, *Proc R Soc Ser B* 143, 380-391.

Thomas, P. K., Landon, D. N., and King, R. H. M. (1984). Diseases of the peripheral nerves. In *Greenfields Neuropathology*, J. H. Adams, J. A. N. Corsellis, and L. W. Duchon, eds. (New York, John Wiley and Sons), pp. 807-920.

Thrower, J. S., Hoffman, L., Rechsteiner, M., and Pickart, C. M. (2000). Recognition of the polyubiquitin proteolytic signal, *Embo J* 19, 94-102.

- Trapp, B. D., and Quarles, R. H. (1982). Presence of the myelin-associated glycoprotein correlates with alterations in the periodicity of peripheral myelin, *J Cell Biol* 94, 877-882.
- Trapp, B. D., Quarles, R. H., and Griffin, J. W. (1984a). Myelin-associated glycoprotein and myelinating Schwann cell-axon interaction in chronic B₂B₁-iminodipropionitrile neuropathy, *J Cell Biol* 98, 1271-1278.
- Trapp, B. D., Quarles, R. H., and Suzuki, K. (1984b). Immunocytochemical studies of quacking mice support a role for the myelin-associated glycoprotein in forming and maintaining the periaxonal space and periaxonal cytoplasmic collar of myelinating Schwann cells., *J Cell Biol* 99, 594-606.
- Treier, M., Staszewski, L. M., and Bohmann, D. (1994). Ubiquitin-dependent c-Jun degradation in vivo is mediated by the delta domain, *Cell* 78, 787-98.
- Tyers, M., and Jorgensen, P. (2000). Proteolysis and the cell cycle: with this RING I do thee destroy, *Curr Opin Genet Dev* 10, 54-64.
- Ulrich, H. D., and Jentsch, S. (2000). Two RING finger proteins mediate cooperation between ubiquitin- conjugating enzymes in DNA repair, *Embo J* 19, 3388-97.
- Varshavsky, A. (1996). The N-end rule: Functions, mysteries, uses, *Proceedings of the National Academy of Science USA* 93, 12142-12149.
- Varshavsky, A. (1997). The Ubiquitin system, *Trends in Biochemical Sciences* 22, 383-387.
- Webster, H., Lampeth, L., Favilla, J. T., Lemke, G., Tesin, D., and Manuelidis, L. (1987). Use of a biotinylated probe and in situ hybridization for light and electron microscopic localization of Po mRNA in myelin- forming Schwann cell., *Histochemistry* 86, 441-444.
- Wellington, C. L., Ellerby, L. M., Hackam, A. S., Margolis, R. L., Trifiro, M. A., Singaraja, R., McCutcheon, K., Salvesen, G. S., Propp, S. S., Bromm, M., *et al.* (1998). Caspase cleavage of gene products associated with triplet expansion disorders generates truncated fragments containing the polyglutamine tract, *J Biol Chem* 273, 9158-67.
- Wiederkehr, A., Avaro, S., Prescianotto-Baschong, C., Haguenaer-Tsapis, R., and Riezman, H. (2000). The F-box protein Rcy1p is involved in endocytic membrane traffic and recycling out of an early endosome in *Saccharomyces cerevisiae*, *J Cell Biol* 149, 397-410.
- Windebank, A. J., Wood, P., Bunge, R. P., and Dyck, P. J. (1985). Myelination determines the calibre of dorsal root ganglion neurons in culture., *J Neurosci* 5, 1563-1569.

- Winder, S. J. (2001). The complexities of dystroglycan, *Trends Biochem Sci* 26, 118-24.
- Winston, J. T., Koepf, D. M., Zhu, C., Elledge, S. J., and Harper, J. W. (1999a). A family of mammalian F-box proteins, *Curr Biol* 9, 1180-2.
- Winston, J. T., Strack, P., Beer-Romero, P., Chu, C. Y., Elledge, S. J., and Harper, J. W. (1999b). The SCF β -TRCP-ubiquitin ligase complex associates specifically with phosphorylated destruction motifs in I κ B and β -catenin and stimulates I κ B ubiquitination in vitro, *Genes Dev* 13, 270-83.
- Wodarz, A., and Nusse, R. (1998). Mechanisms of Wnt signaling in development, *Annu Rev Cell Dev Biol* 14, 59-88.
- Wolf, D. A., McKeon, F., and Jackson, P. K. (1999). F-box/WD-repeat proteins pop1p and Sud1p/Pop2p form complexes that bind and direct the proteolysis of cdc18p, *Curr Biol* 9, 373-6.
- Wu, X., and Haber, J. E. (1996). A 700 bp cis-acting region controls mating-type dependent recombination along the entire left arm of yeast chromosome III, *Cell* 87, 277-85.
- Xie, Y., and Varshavsky, A. (2000). Physical association of ubiquitin ligases and the 26S proteasome, *Proc Natl Acad Sci U S A* 97, 2497-502.
- Yaffe, M. B., and Elia, A. E. H. (2001). Phosphoserine/threonine-binding domains., *Current Opinion in Cell Biology* 13, 131-138.
- Yaglom, J., Linskens, M. H., Sadis, S., Rubin, D. M., Futcher, B., and Finley, D. (1995). p34^{Cdc28}-mediated control of Cln3 cyclin degradation, *Mol Cell Biol* 15, 731-41.
- Yam, C. H., Ng, R. W., Siu, W. Y., Lau, A. W., and Poon, R. Y. (1999). Regulation of cyclin A-Cdk2 by SCF component Skp1 and F-box protein Skp2, *Mol Cell Biol* 19, 635-45.
- Yaron, A., Gonen, H., Alkalay, I., Hatzubai, A., Jung, S., Beyth, S., Mercurio, F., Manning, A. M., Ciechanover, A., and Ben-Neriah, Y. (1997). Inhibition of NF- κ B cellular function via specific targeting of the I- κ B-ubiquitin ligase, *Embo J* 16, 6486-94.
- Yaron, A., Hatzubai, A., Davis, M., Lavon, I., Amit, S., Manning, A. M., Andersen, J. S., Mann, M., Mercurio, F., and Ben-Neriah, Y. (1998). Identification of the receptor component of the I κ B-ubiquitin ligase, *Nature* 396, 590-4.
- Young, J. Z. (1942). The functional repair of nervous tissue, *Physiol Rev* 22, 318.

Zachariae, W., and Nasmyth, K. (1999). Whose end is destruction: cell division and the anaphase-promoting complex, *Genes Dev* 13, 2039-58.

Zachariae, W., Shevchenko, A., Andrews, P. D., Ciosk, R., Galova, M., Stark, M. J., Mann, M., and Nasmyth, K. (1998). Mass spectrometric analysis of the anaphase-promoting complex from yeast: identification of a subunit related to cullins, *Science* 279, 1216-9.

Zhou, P., Bogacki, R., McReynolds, L., and Howley, P. M. (2000). Harnessing the ubiquitination machinery to target the degradation of specific cellular proteins, *Mol Cell* 6, 751-6.

Zhou, P., and Howley, P. M. (1998). Ubiquitination and degradation of the Substrate Recognition Subunits of SCF Ubiquitin-Protein Ligases, *Molecular Cell* 2, 571-580.

Zigmond, M. J., Bloom, F. E., Landis, S. C., Roberts, J. L., and Squire, L. R., eds. (1999). *Fundamental Neuroscience* (San Diego, Academic Press).